

# Physics and phenomenology of large extra dimensions

E.E. Boos, V.E. Bunichev, I.P. Volobuev, V.O. Egorov,  
S.I. Keizerov, E.R. Rakhmetov, M.N. Smolyakov

DOI: <https://doi.org/10.3367/UFNe.2024.12.039820>

## Contents

<b>1. Introduction. Hypothesis on existence of extra spacetime dimensions: a brief history</b>	<b>111</b>
<b>2. Randall–Sundrum model</b>	<b>114</b>
<b>3. Stabilized Randall–Sundrum model</b>	<b>117</b>
<b>4. Phenomenology of Kaluza–Klein excitations</b>	<b>120</b>
<b>5. Comparison of processes involving radion with similar processes involving the Higgs boson</b>	<b>123</b>
5.1 Processes involving a single scalar boson; 5.2 Processes with associated production of radion and Higgs bosons	
<b>6. Nonlinear self-interaction and interaction of radion with fields of the Standard Model</b>	<b>129</b>
6.1 Effective four-dimensional quartic radion Lagrangian	
<b>7. Mixing of Higgs and radion fields</b>	<b>133</b>
7.1 Higgs-dominated state with mass 125 GeV; 7.2 Radion-dominated state with mass 125 GeV	
<b>8. Stability of Randall–Sundrum model with respect to quantum corrections</b>	<b>140</b>
8.1 Quantum corrections from scalar modes to energy–momentum tensor and to equations of motion of Randall–Sundrum model; 8.2 Regularization and renormalization of Casimir energy density of scalar modes; 8.3 Change in model parameters due to Casimir effect	
<b>9. Conclusions</b>	<b>143</b>
<b>References</b>	<b>144</b>

**Abstract.** The history of models of elementary-particle interactions in a spacetime with large extra dimensions is reviewed, and the current state of this approach and its phenomenological implications are considered. The discussion is focused on the stabilized two-brane Randall–Sundrum model—the most interesting one from this perspective—and the most important results it yields. For this model, the connection between the fundamental 5D energy scale and the Planck mass is discussed in detail, as is the isolation of physical degrees of freedom. The interaction of the lowest scalar mode, the radion, and the lowest tensor modes with Standard Model fields is analyzed. The stability of the model with respect to quantum corrections is discussed.

**Keywords:** extra spacetime dimensions, large extra dimensions, field theory, Randall–Sundrum model, brane world

E.E. Boos<sup>(a)</sup>, V.E. Bunichev<sup>(b)</sup>, I.P. Volobuev<sup>(c)</sup>, V.O. Egorov<sup>(d)</sup>,  
S.I. Keyzerov<sup>(e)</sup>, E.R. Rakhmetov<sup>(f)</sup>, M.N. Smolyakov<sup>(g)</sup>  
Lomonosov Moscow State University,  
Skobeltsyn Institute of Nuclear Physics,  
Leninskie gory 1, str. 2, 119991 Moscow, Russian Federation  
E-mail: <sup>(a)</sup>boos@theory.sinp.msu.ru, <sup>(b)</sup>bunichev@theory.sinp.msu.ru,  
<sup>(c)</sup>volobuev@theory.sinp.msu.ru, <sup>(d)</sup>egorov@theory.sinp.msu.ru,  
<sup>(e)</sup>errar@mail.ru, <sup>(f)</sup>rahmetov@theory.sinp.msu.ru,  
<sup>(g)</sup>smolyakov@theory.sinp.msu.ru

Received 29 October 2024, revised 26 November 2024

Uspekhi Fizicheskikh Nauk 195 (2) 116–153 (2025)

Translated by M.Zh. Shmatikov

## 1. Introduction.

### Hypothesis on existence of extra spacetime dimensions: a brief history

The idea that our space may have more than three dimensions appeared long ago. As early as the 19th century, scientists suggested that the dimensions of space may be not limited to just length, width, and height. At the end of the 20th century, this was firmly established in theoretical high-energy physics as one of the most important hypotheses.

V. Rubakov made a significant contribution to the development of theories with extra spacetime dimensions. He and M. Shaposhnikov were the first to suggest the now generally accepted idea of localizing the Standard Model (SM) fields on a four-dimensional hypersurface in multi-dimensional spacetime, which underlies all current brane world models. This approach allows explaining the macroscopic unobservability of large extra dimensions and obtaining a fundamental multidimensional energy scale, which is much smaller than the Planck scale. Rubakov also obtained a number of important results in the theory of brane world models.

The first physical theory with an extra dimension was the unified theory of gravity and electromagnetism, proposed in 1914 by the Finnish physicist Gunnar Nordström [1]. In this relativistic theory, gravity was described by a scalar field, which, together with the four-dimensional vector potential of the electromagnetic field, formed a 5-vector in 5D spacetime. However, the advent of Einstein's general theory of relativity the following year and its subsequent experimental confirma-

tion showed that such a theory was physically inadequate. Therefore, the birth of the multidimensional approach is associated with T. Kaluza's study in 1921 [2], in which an attempt was made to combine electromagnetism with Einstein's four-dimensional theory of gravity in a unified five-dimensional theory. Kaluza's theory was based on three assumptions. First, the presence of one additional spatial dimension was postulated. Second, it was hypothesized that the fifth dimension differs significantly from the other four we are accustomed to. This was manifested, in particular, in the metric of 5D spacetime being not dependent on the fifth coordinate (the cylindricity condition). And, third, Einstein's equations were derived from a geometric generalization of the action for the 4D theory for the case of five dimensions, i.e., the action has the form of a scalar curvature of 5D spacetime integrated over this spacetime.

An interesting implication of Kaluza's assumptions was that the 15 equations of the gravitational field in a multidimensional space were broken down into 10 ordinary Einstein equations in 4D spacetime, 4 Maxwell equations, and one more equation for a scalar field. This automatically yielded the energy–momentum tensor of the electromagnetic field, which had to be introduced into Einstein's 4D theory 'ad hoc.'

Kaluza's ideas are seemingly inconsistent with the apparent unobservability of the fourth spatial dimension in everyday life. This disagreement was resolved in 1926 by O. Klein [3, 4], who clearly showed that the structure of our Universe can allow the existence of not only infinite, but also so-called compact, or curled, dimensions. Such dimensions are inaccessible to our senses due to their small size. In addition, Klein used quantum mechanics to show that the size of the additional cyclic dimension should be of the order of the Planck length  $l_{\text{Pl}} = 1/M_{\text{Pl}}$ , which is far beyond the current capabilities of the experiment. Since then, the Kaluza–Klein theories have been used to refer to a whole class of theories based on the assumption of the existence of additional compact spatial dimensions.

However, the Kaluza–Klein theory encountered a problem that could not be resolved immediately. As noted by Einstein, V. Bargmann, and P. Bergmann [5], in this theory, "it is impossible to explain the empirical fact that the electrostatic forces acting between particles greatly exceed gravitational ones." Therefore, interest in this approach faded for a time.

Interest in the Kaluza–Klein theories rekindled in the 1960s in connection with the development of non-Abelian gauge theories of the interaction of elementary particles. In the mid-1970s, the hypothesis of a multidimensional space became virtually universally accepted, which was due to the advancement in field theory. Many unification schemes, such as theories of supergravity or superstrings, made sense and could be consistently mathematically formulated only in a certain number of dimensions greater than the conventional four [6–10] (these dimensions are called critical). Thus, the ideas of Kaluza–Klein were reborn.

A completely new approach based on Kaluza–Klein theories was proposed in 1983 by V. Rubakov and M. Shaposhnikov [11]. Unlike previous theories, their scenario explained the unobservability of extra dimensions of spacetime not by their small, Planck size, but by the localization of SM fields on a domain wall. In this case, extra dimensions can have a large and even infinite size, remaining unobservable in the region of sufficiently low energies, leading at the same

time to experimentally observable phenomena at high energies [12]. In the limit of an infinitely thin domain wall, an object is obtained that is usually called a membrane, or simply a brane. Theories with localization of fields on an infinitely thin wall based on Rubakov's and Shaposhnikov's ideas are called brane world models.

It should be noted that in [11] a field-theoretical mechanism for the localization of only spinor fields was proposed. The issue of gauge-field localization turns out to be more complicated. Indeed, any such mechanism must ensure charge universality, i.e., provide the independence of the gauge charges of 4D particles from the shape of the wave functions of the corresponding modes in the extra dimension [12]. An option to ensure charge universality is to localize the energy density of the gauge-field zero mode in a certain region in the extra dimension, for example, on a domain wall, with the solution for this zero mode being independent of the coordinate of the extra dimension. This can be done using a field-theoretical mechanism, various variations of which are proposed in [13–15] (in [13], it is the solution for a domain wall that is used to localize the gauge field). In addition, the mechanism of fermion field localization on a domain wall [11] can be combined with a slightly modified mechanism of gauge field localization [13] within a unified theory, which makes it possible to fully reproduce the standard 4D quantum electrodynamics at the level of zero modes [16]. However, due to the presence of Kaluza–Klein (KK) mode towers, the cross sections of some processes in such a model turn out to be infinite, and these infinities are physical and cannot be eliminated using the standard renormalization procedure [16] (it was shown later that similar divergences also arise in a certain type of brane world models [17]). Thus, the issue of constructing a consistent field-theoretical mechanism for localizing fields on a brane persists.

The theory with extra spacetime dimensions was further developed in the so-called ADD scenario (named after the authors: Arkani–Hamed, Dimopoulos, and Dvali) [18, 19]. It was shown that, under the assumption of localization of SM fields on the brane in a multidimensional space and given that the extra dimensions are large, the relationship between the multidimensional gravitational energy scale  $M_{\text{ADD}}$  and the Planck mass  $M_{\text{Pl}}$  (the energy scale of gravity in 4D spacetime) remains the same as in the conventional Kaluza–Klein theory and has the form

$$M_{\text{Pl}}^2 = M_{\text{ADD}}^{n+2} V_n, \quad (1)$$

where  $V_n$  is the total volume of  $n$  extra spatial dimensions. It follows from this formula that, in a multidimensional space, the fundamental energy scale of gravitational interaction can be approximately 1 TeV, which corresponds to the scale of the electroweak interaction, while the effective interaction constant on the brane takes the familiar value of about  $10^{19}$  GeV. In this way, the problem of the hierarchy of gravitational interaction was easily and elegantly solved. The scenario also predicted experimental detectability of extra dimensions in the near future, which was of interest *per se*.

However, while providing a simple and transparent explanation for the weakness of gravitational interaction in 4D spacetime, the ADD scenario has a significant drawback. In this theory, it is assumed that the brane has no energy density — tension — and, in accordance with Einstein's special theory of relativity, no physical frame of reference can be associated with it. If we consider branes with tension in the

ADD scenario, it immediately becomes clear that the gravitational field of the brane cannot be taken into account using perturbation theory, and this problem is very challenging.

The problem of nonperturbative accounting of brane tension was solved in the Randall–Sundrum model (RS model) [20]. In it, an exact solution was found for a system of two branes, one with a positive tension and the other with a negative tension, interacting with gravity in five-dimensional spacetime. The metric of the background solution in the RS model has the form

$$ds^2 = \exp(C - 2k|y|) \eta_{\mu\nu} dx^\mu dx^\nu - dy^2, \quad (2)$$

where  $\eta_{\mu\nu} = \text{diag}(1, -1, -1, -1)$  denotes the Minkowski metric,  $y$  is the coordinate of the extra dimension, and the constant  $C$  is chosen depending on which brane our world is located. The extra dimension is the so-called orbifold, which sets some symmetry on all fields of the model, and two branes are at its fixed points, thus not being dynamic elements of the model: the brane with positive tension is located at the point  $y = 0$ , while the one with negative tension is at the point  $y = L$ .

Apparently, for a nonzero value of the constant  $k$ , the metric (2) is not flat, but contains an exponential conformal factor, the ‘warp factor,’ due to which the problem of the hierarchy of gravitational interaction is solved. If the constant  $C = 0$ , the metric on the brane at  $y = 0$  induced from such a five-dimensional metric coincides with the Minkowski metric, and the corresponding coordinates  $\{x^\mu\}$  are Galilean on this brane (for the definition of Galilean coordinates, see [21]). If the constant  $C = 2kL$ , the coordinates  $\{x^\mu\}$  in Eqn (2) are Galilean on the brane at  $y = L$ .

As in the case of the ADD scenario, the relationship between the four-dimensional Planck scale and the fundamental five-dimensional energy scale can be obtained by integrating the action for the 4D fields over the coordinate of the extra dimension  $y$ , but the results are different for different branes. To find this relationship between the four-dimensional and five-dimensional energy scales, we consider a five-dimensional metric of the form

$$ds^2 = \exp(C - 2k|y|) g_{\mu\nu}(x) dx^\mu dx^\nu - dy^2. \quad (3)$$

If the constant  $C = 0$ , this five-dimensional metric induces a metric  $g_{\mu\nu}(x)$  on the brane at  $y = 0$ , and if  $C = 2kL$ , the metric  $g_{\mu\nu}(x)$  is induced on the brane at  $y = L$ . Substituting the five-dimensional metric (3) into the RS action (see Section 2), we arrive at the following result:

$$S = -2M^3 \int_{-L}^L \exp(C - 2k|y|) dy \int R_4(g) \sqrt{-g} d^4x, \quad (4)$$

where  $M$  is the fundamental five-dimensional energy scale, and  $R_4(g)$  is the four-dimensional scalar curvature corresponding to the metric  $g_{\mu\nu}(x)$ . Integration in Eqn (4) over the extra dimension yields the effective action for the tensor field  $g_{\mu\nu}(x)$  [22]:

$$S_{\text{eff}} = -2M^3 \exp(C) \frac{1 - \exp(-2kL)}{k} \int R_4(g) \sqrt{-g} d^4x. \quad (5)$$

We thus see that the above action is the standard gravitational action, and hence the field  $g_{\mu\nu}(x)$  is indeed a gravitational

field, while the term in front of this action defines the gravitational constants on the branes.

If our world is on a brane at  $y = 0$ , we must set  $C = 0$ , and, as a result, we obtain an expression for the Planck mass in terms of the fundamental five-dimensional energy scale

$$M_{\text{Pl}}^2 = \frac{1 - \exp(-2kL)}{k} M^3. \quad (6)$$

Since  $\exp(-2kL) < 1$ , this relation shows that in this case we should have  $k \sim M \sim M_{\text{Pl}}$ , i.e., the model does not provide a solution to the hierarchy problem of gravitational interaction. If our world is on a brane at  $y = L$ , we must set  $C = 2kL$ , and in this case the expression for the Planck mass in terms of the fundamental five-dimensional energy scale is as follows:

$$M_{\text{Pl}}^2 = \frac{\exp(2kL) - 1}{k} M^3. \quad (7)$$

If now  $k \sim M$  and  $kL \simeq 35$ , then, due to the exponential factor in Eqn (7), we can obtain the correct value of the Planck mass for a model parameter of the order of several TeV. Thus, in this case, the RS model provides a solution to the hierarchy problem of gravitational interaction.

It should be noted that, in the original study by L. Randall and R. Sundrum [20], coordinates that were Galilean on the brane at  $y = 0$  were used to describe the interaction of matter with the KK modes of the gravitational field on the brane at the point  $y = L$ . As a result, an additional exponential factor  $\exp(-2kL)$  appeared in the action for the fields, originating from the induced metric, which was simply removed by redefining the fields and masses. It turned out that the fundamental energy scale of the theory is the Planck mass, as it should be on the brane at  $y = 0$ , while the masses of the lowest KK modes can be of the order of several TeV due to the cutting-off exponential factor. V. Rubakov was the first to note in [12] that such an approach is incorrect, since any theory must be described in coordinates that are Galilean on the observer’s brane (in this study, such coordinates were called physical). A consistent description of the theory on the brane at the point  $y = L$  was subsequently developed in [23], where it was shown that the fundamental energy scale on this brane is a scale of the order of several TeV, while the Planck scale is a derivative and appears due to the exponential factor in the metric.

It should be noted that the absolute majority of studies of the RS model use, following [20], an incorrect physical interpretation of this model. An immense number of studies explore the phenomenology of the unstabilized RS model, and most of them use the Planck energy scale on a brane with negative tension.

However, the RS model, even with the correct physical interpretation, is not flawless. It predicts the existence of a massless four-dimensional scalar mode, radion, first identified in the study by V. Rubakov, R. Gregory, and C. Charmousis [24]. This mode corresponds to fluctuations in the distance between branes, which can be any, implying that it is massless. In this case, we are dealing with an unstabilized distance between branes and, in general, an unstabilized RS model. In such a model, radion should interact with matter on the brane approximately as strongly as gravity. The presence of such a massless scalar particle, ‘strongly’ interacting with SM fields, disagrees with experimental data already at the level of classical gravity.

To solve this problem, a five-dimensional scalar field with a potential in the entire space and additional potentials on the

branes was introduced into the model [25, 26]. This allows the distance between the branes to be stabilized, which leads to the appearance of radion mass. The stabilization of the size of the extra dimension is achieved by using boundary conditions for the scalar field on the branes, and the mass of the radion is determined by the magnitude of the deviation of the background metric from the RS solution. In [27, 28], an option to identify the stabilizing field of the RS model with the SM Higgs field was discussed. Such a unified field propagates throughout the five-dimensional spacetime, and on the brane, where our world is supposedly located, it can play the role of the Higgs field. Namely, all other SM fields, which are considered to be localized on the brane, obtain masses due to interaction with the boundary value of this five-dimensional Higgs field. However, this approach is plagued with serious difficulties [27, 28], so the issue of the possible role of the Higgs field in theories with extra dimensions remains open.

Thus, only the stabilized RS model can be physically adequate, and it is for such a model alone that it makes sense to consider the phenomenological implications. Nevertheless, in some cases, the phenomenological results obtained in an unstabilized model may have physical meaning. This also applies to the variant of the stabilized RS model frequently used in phenomenology, in which, while keeping all the constants of the model unchanged, the required mass for the radion field is simply added ‘ad hoc.’ This variant of stabilization seems inconsistent, since it does not take into account the existence of an infinite tower of scalar excitations, and an arbitrary choice of coupling constants and masses in it may turn out to be contradictory, since they are functions of the parameters of the stabilizing scalar field. Therefore, in our opinion, the only consistent RS model is the one stabilized using a five-dimensional scalar field with a fundamental five-dimensional scale of the order of 5–10 TeV for an observer on a brane with negative tension. Nevertheless, the results of studies where the Planck fundamental scale on this brane is used, generally, coincide with the those obtained in a physically correct interpretation of the model, although the coincidence must be checked each time.

The most famous phenomenological consequence of the RS model, as of any model with extra dimensions, is the existence of KK towers of the gravitational and SM fields, if it is assumed that they can also propagate in the extra dimension. The possible influence of such towers on the interaction between SM particles has been discussed in a plethora of studies, for example, in [29–47]. In this review, we briefly outline the original version of the RS model with a correct physical interpretation, in which the SM fields are localized on one of the branes, and gravity alone can propagate in the entire multidimensional space. Then, we discuss a version of this model with a stabilized distance between branes, which is phenomenologically acceptable. In such a stabilized model, we consider a number of important physical results, including the impact of the KK towers of the graviton and radion on the interaction between SM particles, the similarity of the interactions of the radion and the Higgs boson, and the self-interaction of the radion up to the fourth power, inclusive. We also discuss the mixing of radion and Higgs fields in the stabilized RS model with spontaneous breaking of the SM gauge symmetry due to dynamical gravitational stabilization of the 5D-theory vacuum and the phenomenology of radion- and Higgs-dominated states. Finally, we explore the stability of the stabilized RS model with respect to quantum corrections.

## 2. Randall–Sundrum model

In 1999, L. Randall and R. Sundrum proposed a new solution to the hierarchy problem [20]. The RS model can be briefly described as follows. In a five-dimensional spacetime, which is a direct product of a four-dimensional pseudo-Euclidean spacetime and a one-dimensional space of an extra dimension  $S^1/Z_2$ , a theory of gravity is considered that interacts with two four-dimensional hypersurfaces—branes—on one of which the SM fields are localized, i.e., our observable Universe. Thus, in the RS model, the fifth (extra) dimension is an orbifold, at the fixed points of which branes are located that have proper tensions equal in magnitude and opposite in sign, denoted by  $\lambda_1$  and  $\lambda_2$ , respectively.

We denote the coordinates of the five-dimensional spacetime by  $\{x^M\} \equiv \{x^\mu, y\}$ ,  $M=0, 1, 2, 3, 4$ ,  $\mu=0, 1, 2, 3$ , and assume that the coordinate of the extra dimension  $x^4 \equiv y$  takes values on the interval  $-L \leq y < L$ , and, due to the orbifold symmetry, the points of the five-dimensional spacetime  $(x, -y)$  and  $(x, y)$  should be identified. The components of the five-dimensional metric satisfy the following symmetry conditions:

$$\begin{aligned} g_{\mu\nu}(x, -y) &= g_{\mu\nu}(x, y), \\ g_{4\nu}(x, -y) &= -g_{4\nu}(x, y), \\ g_{44}(x, -y) &= g_{44}(x, y). \end{aligned}$$

The action of the RS model is presented as follows:

$$\begin{aligned} S &= S_1 + S_2, \\ S_1 &= - \int_{M_4} \int_{-L}^L 2M^3 (R - \Lambda) \sqrt{g} d^5x, \\ S_2 &= - \int_{M_4} \int_{-L}^L [\lambda_1 \delta(y) + \lambda_2 \delta(y - L)] \sqrt{-\tilde{g}} d^5x, \end{aligned} \quad (8)$$

where  $R$  is the five-dimensional scalar curvature corresponding to the metric  $g_{MN}$ ,  $\Lambda$  is the five-dimensional cosmological constant, and  $\tilde{g}_{\mu\nu}$  is the metric tensor induced on the four-dimensional hypersurfaces set by the equation  $y = \text{const}$ .

The equations of motion, which are the Euler–Lagrange equations for the action functional (8), can be obtained by varying with respect to the metric tensor of the five-dimensional spacetime  $g_{MN}$ :

$$\begin{aligned} R_{MN} - \frac{1}{2} (R - \Lambda) g_{MN} \\ + \frac{1}{4M^3} [\lambda_1 \delta(y) + \lambda_2 \delta(y - L)] \tilde{g}_{\mu\nu} \delta_M^\mu \delta_N^\nu = 0. \end{aligned} \quad (9)$$

Equation (9) has a solution that is invariant under transformations of the Poincaré group of 4D coordinates  $x^\mu$ :

$$\begin{aligned} g_{MN} &= \gamma_{MN}, \quad \gamma_{\mu\nu} = \exp(C - 2k|y|) \eta_{\mu\nu}, \\ \gamma_{\mu 4} &= 0, \quad \gamma_{44} = -1, \end{aligned} \quad (10)$$

where  $\eta_{\mu\nu}$  is the Minkowski metric tensor, and  $C$  and  $k$  are some constants. The constant  $k$  and the parameters  $M$ ,  $\Lambda$ ,  $\lambda_1$ , and  $\lambda_2$  are related in the following way [20]:

$$k = \sqrt{-\frac{\Lambda}{12}}, \quad \lambda_1 = -\lambda_2 = 24M^3 \sqrt{-\frac{\Lambda}{12}}. \quad (11)$$

$C$  is a constant of integration which is determined from the following considerations. The metric induced on the hyper-

surfaces  $y = \text{const}$  has the form

$$ds^2 = \exp(C - 2k|y|) \eta_{\mu\nu} dx^\mu dx^\nu. \quad (12)$$

In fact, the choice of constant  $C$  is equivalent to the selection of some scale for the coordinates  $\{x^\mu\}$ . The canonical normalization of matter fields assumes that their Lagrangian is presented in Galilean coordinates, i.e., the metric has the form  $ds^2 = \eta_{\mu\nu} dx^\mu dx^\nu$ . Thus, if we assume that the matter is localized exclusively on the brane with coordinate  $y = 0$ , we should choose the constant  $C = 0$ . However, if the matter is localized on the second brane with coordinate  $y = L$ , the constant  $C$  should be chosen as follows:

$$C = 2kL. \quad (13)$$

Next, solution (10) is taken as a background, and small fluctuations of the metric above it are considered [23, 48]. We parameterize the metric as follows:

$$g_{MN} = \gamma_{MN} + \kappa h_{MN}, \quad \kappa \equiv \frac{1}{\sqrt{2M^3}}. \quad (14)$$

It was shown in [48] that the Lagrangian of the zeroth order in  $\kappa$  (i.e., quadratic in  $h$ ), obtained after substituting (14) into (8), after some transformations can be reduced to the form

$$\begin{aligned} L_h = & \frac{1}{4} \nabla_M h_{PQ} \nabla^M h^{PQ} + \frac{1}{4} \nabla_M h \nabla^M h - \frac{1}{2} \nabla_M h^{MP} \nabla_P h \\ & + \frac{1}{2} \nabla_M h^{MP} \nabla^Q h_{PQ} - \frac{k^2}{2} (h_{PQ} h^{PQ} + h^2) \\ & + \left[ 2kh_{PQ} h^{PQ} - kh\tilde{h} + kh_{Pv} h^{Pv} - 3k \left( h_{\mu\nu} h^{\mu\nu} - \frac{1}{2} \tilde{h}^2 \right) \right] \\ & \times [\delta(y) - \delta(y - L)], \end{aligned} \quad (15)$$

where the covariant derivative  $\nabla_P$  is taken with respect to the background metric  $\gamma$ , indices are raised and lowered using the background metric  $\gamma$ , and  $h$  and  $\tilde{h}$  are contractions of the form

$$h \equiv h_{MN} \gamma^{MN}, \quad \tilde{h} \equiv h_{\mu\nu} \gamma^{\mu\nu}. \quad (16)$$

It was also shown in [48] that the action with Lagrangian (15) is invariant with respect to gauge transformations, which allows imposing additional conditions on  $h$ :

$$h_{4v} = 0, \quad h_{44}(x, y) = N_r r(x), \quad (17)$$

where the field  $r(x)$  is called the radion field, and  $N_r$  is some normalization constant. In addition, by representing the components of  $h_{\mu\nu}$  in the form

$$\begin{aligned} h_{\mu\nu} = & b_{\mu\nu} + (k|y| - c) \gamma_{\mu\nu} \\ & + \frac{1}{2k^2} \left( k|y| - c + \frac{1}{2} + \frac{c}{2} \exp(-2k|y|) \right) \partial_\mu \partial_\nu r, \end{aligned} \quad (18)$$

$$c \equiv \frac{kL}{\exp(2kL) - 1}, \quad (19)$$

gauge conditions can be imposed on the fields  $b_{\mu\nu}$ :

$$\eta^{\mu\nu} b_{\mu\nu} \equiv b = 0, \quad \gamma^{\mu\nu} b_{\mu\nu} \equiv \tilde{b} = 0, \quad \partial^\mu b_{\mu\nu} = 0. \quad (20)$$

In such a gauge, the components of the equations of motion with indices  $4\nu$  turn into identities, and the components with indices  $\mu\nu$  and  $44$  acquire the form, respectively,

$$\begin{aligned} & \frac{1}{2} \exp(-2k|y|) \square b_{\mu\nu} + \frac{1}{2} \frac{\partial^2 b_{\mu\nu}}{\partial y^2} - 2k^2 b_{\mu\nu} \\ & + 2k[\delta(y) - \delta(y - L)] b_{\mu\nu} = 0, \end{aligned} \quad (21)$$

$$\square r = 0, \quad (22)$$

where  $\square$  is the 4D d'Alembert operator constructed using the flat metric  $\eta_{\mu\nu}$ .

Equation (22) implies that, in the model under consideration, after the dimensional reduction procedure, one massless scalar field appears. Heavy scalar modes (KK towers of scalar fields) do not arise in this case.

Equation (21) is solved by separation of variables. Representing the five-dimensional field  $b_{\mu\nu}(x, y)$  as an expansion in the basis of wave functions of tensor modes  $\Omega_n(y)$ ,

$$b_{\mu\nu}(x, y) = \sum_n b_{\mu\nu}^n(x) \Omega_n(y), \quad (23)$$

we obtain equations for the modes  $b_{\mu\nu}^n(x)$  and their wave functions  $\Omega_n(y)$ :

$$\square b_{\mu\nu}^n + M_n^2 b_{\mu\nu}^n = 0, \quad (24)$$

$$\begin{aligned} & \left\{ \frac{1}{2} \frac{\partial^2}{\partial y^2} + 2k[\delta(y) - \delta(y - L)] \right. \\ & \left. - 2k^2 + \frac{M_n^2}{2} \exp(2k|y|) \right\} \Omega_n(y) = 0. \end{aligned} \quad (25)$$

Equation (25) at  $M_n = 0$  has a simple solution,

$$\Omega_0 = N_0 \exp(-2k|y|), \quad (26)$$

where  $N_0$  is a constant that can be determined from the normalization condition by requiring the kinetic term to have a canonical form. Solutions with  $M_n \neq 0$  can be represented as a linear combination of the Bessel and Neumann functions

$$\Omega_n(y) = a_n J_2\left(\frac{M_n}{k} \exp(k|y|)\right) + b_n Y_2\left(\frac{M_n}{k} \exp(k|y|)\right). \quad (27)$$

The symmetry conditions at the points  $y = 0$  and  $y = L$  yield the relationship between the parameters  $a_n$  and  $b_n$ , as well as the relation between  $M_n$  and the zeros of the linear combination

$$Y_1\left(\frac{M_n}{k}\right) J_1\left(\frac{M_n}{k} \exp(kL)\right) - J_1\left(\frac{M_n}{k}\right) Y_1\left(\frac{M_n}{k} \exp(kL)\right) = 0. \quad (28)$$

Namely, representing  $M_n$  in the form

$$M_n = \beta_n k \exp(-kL) \quad (29)$$

and taking into account that  $\exp(-kL)$  is a small value (in many studies on the topic under consideration,  $kL$  is assumed to be approximately 30–35; see, for example, [48]), we make an expansion in Eqn (28) in terms of a small argument. We

obtain then for  $\beta_n$  an approximate equation

$$J_1(\beta_n) \approx 0. \quad (30)$$

The normalization condition for the kinetic terms of the fields yields another relation for the parameters  $a_n$  and  $b_n$ . As a result, for the wave functions and normalization constants we obtain the following formulas:

$$\Omega_n(y) = N_n \left[ Y_1(\beta_n k \exp(-kL)) J_2(\beta_n k \exp(k|y| - kL)) - J_1(\beta_n k \exp(-kL)) Y_2(\beta_n k \exp(k|y| - kL)) \right], \quad (31)$$

$$N_0 = \sqrt{\frac{k}{1 - \exp(-2kL)}}, \quad N_r = \sqrt{\frac{\exp(2kL) - 1}{3kL^2}}, \quad (32)$$

$$N_n = \sqrt{\frac{k}{\exp(2kL) f^2(\beta_n) - f^2(\beta_n \exp(-kL))}}, \quad (33)$$

where

$$f(x) \equiv Y_1\left(\frac{M_n}{k}\right) J_2(x) - J_1\left(\frac{M_n}{k}\right) Y_2(x).$$

After integrating over the fifth coordinate  $y$ , the effective four-dimensional action in the quadratic approximation in the fields  $b$  and  $r$  takes the form

$$S_{\text{eff}} = \int_{M_4} d^4x \left( \frac{1}{2} \eta^{\lambda\tau} \partial_\lambda r \partial_\tau r + \frac{1}{4} \sum_n \eta^{\alpha\beta} \eta^{\mu\nu} \times [\eta^{\lambda\tau} (\partial_\lambda b_{\alpha\mu}^n)(\partial_\tau b_{\beta\nu}^n) + M_n^2 b_{\alpha\mu}^n b_{\beta\nu}^n] \right). \quad (34)$$

We now take into account that, in the model under consideration, matter can only be located on branes. The interaction of metric fluctuations with matter fields has the standard form

$$S_{\text{int}} = \frac{\kappa}{2} \int_{M_4, y=0} h^{\mu\nu}(x, 0) T_{\mu\nu}^0 \sqrt{-\gamma_1} d^4x + \frac{\kappa}{2} \int_{M_4, y=L} h^{\mu\nu}(x, L) T_{\mu\nu}^L \sqrt{-\gamma_2} d^4x, \quad (35)$$

where  $\gamma_1$  and  $\gamma_2$  are the determinants of the background metric on the first and second branes, and  $T_{\mu\nu}^{0,L}$  is the energy-momentum tensor (EMT) of matter on branes at the points  $y = 0$  and  $y = L$ , respectively.

We now assume that our Universe is located on the first brane, and consider the interaction on it. We choose coordinates that are Galilean on this brane [23, 48], i.e., we have  $\sqrt{-\gamma_1} = 1$ . Substituting Eqns (18) and (23) into (35), we obtain the following expression for the first term in (35), which describes the action for the brane located at the point  $y = 0$ :

$$S_{\text{int}0} = \frac{1}{2} \int_{M_4} \left[ \kappa_0 b^{0\mu\nu} T_{\mu\nu} + \sum_{n=1}^{\infty} \kappa_n b^{n\mu\nu} T_{\mu\nu} - \kappa_r r T_\mu^\mu \right] d^4x, \quad (36)$$

where

$$\kappa_0 \equiv N_0 \kappa, \quad \kappa_n \equiv \Omega_n(0) \kappa \approx \frac{\exp(-kL)}{|J_2(\beta_n)|} N_0 \kappa, \quad (37)$$

$$\kappa_r \equiv \frac{\exp(-kL)}{\sqrt{3}} N_0 \kappa. \quad (38)$$

We now identify the massless tensor mode  $b_{\mu\nu}^0$  with the graviton. Since our Universe is located specifically on the first brane, to obtain the observable gravitational constant (Newton's constant) on it, the constant  $\kappa_0$  must be chosen equal to  $1/(2M_{\text{Pl}}^2)^{1/2}$ . Thus, we obtain a relationship between the fundamental five-dimensional mass  $M$  and the effective four-dimensional Planck mass

$$M_{\text{Pl}}^2 = \frac{1 - \exp(-2kL)}{k} M^3. \quad (39)$$

As we can see, for  $k \sim M$ , the quantities  $M_{\text{Pl}}$  and  $M$  must also be of the same order. In addition, the scales of interaction of the massless scalar and massive tensor modes with matter fields on this brane are suppressed by the factor  $\exp(-kL)$  compared to the gravitational one. Although this option is plausible, it is not satisfactory, since it does not provide a solution to the hierarchy problem.

We now consider the interaction on the second brane, located at the point with the coordinate  $y = L$ . Since we have chosen coordinates that are Galilean on the first brane, i.e., in which the constant  $C$  in metric (12) is set equal to 0, on the second brane these coordinates are not Galilean. The transition to Galilean coordinates  $\{z^\mu\}$  on the second brane is carried out using the substitution  $x^\mu = \exp(kL) z^\mu$ . In these coordinates, metric (12) corresponds to the value of the constant  $C = 2kL$ . The interaction with matter on the second brane then takes the form

$$S_{\text{int}L} = \frac{\kappa}{2} \int_{M_4, y=L} \exp(-2kL) h^{\mu\nu}(x, L) T_{\mu\nu}^L d^4z, \quad (40)$$

where indices are raised using the flat Minkowski metric. Thus, it is clear that, to find the interaction of five-dimensional gravity with matter on the second brane, it is necessary to switch to Galilean coordinates  $\{z^\mu\}$  also in the effective action (34). To do so, we also redefine the fields and masses of the tensor modes as follows:

$$r' = \exp(kL) r, \quad b_{\alpha\beta}^n = \exp(-kL) b_{\alpha\beta}^n, \quad M'_n = \exp(kL) M_n. \quad (41)$$

This is necessary to bring the kinetic terms of the fields in the action (34) to the canonical form. In the new coordinates, the second term in Eqn (35), describing the action for the second brane, takes the form

$$S_{\text{int}L} = \frac{1}{2} \int_{M_4} \left[ \kappa'_0 b_{\mu\nu}^{'0} T^{\mu\nu} + \sum_{n=1}^{\infty} \kappa'_n b_{\mu\nu}^{'n} T^{\mu\nu} - \kappa'_r r' T_\mu^\mu \right] d^4z, \quad (42)$$

where

$$\kappa'_0 = \exp(-kL) N_0 \kappa, \quad \kappa'_n = \exp(kL) \Omega_n(L) \kappa \approx -N_0 \kappa, \quad \kappa'_r = \frac{1}{\sqrt{3}} N_0 \kappa. \quad (43)$$

Similar to the case of the first brane above, we identify the massless tensor mode  $b_{\mu\nu}^{'0}$  with the graviton and assume that our Universe is now located on the second brane. By requiring that the gravitational constant on it coincide with the experimentally observed one, we find that on the second brane the relationship between the fundamental five-dimensional scale  $M$  and the effective four-dimensional scale  $M_{\text{Pl}}$  is

described by Eqn (7):

$$M_{\text{Pl}}^2 = \frac{\exp(2kL) - 1}{k} M^3. \quad (44)$$

In this case, for  $k \sim M$ , the value of  $M_{\text{Pl}}$  turns out to be approximately  $\exp(kL)$  times greater than that of  $M$ . Thus, if the condition  $kL \sim 30-35$  is satisfied, the observed extremely weak gravitational interaction arises at a value of the fundamental five-dimensional scale  $M$  of the order of several TeV. The values of  $\kappa'_n$  and  $\kappa'_r$  under the same assumptions turn out to be of the order of  $M^{-1}$ , i.e., of the order of  $\text{TeV}^{-1}$ . The masses of the lowest tensor modes  $M'_n = \beta_n k$  are also in the range of several TeV.

Finally, we note here that in studies [49, 50] a scenario was considered where the parameter  $k$  is much smaller than the multidimensional fundamental scale  $M$ . This approach leads to a significantly different phenomenology and is not considered here.

As we have already noted in the Introduction, to describe the interaction of matter with the KK-modes of the gravitational field on the brane at the point  $y = L$ , L. Randall and R. Sundrum used in the original study [20] the coordinates that were Galilean on the brane at  $y = 0$ . As a result, it turned out that the fundamental energy scale of the theory is the Planck mass, as it should be on the brane at  $y = 0$ , and the masses of the lowest KK-modes can be of the order of several TeV due to the cutting-off exponential factor. Rubakov was the first to note that such an approach is incorrect [12], because any theory must be described in coordinates that are Galilean on the observer's brane. Subsequently, it was shown in [23] that the fundamental energy scale on the brane at the point  $y = L$  is of the order of several TeV, and the Planck scale is a derivative and appears due to the exponential factor in the metric. In the absolute majority of studies of the RS model, the authors, following [20], use an incorrect physical interpretation of this model. Nevertheless, the results of such studies usually coincide with those obtained using a physically correct interpretation of the model.

Thus, in the unstabilized RS model, the hierarchy between the gauge and gravitational scales of interactions arises in a natural way. Nevertheless, such a model cannot be considered physically adequate, since the 4D scalar mode arising in it — radion — which describes the relative motion of branes [24], is massless. Indeed, it is easy to show that

$$\int_0^L ds = \int_0^L \sqrt{-g_{44}} dy \approx \left(1 - \frac{N_r}{\sqrt{2}M^3} r\right) L = L - \sqrt{\frac{M_{\text{Pl}}^2}{6M^6}} r. \quad (45)$$

Equation (45) apparently shows that the radion field  $r(x)$  determines the physical distance between the branes. However, the radion being massless implies that, at least in the lowest order, the system must be unstable with respect to small fluctuations; in other words, the distance between the branes is not fixed. Due to this circumstance and the fact that a massless field interacting with the SM fields on the TeV scale would have already been detected experimentally, this model is phenomenologically unacceptable.

### 3. Stabilized Randall–Sundrum model

The above-mentioned shortcomings were removed in the so-called stabilized brane world model (stabilized RS model) [25, 26]. In it, as in the unstabilized RS model, spacetime has

five dimensions, and topologically the fifth dimension is an orbifold. In the 4D space between two branes located at the points 0 and  $L$ , in addition to the gravitational field, a scalar Goldberger–Wise field  $\phi$  propagates, which minimally interacts with the gravitational field. It has some five-dimensional self-interaction potential and certain four-dimensional potentials on the branes. The SM fields are localized on the brane located at the point  $y = L$ . The five-dimensional action in such a model has the form

$$\begin{aligned} S &= S_1 + S_2, \\ S_1 &= \int_{M_4} \int_{-L}^L \left( -2M^3 R + \frac{1}{2} g^{MN} \partial_M \phi \partial_N \phi - V(\phi) \right) \sqrt{g} d^5 x, \\ S_2 &= \int_{M_4} \int_{-L}^L \left[ -\lambda_1(\phi) \delta(y) + (L_{\text{SM}} - \lambda_2(\phi)) \delta(y-L) \right] \sqrt{-g} d^5 x, \end{aligned} \quad (46)$$

where  $V(\phi)$  is the five-dimensional potential of the scalar field,  $\lambda_1(\phi)$  and  $\lambda_2(\phi)$  are additional potentials of the scalar field on the branes, and  $L_{\text{SM}}$  is the Lagrangian of the SM fields. For the gravitational field, account of the orbifold symmetry, as in the case of the unstabilized RS model, sets conditions of the form (8) and, for the scalar field, the condition

$$\phi(x, -y) = \phi(x, y). \quad (47)$$

Action (46) yields the following equations of motion:

$$\begin{aligned} -\frac{1}{2M^3} \frac{1}{\sqrt{-g}} \frac{\delta S}{\delta g^{MN}} &= G_{MN} - \frac{1}{4M^3} T_{MN} = 0, \\ -\frac{1}{\sqrt{-g}} \frac{\delta S}{\delta \phi} &= \square \phi + \frac{dV}{d\phi} + \left[ \frac{d\lambda_1}{d\phi} \delta(y) + \frac{d\lambda_2}{d\phi} \delta(y-L) \right] = 0, \end{aligned} \quad (48)$$

where  $G_{MN}$  is the five-dimensional Einstein tensor, and  $T_{MN}$  is the energy–momentum tensor of the scalar field, defined as follows:

$$\begin{aligned} T_{MN} &\equiv \frac{2}{\sqrt{-g}} \frac{\delta S_\phi}{\delta g^{MN}} = \partial_M \phi \partial_N \phi - g_{MN} \left( \frac{1}{2} g^{PQ} \partial_P \phi \partial_Q \phi - V(\phi) \right) \\ &\quad + [\lambda_1(\phi) \delta(y) + \lambda_2(\phi) \delta(y-L)] g_{\mu\nu} \delta_M^\mu \delta_N^\nu. \end{aligned} \quad (50)$$

It was shown in [26] that the background solutions of equations of motion (48) and (49) with energy–momentum tensor (50) should be sought in the form

$$\begin{aligned} g_{\mu\nu}(x, y) &\equiv \bar{g}_{\mu\nu}(y) = \exp(-2A(y)) \eta_{\mu\nu}, \\ g_{4\mu} &= 0, \quad g_{44} = -1, \quad \phi(x, y) = \bar{\phi}(y). \end{aligned} \quad (51)$$

In this case, the following equations are obtained for the functions  $A(y), \bar{\phi}(y)$ :

$$\frac{dV(\bar{\phi})}{d\bar{\phi}} + \frac{d\lambda_1}{d\bar{\phi}} \delta(y) + \frac{d\lambda_2}{d\bar{\phi}} \delta(y-L) = -4A' \bar{\phi}' + \bar{\phi}'', \quad (52)$$

$$12M^3 (A')^2 + \frac{1}{2} \left( V - \frac{1}{2} (\bar{\phi}')^2 \right) = 0, \quad (53)$$

$$\begin{aligned} \frac{1}{2} \left( \frac{1}{2} (\bar{\phi}')^2 + V(\bar{\phi}) + \lambda_1 \delta(y) + \lambda_2 \delta(y-L) \right) \\ = -2M^3 (-3A'' + 6(A')^2). \end{aligned} \quad (54)$$

Study [51] also showed that, for a certain choice of potentials, the background solutions for the functions  $A(y)$ ,  $\bar{\phi}(y)$  have the form

$$\bar{\phi}(y) = \phi_0 \exp(-2u|y|), \quad (55)$$

$$A(y) = k|y| + \frac{\phi_0^2}{48M^3} \exp(-2u|y|) - \left( kL + \frac{\phi_0^2}{48M^3} \exp(-2uL) \right). \quad (56)$$

In Eqn (56), the term in parentheses is simply the integration constant, which is specifically chosen in such a way that the 4D coordinates  $x^\mu$  on the brane located at the point  $y = L$  are Galilean. The constants  $k$ ,  $u$ , and  $\phi_0$  contained in the solution given by Eqns (51), (55), and (56) are uniquely expressed through the parameters of the potentials  $V$ ,  $\lambda_1$ ,  $\lambda_2$ ; however, for further analysis, it is more convenient to express the potentials through these constants:

$$V(\phi) = -24M^3k^2 + \frac{(u+4k)u}{2} \phi^2 - \frac{u^2}{24M^3} \phi^4, \quad (57)$$

$$\lambda_1 = 24M^3k - u\phi_0^2 - 2u\phi_0(\phi - \phi_0) + \beta_1^2(\phi - \phi_0)^2, \quad (58)$$

$$\lambda_2 = 24M^3k - u\phi_L^2 - 2u\phi_L(\phi - \phi_L) + \beta_2^2(\phi - \phi_L)^2, \quad (59)$$

where

$$\phi_L \equiv \phi_0 \exp(-uL).$$

Assuming now that the solution (51), (55), and (56) is the background one, we consider small fluctuations  $h_{MN}(x, y)$  and  $f(x, y)$  of the gravitational and scalar fields, respectively, above this background. We present the gravitational and scalar fields in the lowest order in the five-dimensional gravitational coupling constant as the following expansion:

$$g_{MN}(x, y) = \bar{g}_{MN}(y) + \kappa h_{MN}(x, y), \quad (60)$$

$$\phi(x, y) = \bar{\phi}(y) + \kappa f(x, y). \quad (61)$$

Presented in [51] is a Lagrangian quadratic in small fluctuations  $h$  and  $f$  and the equations of motion that follow from it. In addition, it is shown in [51] that a gauge exists in which the equations of motion are decoupled. As a result, independent equations are obtained for the tensor, vector, and scalar components, where the tensor and scalar components are physical degrees of freedom, while the vector components can be turned to zero, i.e., they are a pure gauge. In such a gauge, the fields can be represented as follows:

$$h_{\mu\nu} = b_{\mu\nu} - \frac{1}{2} \eta_{\mu\nu} \varphi, \quad h_{44} = \exp(2A) \varphi, \quad h_{4\mu} = 0, \quad (62)$$

$$f = \frac{3}{2} \frac{\exp(2A)}{\kappa^2 \bar{\phi}'} \varphi',$$

where the tensor field  $b_{\mu\nu}$  is transverse-traceless, and the prime sign denotes the derivative with respect to the fifth coordinate  $y$ . The equations for the tensor field  $b_{\mu\nu}$  and the scalar field  $\varphi$  have the following form:

$$\frac{1}{2} (\square b_{\mu\nu} + b_{\mu\nu}'' - (2A'^2 - A'') b_{\mu\nu}) = 0, \quad (63)$$

$$\varphi'' + 2 \left( A' - \frac{\bar{\phi}''}{\bar{\phi}'} \right) \varphi' - \frac{\kappa^2 (\bar{\phi}')^2}{3} \varphi - \square \varphi = 0. \quad (64)$$

Expanding the fields  $b_{\mu\nu}(x, y)$  and  $\varphi(x, y)$  in bases of the wave functions  $\Omega_n(y)$  and  $\Psi_n(y)$ , respectively, we obtain the so-called Kaluza–Klein towers:

$$b_{\mu\nu}(x, y) = \sum_{n=0}^{\infty} b_{\mu\nu}^n(x) \Omega_n(y), \quad (65)$$

$$\varphi(x, y) = \sum_{n=1}^{\infty} \varphi_n(x) \Psi_n(y). \quad (66)$$

In expansion (65) the summation starts from  $n = 0$  to emphasize the presence of the zero (massless) mode with  $\Omega_0 = N_0 \exp(-2A)$  ( $N = 0$  is a normalization factor). It is seen that the term with the zero mode  $b_{\mu\nu}^0 \Omega_0 = b_{\mu\nu}^0 N_0 \exp(-2A)$  has the same structure as the background metric  $\bar{g}_{\mu\nu} = \eta_{\mu\nu} \exp(-2A)$ , so these two terms can be combined, which is equivalent to passing from a flat 4D background to a curved one. The effective 4D action describing such a background exactly coincides with the 4D scalar curvature [52], so the effective 4D gravity in the stabilized RS model coincides with the gravity of general relativity.

Although all scalar modes are massive, the lightest of them can have a mass of the order of the SM energy scale (i.e., much smaller than the masses of the other modes). The equation for the wave functions of the scalar modes  $\Psi_n$  is

$$\left( \frac{\exp(2A)}{(\bar{\phi}')^2} \Psi_n' \right)' - \frac{\kappa^2 \exp(2A)}{3} \Psi_n + m_n^2 \frac{\exp(4A)}{(\bar{\phi}')^2} \times \left( 1 + \frac{2}{\beta_1^2 + u} \delta(y) + \frac{2}{\beta_2^2 - u} \delta(y - L) \right) \Psi_n = 0. \quad (67)$$

The solutions of Eqn (67)—the functions  $\Psi_n(y)$ —form a complete orthogonal system, which can be normalized as follows:

$$\frac{9m_n^2}{4\kappa^2} \int_{-L}^L dy \frac{\exp(4A)}{(\bar{\phi}')^2} \left( 1 + \frac{2}{\beta_1^2 + u} \delta(y) + \frac{2}{\beta_2^2 - u} \delta(y - L) \right) \times \Psi_n \Psi_m = \delta_{nm}. \quad (68)$$

In the approximation of small  $uL$  in Eqns (55) and (56) for the quantities  $A(y)$  and  $\bar{\phi}(y)$ , the exponentials  $\exp(-2u|y|)$  and  $\exp(-2uL)$  can be expanded in a series, retaining in the expansion only the terms linear in  $|y|$  and  $L$ :

$$A(y) \approx \tilde{k}(|y| - L), \quad \bar{\phi}(y) \approx \phi_0(1 - u|y|), \quad (69)$$

where

$$\tilde{k} \equiv k - \frac{u}{12} \kappa^2 \phi_0^2.$$

For the wave functions of the tensor modes  $\Omega_n$ , such an expansion yields an equation similar to Eqn (25) in the unstabilized RS model, in which the symbol  $k$  is replaced by the symbol  $\tilde{k}$ :

$$\left\{ \frac{1}{2} \frac{\partial^2}{\partial y^2} + 2\tilde{k} [\delta(y) - \delta(y - L)] - 2\tilde{k}^2 + \frac{M_n^2}{2} \exp(2\tilde{k}|y|) \right\} \times \Omega_n = 0. \quad (70)$$

To derive a similar equation for the wave functions of the scalar modes  $\Psi_n$ , we substitute the approximate expressions



(69) for the quantities  $A(y)$  and  $\bar{\phi}(y)$  into Eqn (67) and move to the variable  $z = \exp(-\tilde{k}(L-y)) m_n/\tilde{k}$ . As a result, we obtain in the interval  $z \in (m_n \exp(-\tilde{k}L)/\tilde{k}, m_n/\tilde{k})$  an equation of the form

$$\frac{d^2 \Psi_n}{dz^2} + \left(3 + \frac{2u}{\tilde{k}}\right) \frac{1}{z} \frac{d\Psi_n}{dz} + \left(1 - \frac{b^2}{z^2}\right) \Psi_n = 0, \quad (71)$$

where

$$b^2 \equiv \frac{\kappa^2 \phi_0^2}{3} \frac{u^2}{\tilde{k}^2}.$$

The symmetry conditions at the ends of the interval  $z \in (m_n \exp(-\tilde{k}L)/\tilde{k}, m_n/\tilde{k})$ , i.e., at the points of the brane locations  $y = 0$  and  $y = L$ , provide the boundary conditions that the solutions of Eqn (71) must satisfy:

$$\begin{aligned} \left( \tilde{k} z^2 \Psi_n + (\beta_0^2 + u) z \frac{d\Psi_n}{dz} \right) \Big|_{z=m_n \exp(-\tilde{k}L)/\tilde{k}} &= 0, \\ \left( \tilde{k} z^2 \Psi_n - (\beta_L^2 - u) z \frac{d\Psi_n}{dz} \right) \Big|_{z=m_n/\tilde{k}} &= 0. \end{aligned} \quad (72)$$

The solution of Eqn (71) per se can be expressed through a linear combination of Bessel functions:

$$\Psi_n = z^{-1-u/\tilde{k}} (B_n J_\alpha(z) + C_n J_{-\alpha}(z)), \quad (73)$$

where

$$\alpha = \sqrt{\left(1 + \frac{u}{\tilde{k}}\right)^2 + b^2}.$$

If we now assume that the fundamental five-dimensional parameter  $M$  has a value of the order of several TeV, we obtain, as in the unstabilized RS model, the observed effective 4D constant of gravitational interaction, provided  $\tilde{k} \sim M$  and  $\tilde{k}L \sim 35$ . Therefore, since  $m_n/\tilde{k} \ll \exp(\tilde{k}L) \sim 10^{15}$ , the first boundary condition from system (72) yields the relation

$$\begin{aligned} C_n &\approx \frac{\alpha - 1 - u/\tilde{k}}{\alpha + 1 + u/\tilde{k}} \frac{\Gamma(1-\alpha)}{2\Gamma(1+\alpha)} \left( \frac{m_n}{2\tilde{k}} \exp(-\tilde{k}L) \right)^{2\alpha} B_n \\ &\sim 4 \times 10^{-31} \exp[-70(\alpha-1)] \frac{\alpha - 1 - u/\tilde{k}}{\alpha + 1 + u/\tilde{k}} \frac{\Gamma(1-\alpha)}{2\Gamma(1+\alpha)} \\ &\quad \times \left( \frac{m_n}{2\tilde{k}} \right)^{2\alpha} B_n. \end{aligned} \quad (74)$$

Equation (74) apparently shows that the constants  $C_n$  are strongly suppressed compared to the constants  $B_n$ ; therefore, the contribution of the second term in Eqn (73) can be disregarded. Indeed, even on the right boundary of the interval, where  $J_{-\alpha}$  increases like  $z^{-\alpha}$ , the functions  $\Psi_n$  can be approximated as

$$\Psi_n \approx B_n \frac{z^{\alpha-1-u/\tilde{k}}}{2^\alpha \Gamma(1+\alpha)} \left[ 1 + \frac{1}{2} \exp(-2\alpha\tilde{k}L) \frac{\alpha - 1 - u/\tilde{k}}{\alpha + 1 + u/\tilde{k}} \right]. \quad (75)$$

The second term in square brackets in Eqn (75) is the contribution from  $C_n J_{-\alpha}$ . Apparently, it is much smaller than the contribution from the first term; therefore, the second term in Eqn (73) can be ignored over the entire interval. The value of the parameter  $B_n$  can be determined from the normalization condition (see, for example, [52]).

The second boundary condition in (72) yields the mass spectrum of scalar modes:

$$\left( 1 + \alpha + \frac{u}{\tilde{k}} + \frac{1}{\beta_L^2 - u} \frac{m_n^2}{\tilde{k}} \right) J_\alpha \left( \frac{m_n}{\tilde{k}} \right) - \frac{m_n}{\tilde{k}} J_{\alpha-1} \left( \frac{m_n}{\tilde{k}} \right) = 0. \quad (76)$$

Depending on the values of the remaining parameters, this equation can have a solution arbitrarily close to zero, obviously corresponding to the light mode. If its mass satisfies the condition  $m_1^2 \ll \tilde{k}^2$ , in Eqn (76), we can expand the Bessel functions in a series and derive an approximate formula for the mass of the radion, i.e., the lightest mode:

$$m_1^2 = m_r^2 \approx \frac{2}{3} \frac{(\beta_L^2 - u)u^2}{\beta_L^2 + 4\tilde{k}} \kappa^2 \phi_0^2. \quad (77)$$

The next zeros in formula (76) give masses of the order of  $\tilde{k}$  for the remaining scalar modes, and for sufficiently large  $n$  we obtain an approximate formula for the masses of scalar modes,

$$m_n^2 \approx \pi^2 \tilde{k}^2 n^2. \quad (78)$$

Thus, similar to the unstabilized RS model, we obtain the reduced action of the stabilized model in the linear approximation in the form

$$\begin{aligned} S_{\text{eff}} &= -\frac{1}{4} \sum_k \int dx (\partial^\sigma b^{k\mu\nu} \partial_\sigma b_{\mu\nu}^k + M_k^2 b^{k\mu\nu} b_{\mu\nu}^k) \\ &\quad - \frac{1}{2} \sum_k \int dx (\partial_\nu \varphi_k \partial^\nu \varphi_k + m_k^2 \varphi_k \varphi_k). \end{aligned} \quad (79)$$

In the stabilized RS model, the analysis of the interaction of tensor and scalar modes with matter on branes is generally similar to that in the unstabilized RS model. In the first order in the gravitational constant  $\kappa$  for the brane located at the point  $y = L$ , we arrive at the formula

$$S_{\text{int}L} = \frac{1}{2} \int_{M_4} \left[ \kappa_0 b^{0\mu\nu} T_{\mu\nu} + \sum_{n=1}^{\infty} \kappa_n b^{n\mu\nu} T_{\mu\nu} - \sum_{n=1}^{\infty} \kappa_{rn} \varphi_n T_\mu^\mu \right] d^4x, \quad (80)$$

where for each tensor and scalar mode its own coupling constant is obtained:

$$\kappa_0 = \Omega_0(L)\kappa, \quad \kappa_n = \Omega_n(L)\kappa, \quad (81)$$

$$\kappa_{rn} = \Psi_n(L)\kappa. \quad (82)$$

If Galilean coordinates are chosen on the brane located at the point  $y = L$ , the normalized tensor wave functions have the forms  $\Omega_0(L) \approx \sqrt{\tilde{k}} \exp(-\tilde{k}L)$  and  $\Omega_n(L) \approx -\sqrt{\tilde{k}}$ . Then, as was the case in the unstabilized RS model, we obtain the following formula for the coupling constants:

$$\kappa_0 \approx \exp(-\tilde{k}L) \sqrt{\tilde{k}} \kappa, \quad \kappa_n \approx -\exp(\tilde{k}L) \kappa_0. \quad (83)$$

In a completely similar way, we derive the formula for the wave functions of scalar modes on the brane:

$$\Psi_n(L) \approx \frac{1}{2} B_n \left( \frac{m_n}{\tilde{k}} \right)^{-1-u/\tilde{k}} J_\alpha \left( \frac{m_n}{\tilde{k}} \right). \quad (84)$$

As for the formula for the coupling constant of the light scalar mode to the SM fields, it is considered in Section 6, devoted to nonlinear interactions of the radion. Here, we note that, with the range of model parameters chosen above,  $\Lambda \equiv \kappa_{r1}^{-1}$  can easily take values in the range of several TeV.

Thus, in the RS model, a hierarchy naturally arises between the scales of 4D gravitational and gauge interactions. In addition to the massless graviton and an infinite number of heavy tensor modes interacting with the matter EMT with coupling constants of the order of the 4D Planck constant, the unstabilized version of the model contains one massless scalar mode, called the radion, interacting with a trace of the matter EMT with an interaction constant of the order of the fundamental multidimensional scale. This fundamental scale also determines the scale of interaction of the 4D gauge fields and can lie in the range of several TeV. In the stabilized RS model, the hierarchy between the gravitational and gauge energy scales is obtained in a way similar to the unstabilized version of the RS model. However, the effective four-dimensional scalar sector of the stabilized RS model contains an infinite number of massive modes instead of one massless field. The masses of such fields (except, perhaps, the lightest one) start with the values of the order of the multidimensional fundamental scale. The lightest mode can have a mass an order of magnitude smaller (hundreds of GeV), and its interaction with matter fields has a form similar to that in the unstabilized RS model. It should also be noted that the coupling constant of the radion to matter in the stabilized RS model is several times smaller than the similar constant in the unstabilized RS model.

#### 4. Phenomenology of Kaluza–Klein excitations

As already noted in the Introduction, the most noticeable phenomenological implication of the stabilized RS model is the existence of infinite KK towers of tensor and scalar particles with zero SM quantum numbers, which interact in a universal way with all fields of this model with coupling constants of the order of several inverse TeV. Such particles could be produced with a significant cross section in pp collisions at the LHC collider should the energy of this collider be higher than the threshold for the production of KK excitations. If the collider energy is below the threshold of production of even the lowest KK excitation, the interactions generated by the exchange of virtual KK excitations will be reduced with a high accuracy to additional contact interactions of the SM fields and will yield corrections to the collider processes. In this case, the experimental situation may resemble the situation with weak interactions at the times when the energies accessible with accelerators were much lower than the threshold of production of intermediate vector bosons, and weak interactions were described by the four-fermion Fermi interaction. We first consider specifically this option.

The use of contact interactions or effective operators of higher dimensions is a well-known model-independent method for parameterizing possible deviations from the SM, which was proposed in [58–61] and is currently widely used in effective field theories. Such operators are introduced in a fairly arbitrary way in phenomenological extensions of the SM, and the only restriction on their form is usually the requirement to preserve the symmetries of the latter. Experimental verification of the presence of a contribution from such operators to the cross sections of various processes in

hadron and lepton colliders may provide either indications of the manifestation of physics beyond the SM or only constraints on the parameters of the effective Lagrangians (see, for example, [62–65]). However, this would involve a large number of admissible effective operators, each with its own coupling constant, which would significantly complicate extraction of a large number of parameters from experimental data.

At the same time, models with extra dimensions, considered in the energy range below the threshold for the production of KK excitations, lead to effective operators of a certain structure. In particular, the contact interactions arising in such models are universal in the sense that they are characterized by only one dimensional constant. Experimental observation of such contact interactions could be a strong argument in favor of models with large extra dimensions. Following [100], we present such an approach in the stabilized RS model, which also allows taking into account the scalar component of multidimensional gravity.

To do so, we consider a theory with action

$$S = S_{\text{eff}} + S_{\text{intL}} + S_{\text{SM}}, \quad (85)$$

where  $S_{\text{eff}}$  is defined in (79),  $S_{\text{intL}}$  is defined in (80), and  $S_{\text{SM}}$  denotes the SM action, with  $T^{\mu\nu}$  in (80) being the SM energy–momentum tensor. It is easy to see that this theory is in fact a linear approximation of the RS model, which also ignores the interaction of KK modes with each other, considered weaker than their interaction with SM fields.

The free fields in such a theory can be quantized in the standard way, with the KK mode propagators having the form

$$D_{\mu\nu, \rho\sigma}^k(p) = -\frac{b_{\mu\nu, \rho\sigma}^k(p)}{p^2 + M_k^2 - i\epsilon}, \quad (86)$$

$$\begin{aligned} b_{\mu\nu, \rho\sigma}^k(p) &= \left( \eta_{\mu\rho} + \frac{p_\mu p_\rho}{M_k^2} \right) \left( \eta_{\nu\sigma} + \frac{p_\nu p_\sigma}{M_k^2} \right) + \left( \eta_{\mu\sigma} + \frac{p_\mu p_\sigma}{M_k^2} \right) \\ &\quad \times \left( \eta_{\nu\rho} + \frac{p_\nu p_\rho}{M_k^2} \right) - \frac{2}{3} \left( \eta_{\mu\nu} + \frac{p_\mu p_\nu}{M_k^2} \right) \left( \eta_{\rho\sigma} + \frac{p_\rho p_\sigma}{M_k^2} \right), \\ D^k(p) &= -\frac{1}{p^2 + m_k^2 - i\epsilon}. \end{aligned} \quad (87)$$

If we consider the theory with action (85) in the region of energies or momentum transfers much smaller than the masses of the KK excitations  $M_k$ , and  $m_k$ , we can progress to an effective ‘low-energy’ theory, which can be obtained using a standard procedure. Namely, we can omit the momentum dependence in the heavy mode propagators and integrate over these modes in the functional integral constructed based on action (85). As a result, we obtain Lagrangians of contact interactions generated by tensor degrees of freedom,

$$L_T = \frac{1}{8M^3} \left( \sum_{n>0} \frac{\Omega_n^2(L)}{M_n^2} \right) T^{\mu\nu} \Delta_{\mu\nu, \rho\sigma} T^{\rho\sigma}, \quad (88)$$

$$\Delta_{\mu\nu, \rho\sigma} = \frac{1}{2} b_{\mu\nu, \rho\sigma}^k(p)|_{p=0} = \frac{1}{2} \eta_{\mu\rho} \eta_{\nu\sigma} + \frac{1}{2} \eta_{\mu\sigma} \eta_{\nu\rho} - \frac{1}{3} \eta_{\mu\nu} \eta_{\rho\sigma}, \quad (89)$$

and scalar degrees of freedom

$$L_S = \frac{1}{64M^3} \left( \sum_n \frac{\Psi_n^2(L)}{m_n^2} \right) T_\mu^\mu T_\nu^\nu, \quad (90)$$

where  $M$  is the fundamental five-dimensional energy scale.

The effective coupling constants

$$\frac{1}{8M^3} \left( \sum_n \frac{\Omega_n^2(L)}{M_n^2} \right), \quad \frac{1}{64M^3} \left( \sum_n \frac{\Psi_n^2(L)}{m_n^2} \right)$$

in this model can be estimated as follows. In [51], it was shown that in the stabilized RS model it is more convenient to use the parameters  $\tilde{k}$  (69),  $b$  (71), and  $L$  instead of  $\phi_0$ ,  $\phi_L$ , and  $k$ . Also, in Section 3 of this review, it was shown that for  $uL \ll 1$  the metric of the stabilized model virtually coincides with that of the unstabilized model with the inverse anti-de Sitter radius  $\tilde{k}$  instead of  $k$ , and analytical solutions for the wave functions of the tensor and scalar modes and their mass spectra can be found.

In the specified range of values of the model parameters, the spectrum of tensor excitations is presented fairly accurately by solutions of the equation

$$J_1\left(\frac{M_n}{\tilde{k}}\right) = 0,$$

and, in the approximation of an infinitely stiff potential on a brane at  $y = L$ , we obtain  $\Omega_n|_{y=L} = \sqrt{\tilde{k}}$  (see [23, 51]). In this case, the sum over the tensor modes in Eqn (88) can be estimated as

$$\frac{1}{8M^3} \sum_{n>0} \frac{\Omega_n^2(L)}{M_n^2} \approx \frac{1.82}{\Lambda_\pi^2 M_1^2},$$

where we introduced the coupling constant of the first KK resonance  $A_\pi$  and its mass  $M_1$ :

$$\frac{1}{A_\pi} = -\frac{\Omega_1(L)}{\sqrt{8M^3}}, \quad M_1 = 3.83\tilde{k}.$$

It should be noted that the contribution of the first KK resonance to this sum is exactly  $1/\Lambda_\pi^2 M_1^2$ , while the value 1.82 is determined by the nonfactorizable spacetime geometry of the RS model. For example, for a factorizable geometry with a space of extra dimension  $S^1$ , we would get instead

$$\sum_{n=1}^{\infty} \frac{1}{n^2} \equiv \zeta(2) = \frac{\pi^2}{6}.$$

It is also easy to verify that

$$-\frac{\Omega_n(L)}{\sqrt{8M^3}} \approx \frac{1}{A_\pi}$$

for sufficiently small  $n$ .

In this parameterization, often applied in the RS model, the effective Lagrangian takes the form

$$L_{\text{eff}} = L_T + L_S = \frac{1.82}{\Lambda_\pi^2 M_1^2} T^{\mu\nu} \tilde{A}_{\mu\nu, \rho\sigma} T^{\rho\sigma}, \quad (91)$$

$$\tilde{A}_{\mu\nu, \rho\sigma} = \frac{1}{2} \eta_{\mu\rho} \eta_{\nu\sigma} + \frac{1}{2} \eta_{\mu\sigma} \eta_{\nu\rho} - \left( \frac{1}{3} - \frac{\delta}{2} \right) \eta_{\mu\nu} \eta_{\rho\sigma}, \quad (92)$$

where the constant  $\delta$  takes into account the contribution of scalar modes and, according to the results of Section 3, is approximately equal to 0.7 [100].

As we have already noted, such an interaction Lagrangian generates well-defined processes with SM fields, which are determined by the structure of its energy–momentum tensor  $T^{\mu\nu}$ , the sum of the energy–momentum tensors of the free SM fields and the contribution of the interaction terms proportional to the SM coupling constants. The energy–momentum tensors of free SM fields, which are quadratic in the fields, are presented in an explicit form in [100].

For free massless fields, the trace of the energy–momentum tensor is zero, and the scalar degrees of freedom do not contribute to the effective interaction. They can contribute to such an interaction only if the conformal anomaly of massless fields is taken into account. The anomalous part of the energy–momentum tensor turns out to be

$$\Delta T_{\mu\nu} = \frac{\beta(g)}{6g} \left( \eta_{\mu\nu} - \frac{\partial_\mu \partial_\nu}{\square} \right) F_{\rho\sigma} F^{\rho\sigma},$$

which leads to the well-known formula for the anomalous trace of this tensor

$$\Delta T_\mu^\mu = \frac{\beta(g)}{2g} F_{\rho\sigma} F^{\rho\sigma},$$

where  $\beta(g)$  is the beta function. The structure of this anomalous contribution to the energy–momentum tensor is such that the interaction via tensor particle exchange in Eqn (88) disappears, and only the interaction via scalar particle exchange (90) persists. However, this anomalous interaction turns out to be suppressed compared to the interaction via tensor particle exchange, because the trace of the energy–momentum tensor is proportional to the particle mass, which is much smaller than both  $M_1$ , and  $A_\pi$ . Therefore, the observation of the scalar component of the effective interaction is most likely possible only due to the mixing of the Higgs and radion fields [72, 73, 85] (this issue is discussed below in Section 7).

Thus, in the lowest nonvanishing order in the SM coupling constants, the effective Lagrangian (91) is a sum of four-particle effective operators (not only four-fermion ones, but also those corresponding to the interaction of two fermions and two vector particles, four vector particles, etc.). Experimental observation of production processes that follow from the effective Lagrangian (91) or constraints on their cross sections allows one to estimate the multidimensional fundamental energy scale  $M$ , provided theoretical estimates for the product of the parameters  $M_1$  and  $A_\pi$  in (91) can be obtained. Their ratio can be evaluated based on the fact that the width of the first KK resonance must be smaller than its mass.

As noted above, in the lowest order in SM couplings, the effective Lagrangian includes a sum of various four-particle effective operators (not only four-fermion, but also two-fermion–two-boson and four-boson), which are invariant under the SM gauge group and lead to a well-defined phenomenology. Such a Lagrangian contains only three free parameters,  $A_\pi$ ,  $M_1$ , and  $\delta$ , where  $A_\pi$  and  $M_1$  parameterize the overall coupling and  $\delta$  characterizes the relative contribution of the scalar field radion (or a set of scalar fields, as is the case in the stabilized RS model). Some interesting points are worth noting.

First and foremost, the lowest order only involves neutral currents of particles from the same SM generation. Such new interactions do not lead to additional decay modes. New possible decays of SM particles following from a given effective Lagrangian can only arise in the next order in the SM couplings, when charged currents appear in the energy–momentum tensor. The new effective four-particle operators obtained from the energy–momentum tensor do not lead to flavor-changing neutral currents either. In the tree approximation, the effective Lagrangian leads to a number of processes that appear in the SM only at the loop level:  $gg \rightarrow l^+l^-$ ,  $gg \rightarrow ZZ (W^+W^-)$ ,  $e^+e^- \rightarrow gg$ ,  $\gamma\gamma \rightarrow gg$ , etc. Study [100] presents analytical expressions for the differential cross sections of these processes, taking into account the nonzero masses of the particles in the final state. In the case of massless fermions, these formulas for the total and differential cross sections of the Drell–Yan processes  $gg \rightarrow l^+l^-$  and  $q\bar{q} \rightarrow l^+l^-$  are in complete agreement with the formulas reported in [101–103].

The scalar radion also contributes to the production of massive particles by colliding gluons. This contribution, which is calculated using Eqns (91) and (92), turns out to be proportional to the parameter  $\delta^2$  of order 1 and the anomalous trace coefficient  $(b(g_s)/2g_s)^2$ ; numerically, it turns out to be approximately 1% of the contribution from the tensor modes.

Following study [100] again, we present below the results of numerical calculations of the Drell–Yan processes, because this channel is most sensitive to new physics. Such analytical and numerical calculations, including modeling of the SM background in a gedankenexperiment for the LHC, were carried out using a version of the CompHEP package [89] developed on the basis of the FORM symbolic computing package [104]. This version of the CompHEP package incorporates Feynman rules obtained from the derived effective Lagrangian, which allows using the code for generating events and subsequently for analyzing data under real experimental conditions.

Using the standard criterion  $\chi^2$ , which takes into account systematic errors (characteristic detector resolution, uncertainties related to the factorization/normalization scales of the QCD and PDF distribution functions, errors in measuring the electroweak parameters and luminosity) and statistical uncertainties in the SM dilepton invariant mass distribution, we estimated experimental constraints on the coupling constant parameter with 95% confidence that can be achieved at the LHC for two values of the integrated luminosity:

$$\begin{aligned} 50 \text{ fb}^{-1} : \frac{0.91}{\Lambda_\pi^2 M_1^2} &< 0.00164 \text{ TeV}^{-4}, \\ 100 \text{ fb}^{-1} : \frac{0.91}{\Lambda_\pi^2 M_1^2} &< 0.0014 \text{ TeV}^{-4}. \end{aligned} \quad (93)$$

It is seen that these constraints slowly weaken with increasing luminosity.

Figure 1 shows the distributions for (standard) SM and SM taking into account the contribution of KK gravitons, corresponding to the maximum luminosity value in Eqn (93) and also taking into account the subprocess  $gg \rightarrow \mu^+\mu^-$ . We see that, in the RS model, the exchange with a tower of KK gravitons in the energy region below the threshold of their production leads to a rise in the tail of the distribution of the invariant mass of the produced particles; this was pointed out

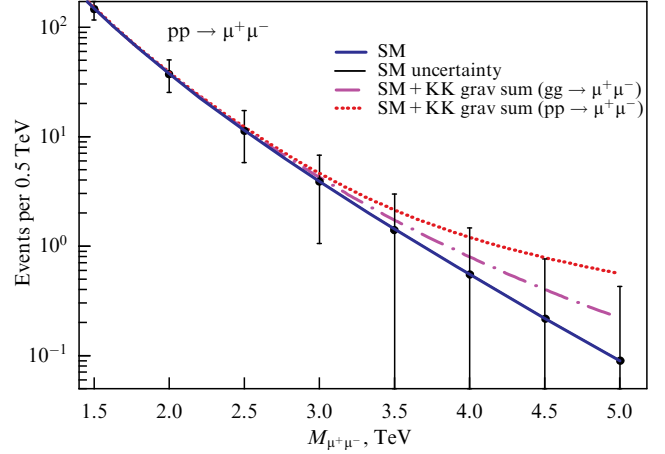


**Figure 1.** Distribution of invariant mass of dileptons at a 95% confidence level of parameter  $0.91/(\Lambda_\pi^2 M_1^2) = 0.0014 \text{ TeV}^{-4}$  for the LHC accelerator ( $L = 100 \text{ fb}^{-1}$ ). Dashed-dotted line corresponds to sum SM + KK for the  $gg \rightarrow \mu^+\mu^-$  process; dotted line corresponds to sum SM + KK for the  $pp \rightarrow \mu^+\mu^-$  process.

in [67]. It is especially important to emphasize the characteristic feature of the search for KK resonances below the threshold of production of the first mode. It consists in a significant increase in the effective coupling constant compared to the contribution of the first mode alone, which is a consequence of the summation of the contributions of the KK modes. As was shown above, for the considered case of the stabilized model, the following enhancement factor is obtained:

$$\sum_{n \neq 0} \frac{(\Omega_n(L))^2}{M_n^2} \approx 1.82 \frac{(\Omega_1(L))^2}{M_1^2}.$$

This leads to an increase in the production cross sections by a factor of  $(1.82)^2 \approx 3.3$  (in the case of one flat extra dimension, this factor is equal to

$$(1.64)^2 \Rightarrow \left( \sum_n \frac{1}{n^2} \right)^2 = \left( \frac{\pi^2}{6} \right)^2 \approx 2.7,$$

which is close in magnitude to the case of a nonflat dimension.)

The constraints from Eqn (93) can also be used to estimate the lower value of the parameter  $\Lambda_\pi$  based on the requirement that the resonance width be less than its mass,  $\Gamma_1 < M_1$ , which leads to the restriction  $\Lambda_\pi > 2.82 \text{ TeV}$  [100].

The LHC collider has also been used to search for resonances in Drell–Yan processes. The maximum integrated luminosity currently measured in these experiments is  $139 \text{ fb}^{-1}$  [53], and the lower bounds found on the mass of the first KK graviton range from about 2.5 to 5 TeV, depending on the  $\tilde{k}/M$  parameter ratio, which determines the value of the resonance coupling constant [53, 54]. To illustrate the changes in the distributions due to the contributions of the KK graviton towers for the case when the resonance masses are less than the maximum collider energy, we carried out simulations for two points in the parameter space, such that for one point the first KK resonance is in the region of direct observation, while for the other point it is outside the region.

The first point corresponds to the model parameter values  $M_1 = 3.83 \text{ TeV}$ ,  $\Lambda_\pi = 8 \text{ TeV}$ ,  $\Gamma_1 = 0.08 \text{ TeV}$ . This resonance in the RS model lies close to the boundary of direct

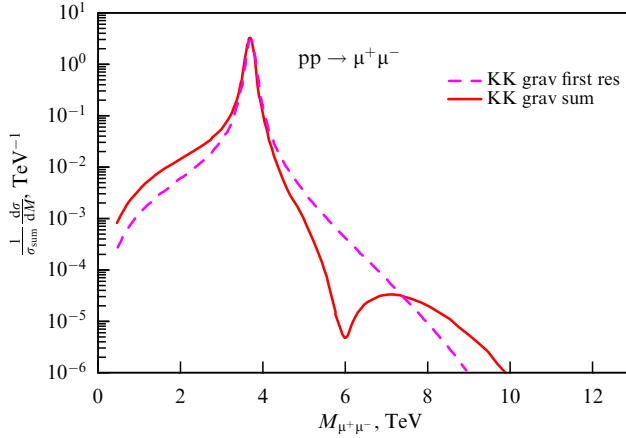


**Figure 2.** Normalized distribution by invariant mass of dilepton for the first KK resonance plus the sum of KK tower states starting from the second mode (solid line) and for the first KK resonance alone (dashed line) at  $M_{\text{res}} = 3.83$  TeV,  $\Gamma_{\text{res}} = 0.08$  TeV,  $A_\pi = 8$  TeV for LHC accelerator.

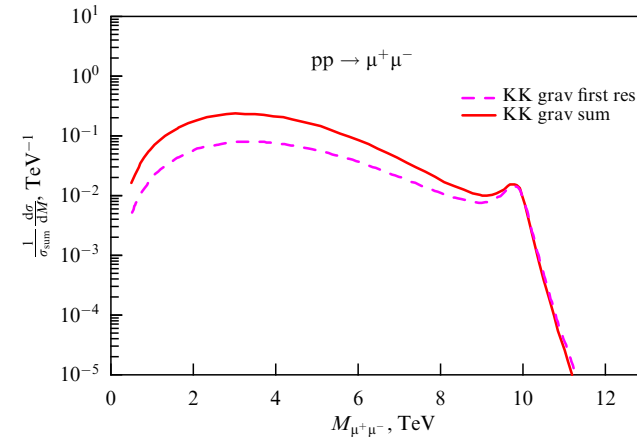


**Figure 3.** Normalized distribution by invariant mass of dilepton for the sum of KK tower states starting from the first mode (solid line) and for the first KK resonance alone (dashed line) at  $M_{\text{res}} = 10$  TeV,  $\Gamma_{\text{res}} = 0.5$  TeV,  $A_\pi = 14$  TeV for LHC accelerator.

observation of the LHC collider. For the second point with  $M_1 = 10$  TeV,  $A_\pi = 14$  TeV,  $\Gamma_1 = 0.5$  TeV, the mass of the first KK resonance is close to the maximum collider energy, and it is not directly observable. For both points, we can use the method of low-energy effective Lagrangians. To do so, we must sum either the contributions of all KK modes, or of all modes except the first, and thus take into account their influence on the tail of the distribution. Figures 2 and 3 show that the additional contribution from the KK tower increases the production cross section more than three times in the region of invariant masses smaller than the mass of the first KK resonance. However, the behavior of the cross section changes drastically in the region above the mass of the first resonance, where, along with the resonance peak, a dip appears due to the destructive interference between the contribution of the first KK resonance and that of the rest of the KK tower. This local minimum is located at point  $M_{\text{min}} \approx 1.5M_1$ . The growth of the cross section after this minimum is strongly suppressed by the parton structure functions, which leads to an additional bump in the distribution over the invariant mass. However, experimentally observing such a bump against the background of the SM

cross section is extremely difficult. Therefore, for a correct search for KK resonances in calculations and modeling of signal processes, it is necessary to not only take into account the interference with the SM amplitude (if it does not disappear) and calculate the NLO correction of the QCD, but also take into account the contribution to the process amplitude of those KK modes that are inaccessible for direct observation and the interference with it.

As we mentioned in the Introduction, a variant of the RS model is also considered, where the SM gauge fields also propagate in the 4D space between the branes. The reason for such an extension of the RS model is that the original approach of Rubakov and Shaposhnikov does not contain a consistent mechanism for localizing the gauge fields on the domain wall. In this case, the SM gauge fields should also have KK modes, which were sought in LHC experiments [55, 56]. Currently, the lower bound on the masses of such excitations is approximately 3.7 TeV. The impact of these KK modes on SM processes is considered in detail, for example, in [43–47, 57].

## 5. Comparison of processes involving radion with similar processes involving the Higgs boson

In the previous sections, it was shown that the effective four-dimensional interaction of radion with SM fields is described in the lowest order by a Lagrangian of the form [51, 66]

$$L_{\text{int}} = -\frac{1}{A} r T_\mu^\mu, \quad (94)$$

where  $T_\mu^\mu$  is the trace of the EMT of the SM fields,  $r$  is the radion field, and  $A$  is a constant with the dimension of energy. Since in this case the radion actually performs as a dilaton, it also interacts with the massless SM vector fields (photon and gluon) via a conformal anomaly, which must be included in the EMT trace. Taking into account the last remark, the EMT trace is presented as

$$\begin{aligned} T_\mu^\mu = & \sum_f \left\{ \frac{3i}{2} [(D_\mu \bar{f}) \gamma^\mu f - \bar{f} \gamma^\mu (D_\mu f)] + 4m_f \bar{f} f \left(1 + \frac{h}{v}\right) \right\} \\ & - (\partial_\mu h)(\partial^\mu h) + 2m_h^2 h^2 \left(1 + \frac{h}{2v}\right)^2 \\ & - (m_Z^2 Z_\mu Z^\mu + 2m_W^2 W_\mu^+ W^{-\mu}) \left(1 + \frac{h}{v}\right)^2 + \\ & + \frac{\beta(g_s)}{2g_s} G_{\mu\nu}^{ab} G^{\mu\nu}_{ab} + \frac{\beta(e)}{2e} F_{\mu\nu} F^{\mu\nu}, \end{aligned} \quad (95)$$

where the summation in the first term is carried out over all SM fermions, and  $D_\mu$  is the covariant derivative of the SM. The last two terms in Eqn (95) describe the gluon and photon anomalies, and the factors  $\beta(g_s)$  and  $\beta(e)$  are the beta functions of quantum chromodynamics and quantum electrodynamics, respectively. When considering specific processes involving radion, many studies assume that the fields are on the mass shell (i.e., satisfy the equations of motion). In this case, the trace of the energy–momentum tensor for spinor and vector fields takes a particularly simple form:

$$\begin{aligned} T_\mu^\mu = & \frac{\beta(g_s)}{2g_s} G_{\mu\nu}^{ab} G^{\mu\nu}_{ab} + \frac{\beta(e)}{2e} F_{\mu\nu} F^{\mu\nu} - m_Z^2 Z_\mu Z^\mu \\ & - 2m_W^2 W_\mu^+ W^{-\mu} + \sum_f m_f \bar{f} f. \end{aligned} \quad (96)$$

If, for some reason, it turns out that the anomalous terms can be disregarded in Eqn (96), it is apparent that, on the mass shell, the interaction of spinor and vector fields with the radion takes the same form as the interaction of such fields with the Higgs boson (with the coupling constant replaced by  $\Lambda \rightarrow v$ ).

The off-mass-shell situation is different. The interaction of the radion with fermions contains terms with derivatives with respect to coordinates, and, therefore, the corresponding vertices in the momentum representation depend on the momenta of the fermions. Therefore, it would be natural to expect that processes involving fermions, gauge bosons, and radions should in principle differ from similar processes where the Higgs boson is produced instead of the radion. However, as shown in [68, 69], the amplitudes of any scattering processes involving one radion and an arbitrary number of fermions and vector bosons have the same structure as the amplitudes of similar processes involving the Higgs boson. Additional (compared to processes involving the Higgs boson) contributions are canceled out when summing the amplitudes in both the tree and one-loop approximations. In particular, the processes of single radion production coincide with similar processes of Higgs boson production up to replacing the Higgs boson mass with the radion mass and replacing the vacuum expectation value  $v$  with the constant  $\Lambda$ . Moreover, it is shown in [70, 71] that a similar cancellation also occurs in the case of associative radion and Higgs boson production in comparison with the pair production of the Higgs boson—the difference is reduced to replacing the masses and interaction constants, and rescaling the third-power self-interaction constant for the Higgs boson, the constant not altering for scalars of equal masses. In this section, we consider in detail how such a cancellation of additional contributions to the radion scattering amplitude occurs in various processes, resulting in processes that involve such seemingly differently interacting scalars as the radion and the Higgs boson being potentially indistinguishable.

### 5.1 Processes involving a single scalar boson

**5.1.1 Radion production.** The simplest example that can demonstrate the cancellation of additional ‘kinetic’ contributions to the total scattering amplitude might be radion production in a pair with a Z-boson in  $e^+e^-$ -collisions. In the lowest order, this process is described by the four Feynman diagrams displayed in Fig. 4.

We now compare the four amplitudes for the  $e^+e^- \rightarrow Zr$  process shown in Fig. 4 with similar amplitudes for the Higgs boson emission. The fourth diagram in Fig. 4 has the same structure (up to replacing radion with the Higgs boson) as the similar diagram for the production of the Higgs boson. The analogues of the second and third diagrams shown in Fig. 4, in principle, also contribute to the total amplitude of this process, but they are usually not considered due to the negligible mass of the electron, to which the vertex function  $e^+e^-h$  is proportional. When considering the emission of the radion, a similar amplitude cannot be straightforwardly ignored, since, in addition to the masses of the fermions, the momenta of the incoming fermions obviously contribute to it. The first diagram in Fig. 4, which contains a vertex coming from the term with the product of the radion and the covariant derivative of the fermion, has no analogue for the process of radiation of the Higgs boson.

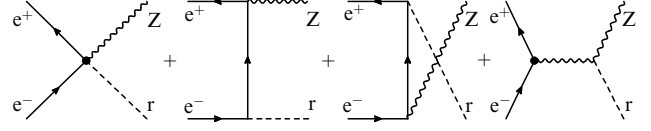


Figure 4. Feynman diagrams contributing to process  $e^+e^- \rightarrow Zr$ .

If we use the formula in the 't Hooft–Feynman gauge for the gauge boson propagator and ignore the electron mass, the four diagrams displayed in Fig. 4, which describe radion emission, correspond to the following analytical formulas:

$$M_1 = i3C\bar{e}(p_+) \Gamma^\mu e(p_-) \varepsilon_\mu(q_Z) r(q_r), \quad (97)$$

$$M_2 = -iC\bar{e}(p_+) \Gamma^\mu \frac{\hat{l}}{l^2} \left[ \frac{3}{2} (\hat{l} + \hat{p}_-) \right] e(p_-) \varepsilon_\mu(q_Z) r(q_r), \quad (98)$$

$$M_3 = -iC\bar{e}(p_+) \left[ \frac{3}{2} (\hat{p}_+ + \hat{l}') \right] \frac{\hat{l}'}{l'^2} \Gamma^\mu e(p_-) \varepsilon_\mu(q_Z) r(q_r), \quad (99)$$

$$M_4 = -i2C\bar{e}(p_+) \Gamma^\mu e(p_-) \frac{1}{k^2 - m_Z^2} m_Z^2 \varepsilon_\mu(q_Z) r(q_r), \quad (100)$$

where the following notations are introduced:

$$C \equiv \frac{1}{\Lambda} \frac{e}{2 \sin \theta_W \cos \theta_W}, \quad \Gamma^\mu = \gamma^\mu \left( 2 \sin^2 \theta_W - \frac{1}{2} (1 - \gamma_5) \right), \quad (101)$$

$\hat{l} = l_\mu \gamma^\mu$ , and the following relations are satisfied for momenta:

$$k = p_+ + p_- = q_r + q_Z, \quad l = q_Z - p_+ = p_- - q_r, \\ l' = q_r - p_+ = p_- - q_Z. \quad (102)$$

Using the Dirac equation for a massless particle in the momentum representation  $\hat{p}_- e(p_-) = 0$ ,  $\bar{e}(p_+) \hat{p}_+ = 0$  and the apparent identity  $\hat{l}(\hat{l}/l^2) = 1$ , it can be easily verified that the sum of the second and third diagrams is exactly equal to the first diagram with the opposite sign and, consequently,

$$M_1 + M_2 + M_3 = 0. \quad (103)$$

Therefore, for the modulus squared of the matrix element of radion emission  $|M|^2$ , the equality  $|M|^2 = |M_4|^2$  holds, i.e.,  $|M|^2$  has a structure that exactly coincides with that for Higgs boson production, and, thus, the cross section has the well-known form (with the corresponding replacement of  $\Lambda \leftrightarrow v$  and  $m_r \leftrightarrow m_h$ )

$$\sigma(e^+e^- \rightarrow rZ) = \frac{m_Z^2}{\Lambda^2} \frac{\alpha(8 \sin^4 \theta_W - 4 \sin^2 \theta_W + 1)}{24 \sin^2 \theta_W \cos^2 \theta_W} \\ \times \frac{\sqrt{\lambda_r} \lambda_r + 12 m_Z^2 s}{4 s^2 (s - m_Z^2)^2}, \quad (104)$$

where, by definition,  $\lambda_r \equiv (m_Z^2 + m_r^2 - s)^2 - 4 m_Z^2 m_r^2$ .

As can be seen from Eqn (103), all contributions from the additional diagrams presented in Fig. 4 cancel each other out, and therefore the cross section of radion emission is described by the same formula as the cross

section of Higgs boson emission (up to rescaling of the scalar boson mass and the interaction constant). Using similar reasoning, it can be easily demonstrated that the amplitudes also cancel in a similar way for the associative production of the radion and  $W^\pm$  bosons, for example, in the  $ud \rightarrow rW^+$  process.

**5.1.2 Cancellation of additional contributions to the total amplitude for tree-level processes involving a single radion.** In this section, we consider tree-level processes involving a single radion and an arbitrary number of gauge bosons in the initial and final states. For such processes, the declared cancellation of additional contributions to the total scattering amplitude follows from the structure of the fermion current emitting the radion and gauge bosons.

To understand how such a cancellation occurs in the general case, it is useful first to consider in detail the simplest example with the radiation by a fermion current of one gauge boson and one radion, which corresponds to the three diagrams displayed in Fig. 5.

We represent the vertex

$$\frac{i}{\Lambda} \left[ \frac{3}{2} (\hat{p} + \hat{q}) - 4m_f \right]$$

of the fermion-radion interaction as follows:

$$\begin{aligned} \frac{i}{\Lambda} \left[ \frac{3}{2} (\hat{p} + \hat{q}) - 4m_f \right] &= \frac{i}{\Lambda} \left[ \frac{3}{2} (\hat{p} - m_f) + \frac{3}{2} (\hat{q} - m_f) - m_f \right] \\ &= \frac{i}{\Lambda} \left[ \frac{3}{2} S^{-1}(p) + \frac{3}{2} S^{-1}(q) - m_f \right], \end{aligned} \quad (105)$$

where  $p$  and  $q$  are the momenta of the fermions entering the fermion vertex, and  $S^{-1}(p)$  is the inverse fermion propagator. Note that, in Eqn (105), which describes the interaction vertex, the last term in square brackets is proportional to the fermion mass  $m_f$ , just as is the case of the vertex of interaction between the Higgs boson and fermions. Taking into account transformation (105) for the vertices of the fermion-radion interaction, we can present analytical formulas for the diagrams shown in Fig. 5 as follows:

$$M_1 = +i3C\bar{u}_{\text{out}}(p_{\text{out}}) \Gamma^\mu u_{\text{in}}(p_{\text{in}}), \quad (106)$$

$$\begin{aligned} M_2 &= -iC\bar{u}_{\text{out}}(p_{\text{out}}) \left[ \frac{3}{2} S^{-1}(p_{\text{out}}) + \frac{3}{2} S^{-1}(q_1) - m_f \right] \\ &\times S(q_1) \Gamma^\mu u_{\text{in}}(p_{\text{in}}) = -i \frac{3}{2} C\bar{u}_{\text{out}}(p_{\text{out}}) \Gamma^\mu u_{\text{in}}(p_{\text{in}}) \\ &+ im_f C\bar{u}_{\text{out}}(p_{\text{out}}) S(q_1) \Gamma^\mu u_{\text{in}}(p_{\text{in}}), \end{aligned} \quad (107)$$

$$\begin{aligned} M_3 &= -iC\bar{u}_{\text{out}}(p_{\text{out}}) \Gamma^\mu S(k_1) \left[ \frac{3}{2} S^{-1}(k_1) + \frac{3}{2} S^{-1}(p_{\text{in}}) - m_f \right] \\ &\times u_{\text{in}}(p_{\text{in}}) = -i \frac{3}{2} C\bar{u}_{\text{out}}(p_{\text{out}}) \Gamma^\mu u_{\text{in}}(p_{\text{in}}) \\ &+ im_f C\bar{u}_{\text{out}}(p_{\text{out}}) \Gamma^\mu S(k_1) u_{\text{in}}(p_{\text{in}}), \end{aligned} \quad (108)$$

where the symbol  $C$  denotes the product of constants at all vertices included in the amplitude, and the expression  $\Gamma^\mu$  denotes the Lorentz structure, which is the same for the fermion–boson and fermion–boson–radion vertices. The initial and final fermions are the same in the case of the  $Z$  boson (neutral current) and different in the case of the

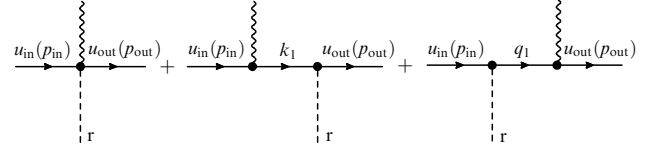


Figure 5. Emission by fermion current of radion and one gauge boson.

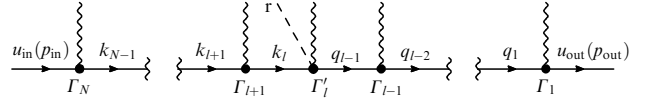


Figure 6. Example of one of  $N$  possible variants of radiation of a single radion by a fermion current from a type  $\Gamma'_l$  vertex with four lines and  $N$  gauge bosons from type  $\Gamma_l$  vertices.

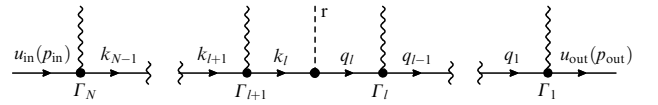


Figure 7. Example of one of  $N + 1$  possible variants of radiation of a single radion by a fermion current from a vertex with three lines and  $N$  gauge bosons from type  $\Gamma_l$  vertices.

$W$  boson (charged current). As can be seen from Eqns (106)–(108), after summing all three diagrams, the contribution to the total amplitude of the process involving a single radion is ultimately given by only two terms proportional to the fermion masses,

$$\begin{aligned} M &= M_1 + M_2 + M_3 = im_f C\bar{u}_{\text{out}}(p_{\text{out}}) \\ &\times [\Gamma^\mu S(k_1) + S(q_1) \Gamma^\mu] u_{\text{in}}(p_{\text{in}}). \end{aligned} \quad (109)$$

Comparing Eqn (109) with a similar formula for the total amplitude of the process involving a single Higgs boson, we find that the total amplitudes of these two processes coincide if we replace the interaction constants  $\Lambda \leftrightarrow v$ .

In the processes involving a radion, a similar cancellation of additional (if compared with processes involving the Higgs boson) contributions also occurs when an arbitrary number  $N$  of gauge bosons and a single radion are emitted by the fermion current. Two types of diagrams characteristic of such a process are displayed in Figs 6 and 7.

Looking at Fig. 7, we can conclude that there are only  $N + 1$  diagrams with single-radion emission containing a three-prong vertex, since the vertex containing a radion can be included in the diagram of Fig. 7 in exactly  $N + 1$  ways. Similarly, examining Fig. 6, we can conclude that there are only  $N$  diagrams with single-radion emission containing four-prong vertices. Indeed, in the diagram of Fig. 6, there are exactly  $N$  three-prong type  $\Gamma_l$  vertices that could be converted into four-prong type  $\Gamma'_l$  vertices, where the radion is emitted from a single vertex together with a gauge boson. It should be noted that the primed four-prong vertex of the interaction of a radion with two fermions and a gauge boson in Fig. 6 can be expressed in terms of a three-prong (unprimed) vertex:  $\Gamma_j^{\prime\mu} = -3\Gamma_j^\mu/\Lambda$ . Thus, the sum of all diagrams for this process can be represented as

$$M = M_0 + \sum_{l=1}^N (M_l + M'_l), \quad (110)$$

where the amplitudes  $M_l$ , similar to the amplitude shown in Fig. 7, contain a vertex with the emission of a radion of only the three-prong type:

$$M_l = i^{2N+1} C\bar{f}_{\text{out}}(p_{\text{out}}) \left[ \prod_{j=1}^l \Gamma_j^{\mu_j} S(q_j) \right] \left[ -\frac{3}{2} S^{-1}(q_l) - \frac{3}{2} S^{-1}(k_l) + m_{f_l} \right] \left[ \prod_{j=l+1}^N S(k_{j-1}) \Gamma_j^{\mu_j} \right] f_{\text{in}}(p_{\text{in}}) \quad (111)$$

for  $l = 0, \dots, N$ ,

while the primed amplitudes  $M'_l$ , similar to the amplitude presented in Fig. 6, contain only a fourth-order vertex with the emission of the radion:

$$M'_l = i^{2N-1} C\bar{f}_{\text{out}}(p_{\text{out}}) \left[ \prod_{j=1}^{l-1} \Gamma_j^{\mu_j} S(q_j) \right] [-3\Gamma_l^{\mu_l}] \times \left[ \prod_{j=l+1}^N S(k_{j-1}) \Gamma_j^{\mu_j} \right] f_{\text{in}}(p_{\text{in}}) \quad (112)$$

for  $l = 1, \dots, N$ ;

in Eqns (111) and (112), it is implied that all products of the form  $\prod_{j=l+1}^N$  and  $\prod_{j=1}^{l-1}$  in which the number of the first factor exceeds that of the last factor are identically equal to one. In addition, the following notations are introduced for momenta and their linear combinations:

$$k_l = p_{\text{in}} - \sum_{j=l}^N p_{V_j}, \quad q_l = k_l - p_r = p_{\text{out}} + \sum_{j=1}^l p_{V_j}, \quad q_0 = p_{\text{out}}, \quad (113)$$

where  $q_l$  and  $k_l$  are the momenta of fermions in intermediate states,  $p_r$  is the radion momentum, and  $m_{f_{\text{in}}}$ ,  $m_{f_{\text{out}}}$ , and  $m_{f_l}$  are the masses of fermions in the initial, final, and intermediate states, respectively. It is worth noting that, in diagrams (111) and (112), the factors  $i^{2N+1}$  and  $i^{2N-1}$  differ, since, in diagrams of the  $M$  and  $M'$  type, the number of propagators and vertices differs by one, which ultimately leads to opposite signs of the contributions of these diagrams.

From Eqns (110)–(113), using the apparent identities  $S^{-1}(q_l) S(q_l) = 1$  and the Dirac equation, which the initial  $f_{\text{in}}(p_{\text{in}})$  and final  $\bar{f}_{\text{out}}(p_{\text{out}})$  fermion states satisfy, we obtain

$$M_0 = M_0^{\text{H}} - \frac{1}{2} M'_1, \quad M_N = M_N^{\text{H}} - \frac{1}{2} M'_N, \quad (114)$$

$$M_l = M_l^{\text{H}} - \frac{1}{2} M'_l - \frac{1}{2} M'_{l+1}, \quad l = 1, \dots, N-1. \quad (115)$$

By  $M_l^{\text{H}}$  we mean amplitudes whose structure is similar to those of processes where the Higgs boson is involved instead of a radion, i.e., contributions proportional to the fermion masses:

$$M_l^{\text{H}} = i^{2N+1} \bar{f}_{\text{out}}(p_{\text{out}}) \left[ \prod_{j=1}^l \Gamma_j^{\mu_j} S(q_j) \right] [m_{f_l}] \times \left[ \prod_{j=l+1}^N S(k_{j-1}) \Gamma_j^{\mu_j} \right] f_{\text{in}}(p_{\text{in}}). \quad (116)$$

It is assumed in Eqn (116) that the index  $l$  varies from zero to  $N$  and that all products  $\prod_{j=1}^l$  in which the number of the first

factor exceeds that of the last factor are identically equal to one.

Substituting Eqns (114) and (115) into the formula for the total amplitude of the process under consideration (110), we obtain the following equality:

$$M = \sum_{l=0}^N M_l + \sum_{l=1}^N M'_l = \sum_{l=0}^N M_l^{\text{H}}. \quad (117)$$

Equation (117) apparently shows that, in addition to the Higgs-like contributions  $M_l^{\text{H}}$ , all other contributions to the total amplitude  $M$  of the process involving a single radion cancel each other out and only the Higgs-like part  $\sum_{l=0}^N M_l^{\text{H}}$  remains.

**5.1.3 Cancellation of additional contributions to total amplitude for processes involving a single radion at the loop level.** The result formulated in the previous section for tree diagrams can easily be generalized to the case of fermion loops, when none of the fermions is on the mass shell. In this case, the number of type  $M_l$  diagrams is one less than in the tree case, since, as can be seen from Figs 6 and 7, for a closed loop, the radiation from the radion to the right of the first gauge vertex is identical to that from the radion to the left of the  $N$ th gauge vertex. This implies that, for the total amplitude of such a process, we can write

$$M = \sum_{l=1}^N M_l + \sum_{l=1}^N M'_l, \quad (118)$$

where, as in the tree case,  $M_l$  are diagrams containing the cubic type radion interaction vertex, and  $M'$  are diagrams containing the quartic radion interaction vertex.

Arguing in the same way as in the tree case, we obtain formulas in which the Higgs-like contributions are separated:

$$M_l = M_l^{\text{H}} - \frac{1}{2} M'_l - \frac{1}{2} M'_{l+1}, \quad (119)$$

$$M_N = M_N^{\text{H}} - \frac{1}{2} M'_N - \frac{1}{2} M'_1. \quad (120)$$

Substituting Eqns (119) and (120) into the formula for the total amplitude of process (118), similarly to the tree case, we find that all additional contributions to the total amplitude of process  $M$  are canceled out, and only contributions similar to the Higgs-boson contributions remain:

$$M = \sum_{l=1}^{N-1} M_l^{\text{H}}. \quad (121)$$

## 5.2 Processes with associated production of radion and Higgs bosons

In the previous section, it was shown that, in the production of a single fermion accompanied by an arbitrary number of any gauge bosons, despite the presence of terms at the vertices of the interaction of a radion and fermions that depend on the fermion momenta and four-prong vertices of the fermion–gauge boson–radion type, all additional contributions are canceled out in such a way that only that part remains whose form is the same as in similar processes with the production of the Higgs boson. This result holds both at the tree level and in the case of a fermion loop; the vector bosons involved in the process can be either on or off the mass shell. The amplitudes



of processes involving radion can be derived from the amplitudes of similar processes involving the Higgs boson by simply replacing the Higgs boson mass  $m_h$  with the radion mass  $m_r$  and the Higgs vacuum expectation value  $v$  with the inverse interaction constant of radion  $\Lambda$ . We now show that, if, in addition to gauge bosons, radion production is accompanied by an arbitrary number of Higgs bosons, a similar cancellation also occurs; however, this time, in addition to the indicated replacements, it is also necessary to change the constant in the three-prong vertex of the Higgs boson self-interaction.

**5.2.1 Annihilation of a fermion-antifermion pair.** We start with a simple example of the associated production of radion and the Higgs boson in the fermion-antifermion annihilation. Diagrams of this process are shown in Fig. 8.

The last three diagrams are similar to the those of pair production of Higgs bosons (if the outgoing radion is replaced by the Higgs boson, and the vertices of the interaction of fermions with the radion and the Higgs boson with the radion are replaced, respectively, by the vertices of the interaction of fermions with the Higgs boson and its vertex of third-power self-interaction). According to Feynman rules, each of the four graphs presented in Fig. 8 can be associated with analytical formulas presented below in Eqns (122)–(125). For the first diagram in Fig. 8, we obtain

$$M_1 = -4 \frac{i}{v\Lambda} \bar{f}(p_1)[m_f]f(p_2)r(q_r)h(q_h). \quad (122)$$

The second and third diagrams displayed in Fig. 8 are described by the formulas

$$M_2 = -\frac{i}{v\Lambda} \bar{f}(p_1) \left[ -\frac{3}{2} S^{-1}(p_1) - \frac{3}{2} S^{-1}(l) + m_f \right] \times S(l)[m_f]f(p_2)r(q_r)h(q_h), \quad (123)$$

$$M_3 = -\frac{i}{v\Lambda} \bar{f}(p_1)[m_f]S(l') \left[ -\frac{3}{2} S^{-1}(l') - \frac{3}{2} S^{-1}(p_2) + m_f \right] \times f(p_2)r(q_r)h(q_h). \quad (124)$$

Finally, the following analytical formula corresponds to the fourth diagram in Fig. 8:

$$M_4 = -\frac{i}{v\Lambda} \bar{f}(p_1)[m_f]f(p_2) \frac{1}{k^2 - m_h^2} \times [-2(kq_h) + 4m_h^2]r(q_r)h(q_h), \quad (125)$$

where

$$k = p_1 + p_2 = q_h + q_r, \quad l = p_2 - q_r = q_h - p_1, \\ l' = p_2 - q_h = q_r - p_1. \quad (126)$$

Using simple kinematic relations and the Dirac equation in the momentum representation, we can represent the analytical

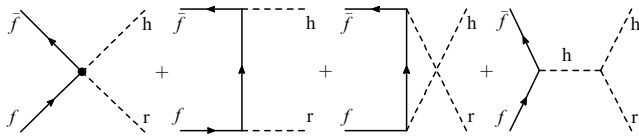


**Figure 8.** Production of a radion and a Higgs boson in annihilation of a fermion-antifermion pair.

formulas corresponding to the last three diagrams as follows:

$$M_2 = \frac{3}{2} \frac{i}{v\Lambda} \bar{f}(p_1)[m_f]f(p_2)r(q_r)h(q_h) - \frac{i}{v\Lambda} \bar{f}(p_1)[m_f^2 S(l)]f(p_2)r(q_r)h(q_h), \quad (127)$$

$$M_3 = \frac{3}{2} \frac{i}{v\Lambda} \bar{f}(p_1)[m_f]f(p_2)r(q_r)h(q_h) - \frac{i}{v\Lambda} \bar{f}(p_1)[m_f^2 S(l')]f(p_2)r(q_r)h(q_h), \quad (128)$$

$$M_4 = \frac{i}{v\Lambda} \bar{f}(p_1)[m_f]f(p_2)r(q_r)h(q_h) - \frac{i}{v\Lambda} \bar{f}(p_1)[m_f]f(p_2) \frac{1}{k^2 - m_h^2} [m_r^2 + 2m_h^2]r(q_r)h(q_h). \quad (129)$$

As we can see, the first terms in Eqns (127)–(129), up to the coefficients, coincide with the first diagram, and the coefficients of these four diagrams are such that their sum is zero ( $1 + 3/2 + 3/2 - 4 = 0$ ). Therefore, the sum of all four diagrams has the form

$$M \equiv M_1 + M_2 + M_3 + M_4 = -\frac{im_f}{v\Lambda} \bar{f}(p_1)f(p_2) \frac{m_r^2 + 2m_h^2}{k^2 - m_h^2} \times r(q_r)h(q_h) - \frac{im_f^2}{v\Lambda} \bar{f}(p_1)[S(l) + S(l')]f(p_2)r(q_r)h(q_h). \quad (130)$$

We now compare the derived equation (130) with the formula for the amplitude of pair production of Higgs bosons in the annihilation of a fermion-antifermion pair, where the diagrams of the corresponding process are presented in Fig. 9. The analytical formulas for these diagrams are

$$M_1^H = -\frac{im_f^2}{v^2} \bar{f}(p_1)S(l')f(p_2)h(q_1)h(q_2), \quad (131)$$

$$M_2^H = -\frac{im_f^2}{v^2} \bar{f}(p_1)S(l)f(p_2)h(q_1)h(q_2), \quad (132)$$

$$M_3^H = -\frac{im_f}{v^2} \bar{f}(p_1)f(p_2) \frac{3m_h^2}{k^2 - m_h^2} h(q_1)h(q_2), \quad (133)$$

and their sum is

$$M^H \equiv M_1^H + M_2^H + M_3^H = -\frac{im_f}{v^2} \bar{f}(p_1)f(p_2) \frac{3m_h^2}{k^2 - m_h^2} \times r(q_r)h(q_h) - \frac{im_f^2}{v^2} \bar{f}(p_1)[S(l) + S(l')]f(p_2)r(q_r)h(q_h). \quad (134)$$

As we can see, Eqn (130) can be derived from Eqn (134) by replacing one vacuum expectation value  $v$  in the factor  $v^{-2}$  with the constant  $\Lambda$  and the self-interaction constant of the

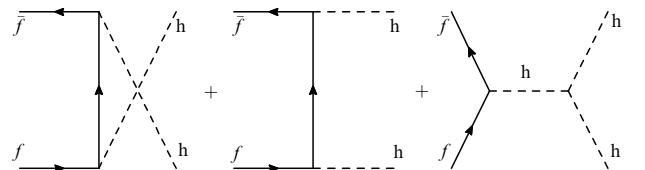


**Figure 9.** Annihilation of two fermions with production of two Higgs bosons.

Higgs boson  $3m_h^2/v$  with a new constant of the following form:

$$\frac{1}{A} (2m_h^2 + m_r^2) = (1 + \zeta) \frac{3m_h^2}{A}, \quad (135)$$

where

$$\zeta \equiv \frac{m_r^2 - m_h^2}{3m_h^2}.$$

The same similarity property also holds for the fusion of two gluons with the production of a pair of scalar particles, in particular for the joint production of a Higgs boson and a radion ( $gg \rightarrow hr$ ) and pair production of Higgs bosons ( $gg \rightarrow hh$ ). The number of diagrams required to describe such processes is much higher than that needed to describe the previously considered processes, so we do not present them here. The processes mentioned are considered in detail in study [68], where it is shown that the amplitudes of these two processes also coincide up to the parameter  $\zeta$  and the replacement of the masses of scalars and coupling constants. In other words, the participation of a radion in the process can imitate the deviation of the constant of Higgs boson cubic self-coupling from its SM value.

**5.2.2 General case of cancellation of additional contributions in associated production of rados and Higgs bosons.** We now show that the cancellation of radiation-type contributions considered in the previous sections also occurs in the general case of the production of a single radion accompanied by an arbitrary number of gauge and Higgs bosons. We consider a fermion current (or a fermion loop) emitting a certain number  $N$  of bosons (gauge bosons  $V_j$  or Higgs bosons  $h_j$ ; the subscript  $j$  numbers the bosons). We denote the number of gauge bosons by  $N_V$ , the number of Higgs bosons by  $N_h$ , so  $N_V + N_h = N$ , and the process is  $\bar{f}f \rightarrow h_1 \dots h_{N_h} V_1 \dots V_{N_V}$ . We add either one more Higgs boson (thereby converting the process into  $\bar{f}f \rightarrow h_1 \dots h_{N_h+1} V_1 \dots V_{N_V}$ ) or a radion (converting the process into  $\bar{f}f \rightarrow rh_1 \dots h_{N_h} V_1 \dots V_{N_V}$ ) in an arbitrary possible place in the process diagram. Apparently, a single Higgs boson can be added in two possible ways:

- (a) with emission from a fermion line and
- (b) with emission from a boson line ( $V$  or  $h$ )

for a single radion, and a third option is added to these two:

- (c) with emission of a radion from an already existing fermion-boson vertex (in this way, a three-prong vertex turns into a four-prong one).

All three options are displayed in Fig. 10.

We now present analytical formulas for the vertices corresponding to different options of the emission of a radion or Higgs boson.

- a. Vertices of emission of a Higgs boson  $\Gamma_{hff}$  or a radion  $\Gamma_{rff}$  from a fermion line:

$$\Gamma_{hff} = i \frac{m_f}{v}. \quad (136)$$

The vertex  $\Gamma_{rff}$  of radion emission from a fermion line is a function of the fermion momenta it contains, for example,  $p$  and  $l$ , and can be represented in terms of the corresponding propagators:

$$\begin{aligned} \Gamma_{rff}(p, l) &= \frac{i}{A} \left\{ \frac{3}{2} [S^{-1}(l) + S^{-1}(-p)] - m_f \right\} \\ &= \frac{v}{A} \Gamma_{(h)} + \frac{i3}{2A} [S^{-1}(l) + S^{-1}(-p)]. \end{aligned} \quad (137)$$

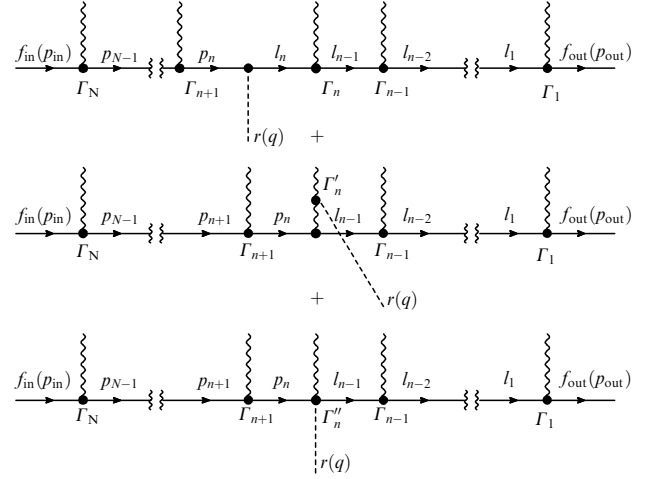


**Figure 10.** Possible variants of adding a radion to a fermion current emitting  $N$  Higgs and gauge bosons.

- b. Vertices of the emission of a Higgs boson  $\Gamma_{hVV}$  or a radion  $\Gamma_{rVV}$  from a vector boson line:

$$\Gamma_{hVV} = i \frac{2m_V^2}{v} \delta_\beta^\alpha. \quad (138)$$

A similar vertex  $\Gamma_{rVV}$  of the radion radiation coincides with the vertex  $\Gamma_{hVV}$  up to the replacement of the constant  $v$  by the constant  $A$ :

$$\Gamma_{rVV} = i \frac{2m_V^2}{A} \delta_\beta^\alpha. \quad (139)$$

- c. Three-prong vertices of the radiation of the Higgs boson  $\Gamma'_{hhh}$  or radion  $\Gamma'_{rhh}$  from the Higgs boson line:

$$\Gamma'_{hhh} = -i \frac{3m_h^2}{v}. \quad (140)$$

A similar vertex of the radion emission from the Higgs boson line is momentum dependent; it can be represented as the sum of three propagators and a Higgs-like contribution:

$$\begin{aligned} \Gamma'_{rhh} &= \frac{i}{A} \{2(pq) + 4m_h^2\} = \frac{i}{A} \{D_r^{-1}(p - q) - D_h^{-1}(p) - \\ &\quad - D_h^{-1}(q)\} + \frac{v}{A} (1 + \zeta) \Gamma'_{hhh}. \end{aligned} \quad (141)$$

- d. A four-prong vertex  $\Gamma''_{rffV}$  from which a radion, a vector boson, and two fermions are emitted:

$$\Gamma''_{rffV} = \frac{i3}{A} \gamma_\mu (a_f + b_f \gamma_5) = \frac{3}{A} \Gamma_{ffV}. \quad (142)$$

- e. A four-prong vertex  $\Gamma''_{rffh}$  from which a radion, a Higgs boson, and two fermions are emitted:

$$\Gamma''_{rffh} = -\frac{i}{A} \frac{4m_f}{v} = \frac{4}{A} \Gamma_{hff}. \quad (143)$$

We now consider some vertex  $\Gamma_n$  on the fermion line from which a vector boson is emitted and which for convenience we call the ‘central’ vertex. We now select from the entire set of diagrams corresponding to the process under consideration four diagrams in which a radion is emitted in the immediate vicinity of the central vertex. The first diagram corresponds to

the case when a radion is emitted from the fermion line to the left of the central vertex. The second diagram corresponds to the case when a radion is emitted from the fermion line to the right of the central vertex. The third diagram shows radion emission from the line of the emitted vector boson. The fourth diagram presents radion emission directly from the central vertex. We denote the amplitudes of such diagrams by  $M[r]_j$ , where  $j = 1, 2, 3, 4$ . Using Eqn (137) for vertex  $\Gamma_{\text{eff}}$ , the amplitude of the first diagram  $M[r]_1$  can be represented as a sum of three terms, the first of which coincides with the similar diagram with Higgs boson emission up to the replacement of  $v$  by the constant  $A$ , while, in the other two, the inverse propagators cancel each other out with the propagators on the left or right, thus ‘eliminating’ the fermion line either between the radion emission vertex and the central vertex, or a vertex located even further to the left (if there is no such vertex, such a term is zero, since the inverse propagator acts on the fermion on the mass shell). As a result of such a reduction, an additional term of the type  $-1/2 M[r]_4$  emerges, where the factor  $-1/2$  arises due to the factors of the inverse propagators and in the vertex  $\Gamma''_{\text{eff}}$ . Therefore, we obtain

$$M[r]_1 = \dots + \frac{v}{A} M[h]_1 - \frac{1}{2} M[r]_4, \quad (144)$$

where the ellipsis denotes the third term, which is of no interest to us in this case, since, if it is other than zero, it must be assigned to the block of diagrams related to the next central vertex  $\Gamma_{n+1}$ . Here,  $M[h]_j$  denotes an amplitude similar to  $M[r]_j$ , but with the emission of a Higgs boson instead of a radion. A similar reduction for the amplitude of the second diagram yields

$$M[r]_2 = -\frac{1}{2} M[r]_4 + \frac{v}{A} M[h]_1 + \dots \quad (145)$$

The amplitude of the third diagram coincides with  $v/A$  up to a factor of  $M[h]_3$ , and thus, for this group of four diagrams, we obtain

$$M[r]_1 + M[r]_2 + M[r]_3 + M[r]_4 = \frac{v}{A} M[h]_1 + \frac{v}{A} M[h]_2 + \frac{v}{A} M[h]_3 + \left(1 - \frac{1}{2} - \frac{1}{2}\right) M[r]_4.$$

Since the expression in parentheses is zero, it is apparent that only the contributions of the amplitudes of the Higgs-type diagrams remain. The fermion line in Fig. 10 can be either open, when the initial and final fermions are on the mass shell, or a loop, so the result obtained for tree diagrams can easily be generalized to the case of fermion loops [70, 71].

## 6. Nonlinear self-interaction and interaction of radion with fields of the Standard Model

In Section 5, it was shown that the processes of production of a single radion accompanied by an arbitrary number of vector bosons at both the tree and loop levels coincide with similar processes with the production of a Higgs boson up to the replacement of masses and the interaction constant. Moreover, for processes with the associated production of a radion and a Higgs boson, a similar result is obtained (up to the replacement of masses, the interaction constant, and the self-interaction constant in the three-prong vertex of the Higgs boson self-interaction). Current experimental data rule out the existence of scalar particles with masses less than 1 TeV

and with constants of interaction with SM fields of the order of the Higgs boson coupling constant, but do not rule out the existence of scalar particles with masses of the order of the Higgs boson with coupling constants much smaller than those of the Higgs boson. Consequently, if the radion mass is close to the Higgs boson mass, a problem occurs related to identifying the scalar particles participating in the processes. Due to this, it is of importance to study in more detail the possible properties of radions, in particular, to derive the potential of radion self-interaction of a power higher than the second and the nonlinear terms of the interaction of a radion with SM fields, as we did in [52].

### 6.1 Effective four-dimensional quartic radion Lagrangian

We retain in expansions (65) and (66) for the tensor and scalar fields only the zero mode of the gravitational field and the radion field. Thus, with an accuracy of terms of the order of  $1/M^3$ , the fields  $g_{MN}$  and  $\phi$  are represented as

$$g_{\mu\nu}(x, y) = \exp(-2A(y)) (1 - \chi(y)r(x)) g_{\mu\nu}^{(0)}(x),$$

$$g_{\mu\nu}^{(0)}(x) = \eta_{\mu\nu} + N_0 b_{\mu\nu}^{(0)}(x), \quad (146)$$

$$g_{4\mu} = 0, \quad g_{44}(x, y) = 1 + 2\chi(y)r(x), \quad (147)$$

$$\phi(x, y) = \bar{\phi}(y) + \Phi(y)r(x), \quad (148)$$

where

$$\chi(y) \equiv \frac{1}{2\sqrt{2}M^3} \exp(2A(y)) \Psi_1(y),$$

$$\Phi(y) \equiv \frac{3}{2} \frac{\sqrt{2}M^3 \exp(2A(y))}{\bar{\phi}'(y)} \Psi_1'(y). \quad (149)$$

The functions  $A$ ,  $\bar{\phi}$ , and  $\Psi_1$  depending on the fifth coordinate have the form (55), (56), and (73). Substituting Eqns (146)–(148) into the gravitational part of the multi-dimensional Lagrangian (46), we obtain

$$\begin{aligned} \sqrt{-g}R[g] = & \partial^\mu \left[ \exp(-2A) \sqrt{-g^{(0)}} g_{\mu\nu}^{(0)} \frac{(1+8\chi r)\chi}{\sqrt{1+2\chi r}} \partial^\nu r \right] \\ & - \partial_4 \left[ \exp(-2A) \sqrt{-g^{(0)}} \frac{4(1-\chi r)\chi}{\sqrt{1+2\chi r}} \partial_4 (\exp(-2A)(1-\chi r)) \right] \\ & + \sqrt{-g^{(0)}} \left\{ \frac{3}{\sqrt{1+2\chi r}} (\exp(-2A)(1-\chi r))^2 - \exp(-2A) \right. \\ & \times \left. \frac{3(1-4\chi r)\chi^2}{2\sqrt{1+2\chi r}(1-\chi r)} g_{\mu\nu}^{(0)} \partial^\mu r \partial^\nu r \right\} \\ & + \exp(-2A)(1-\chi r) \sqrt{1+2\chi r} \sqrt{-g^{(0)}} R[g^{(0)}]. \end{aligned} \quad (150)$$

The first term in Eqn (150) is a complete 4D divergence, and is therefore discarded in the effective 4D action obtained after the reduction. The second term is the derivative with respect to the fifth coordinate of a certain function that is periodic with respect to this coordinate (since the extra dimension is an orbifold  $S^1/Z_2$ , i.e., a circle of length  $2L$  with additional symmetry conditions; see Section 2 above). Therefore, its integral over the fifth coordinate on the interval  $(-L, L)$  is zero, and, therefore, it does not contribute to the effective action. The third and fourth terms in Eqn (150) describe the nonlinear self-interaction of a radion.

The last term in Eqn (150) is the product of the curvature of the four-dimensional space  $R[g^{(0)}]$  with the metric tensor  $g_{\mu\nu}^{(0)}$  and some function of the radion field  $r$ . After integration over the fifth coordinate, this term describes the nonminimal interaction of the radion field with four-dimensional gravity, and in the lowest approximation it has the form  $\lambda r^2 R$ , with some constant  $\lambda$  of the order of unity. Such terms are unimportant in the present epoch for processes involving SM fields on scales of the order of TeV. Since the process of evolution of the early Universe is not the subject of this review, we do not consider such interactions here and restrict ourselves to only the part  $\exp(-2A)\sqrt{-g^{(0)}}R[g^{(0)}]$  that does not depend on the radion. Note that the integration of this term with respect to the fifth coordinate enables the introduction of the 4D gravitational constant in a way [52] that is alternative to the one presented in Section 2 of this review (see also the discussion and references in [51, 66]).

Substituting Eqns (146)–(148) into the scalar part of the five-dimensional Lagrangian (46) and adding the resulting formula to (150), we obtain the effective four-dimensional action of the radion in the form

$$S_{\text{eff}} = \int [-P(r) g^{(0)\mu\nu} \partial_\mu r \partial_\nu r - U(r)] d^4x, \quad (151)$$

where  $P(r)$  and  $U(r)$  are nonpolynomial functions of  $r$  and have the following implicit representations:

$$P(r) = \frac{1}{2} \int_{-L}^L \left\{ 2M^3 \frac{3(1-4\chi r)\chi^2}{\sqrt{1+2\chi r}(1-\chi r)} + (1-\chi r)\sqrt{1+2\chi r} \Phi^2 \right\} \times \exp(-2A) dy, \quad (152)$$

$$U(r) = \int_{-L}^L \left\{ \frac{6M^3}{\sqrt{1+2\chi r}} (\exp(-2A)(1-\chi r))^2 - \exp(-4A)(1-\chi r)^2 \sqrt{1+2\chi r} \left[ \frac{(\varphi + \Phi r)^2}{2(1+2\chi r)} + V(\varphi + \Phi r) \right] - \exp(-4A)(1-\chi r)^2 [\lambda_0(\varphi + \Phi r) \delta(y) + \lambda_L(\varphi + \Phi r) \delta(y-L)] \right\} dy. \quad (153)$$

Since  $\chi$  and  $\Phi$  are some complex functions of the fifth coordinate, it is not possible to derive an exact analytical formula for  $P(r)$  and  $U(r)$ . Therefore, we seek expansions for  $P(r)$  and  $U(r)$  in power series with respect to  $r$ , reduced to a dimensionless form using some dimensional parameters. To do so, in Eqns (152) and (153), we expand the nonpolynomial functions of  $1+2\chi r$  and  $1-\chi r$  in series in  $\chi r$  in the integrands, assuming  $|2\chi r| < 1$ . Since  $\chi$  is maximum at  $y = L$ , and it follows from (149) and (76) that

$$2\chi(L) = \frac{1}{\sqrt{2M^3}} \Psi_1(L) = \frac{4}{A},$$

we obtain the following restriction on the amplitude of the radion field:

$$|r| < \frac{4}{A}. \quad (154)$$

It is shown below that the minimum of the radion potential is realized at  $r = 0$ , which implies that there are no conditions for a significant deviation of the radion field from zero, so the approximation applied is valid.

In Section 2 (see also [51, 66]), the effective action was presented in the quadratic approximation in  $r$  with terms, linear in  $r$ , of interaction with the SM fields and the interaction constant  $\Lambda^{-1}$ . The next term of interaction with the SM fields, quadratic in  $r$ , has the order  $\Lambda^{-2}$ . It is this order that our consideration in this review is limited to. The terms of the self-interaction of the fourth power in  $r$  in the kinetic term have the order  $\Lambda^{-2}$ , and in the potential term,  $\tilde{\kappa}^2 \Lambda^{-2}$ . Thus, generalizing the results of studies [51, 66], we derive the effective action for the radion with an accuracy of up to the fourth power in  $r$  for the self-interaction of the radion and the second power for the interaction of the radion with the SM fields. Taking into account the above, we represent the functions  $P(r)$  and  $U(r)$  in the form

$$P(r) = \alpha_0 + \alpha_1 r + \alpha_2 r^2, \quad (155)$$

$$U(r) = \beta_0 + \beta_1 r + \beta_2 r^2 + \beta_3 r^3 + \beta_4 r^4, \quad (156)$$

where the coefficients  $\alpha_j$  are determined by the following formulas:

$$\alpha_0 = \frac{1}{2} \int_{-L}^L \{ 6M^3 \chi^2 + \Phi^2 \} \exp(-2A) dy, \quad (157)$$

$$\alpha_1 = -12M^3 \int_{-L}^L \chi^3 \exp(-2A) dy, \quad (158)$$

$$\alpha_2 = \frac{1}{4} \int_{-L}^L \{ 18M^3 \chi^4 - 3\Phi^2 \chi^2 \} \exp(-2A) dy, \quad (159)$$

and the coefficients  $\beta_j$ , which have a similar but somewhat more cumbersome structure, are presented in [52].

We now consider the form of the interaction of the radion field with the SM fields with an accuracy of up to the second order. The first-order interaction in metric fluctuations was presented in Section 3 of this review (see Eqn (80)); we rewrite this formula here for only the radion field:

$$L_r = \frac{1}{2} \int_{-L}^L \chi r \eta^{\mu\nu} T_{\mu\nu} \delta(y-L) dy = \frac{1}{2} \chi(L) r \eta^{\mu\nu} T_{\mu\nu} \equiv \frac{1}{A} r T_\mu^\mu, \quad (160)$$

whence it follows that  $\Lambda^{-1} = \chi(L)/2$ , which coincides with the general formula (82) for  $\kappa_{rn}$  at  $n = 1$  presented in Section 2.

The next order of interaction of the radion field with the SM fields could be obtained by varying  $\sqrt{-g} T_\mu^\mu$  with respect to the metric once again. However, it can be done in a simpler way by expanding the original formula for  $\sqrt{-g} L_{\text{SM}}$  directly in terms of the field  $r$  it contains. To do so, we represent the Lagrangians on the brane at the point  $y = L$  for the scalar ( $h$ ), vector ( $V_\mu$ ), and spinor ( $\psi$ ) fields for the case of the metric  $\tilde{g}_{\mu\nu}$  induced from the metric (146) with  $b_{\mu\nu}^0 = 0$ . For a scalar field, we obtain

$$\begin{aligned} \sqrt{-\tilde{g}} L_{h,\tilde{g}} &= \sqrt{-\tilde{g}} \left\{ -\frac{1}{2} \tilde{g}^{\mu\nu} h_{,\mu} h_{,\nu} - V(h) \right\} \\ &= -\frac{1}{2} \exp(-2A)(1-\chi r) \eta^{\mu\nu} h_{,\mu} h_{,\nu} \\ &\quad - \exp(-4A)(1-\chi r)^2 V(h) = L_{h,\eta} \\ &\quad + r \chi \left[ \frac{1}{2} \exp(-2A) \eta^{\mu\nu} h_{,\mu} h_{,\nu} + 2 \exp(-4A) V(h) \right] \\ &\quad - \chi^2 r^2 \exp(-4A) V(h), \end{aligned} \quad (161)$$

where  $L_{h,\tilde{g}}$  is the Lagrangian with the metric  $\tilde{g}_{\mu\nu}$ ,  $L_{h,\eta}$  is the same Lagrangian with the flat metric  $\eta^{\mu\nu}$ , and  $V(h)$  is the scalar potential. Since on the brane  $y = L$  the function  $A(L) = 0$ , the exponentials in Eqn (161) vanish, and the Lagrangian of the interaction of a radion with a scalar field has the form

$$L_{rh} = -\frac{r}{A} T_\mu^\mu(h) - \frac{4r^2}{A^2} V(h). \quad (162)$$

Similarly, for a vector field, we have

$$\begin{aligned} \sqrt{-\tilde{g}} L_{V,\tilde{g}} &= \sqrt{-\tilde{g}} \left\{ -\frac{1}{4} \tilde{g}^{\mu\nu} \tilde{g}^{\alpha\beta} F_{\mu\nu} F_{\alpha\beta} + \frac{\mu_V^2}{2} \tilde{g}^{\mu\nu} V_\mu V_\nu \right\} \\ &= -\frac{1}{4} \eta^{\mu\nu} \eta^{\alpha\beta} F_{\mu\nu} F_{\alpha\beta} + \exp(-2A)(1-\chi r) \frac{\mu_V^2}{2} \eta^{\mu\nu} V_\mu V_\nu. \end{aligned} \quad (163)$$

As we see, the exact interaction of a radion with a vector field is limited to only one linear term (anomalous type terms, similar to those presented in Eqn (95), are not considered here):

$$L_{rV} = -\frac{r}{A} T_\mu^\mu(V). \quad (164)$$

Finally, for the Lagrangian of a spinor field, we have the following formula:

$$\sqrt{-\tilde{g}} L_{\psi,\tilde{g}} = \sqrt{-\tilde{g}} \left[ \frac{i}{2} \bar{\psi} \gamma^\mu (\nabla_\mu \psi) - \frac{i}{2} (\nabla_\mu \bar{\psi}) \gamma^\mu \psi + m_\psi \bar{\psi} \psi \right], \quad (165)$$

where  $\nabla_\mu \psi$  is the total covariant derivative of the spinor field (including both the metric (tetrad) and gauge parts). However, for a metric that differs from the Minkowski spacetime metric by only some conformal factor, the equality

$$\bar{\psi} \gamma^\mu (\nabla_\mu \psi) - (\nabla_\mu \bar{\psi}) \gamma^\mu \psi = \frac{\exp(A)}{\sqrt{1-\chi r}} (\bar{\psi} \gamma^\mu (D_\mu \psi) - (D_\mu \bar{\psi}) \gamma^\mu \psi) \quad (166)$$

holds, where  $D_\mu \psi$  is the usual covariant derivative (without the tetrad part). As a result, we obtain

$$\begin{aligned} \sqrt{-\tilde{g}} L_{\psi,\tilde{g}} &= \exp(-3A)(1-\chi r)^{3/2} \left( \frac{i}{2} \bar{\psi} \gamma^\mu (D_\mu \psi) - \frac{i}{2} (D_\mu \bar{\psi}) \gamma^\mu \psi \right) \\ &+ \exp(-4A)(1-\chi r)^2 m_\psi \bar{\psi} \psi. \end{aligned} \quad (167)$$

As we can see, the exact formula for the interaction of a radion with a spinor field has a nonpolynomial form. Expanding in  $r$  and retaining terms up to the second power in  $r$  inclusive, we obtain

$$\begin{aligned} L_{r\psi} &= -\frac{r}{A} T_\mu^\mu(\psi) + \frac{r^2}{A^2} \left[ \frac{3}{4} (i \bar{\psi} \gamma^\mu (D_\mu \psi) \right. \\ &\left. - i (D_\mu \bar{\psi}) \gamma^\mu \psi) + 4m_\psi \bar{\psi} \psi \right]. \end{aligned} \quad (168)$$

We now return to the parameters of radion self-interaction. We consider definition (157) for the parameter  $\alpha_0$ . Substituting into it the formulas for  $\chi$  and  $\Phi$  from equations

(149), we obtain

$$\begin{aligned} \alpha_0 &= \frac{9}{4} M^3 \int_{-L}^L \left\{ \frac{\exp(4A)}{\bar{\phi}^2} m_r^2 \left( 1 - \frac{2}{\beta_1^2 + u} \delta(y) \right. \right. \\ &\left. \left. - \frac{2}{\beta_2^2 - u} \delta(y-L) \right) \Psi^2 \right\} dy. \end{aligned} \quad (169)$$

Since  $\alpha_0 \eta^{\mu\nu} \partial_\mu r \partial_\nu r$  is the kinetic term of the free scalar field,  $\alpha_0$  must be equal to  $1/2$ , which, taking into account Eqn (169), yields the normalization condition for the function  $\Psi$ .

Next, substituting Eqns (55) and (56) for  $\phi$  and  $A$ , respectively, into the formula for  $\beta_0$  (see [52]), we can verify that  $\beta_0 = 0$ , i.e., the effective 4D cosmological constant in this model is zero. In a similar way, we can verify that  $\beta_1 = 1$ , as it should be for the Lagrangian of fluctuations over the background, which is a solution to the equations of motion. Finally, the formula for  $\beta_2$  coincides with  $-m_r^2$  (see [52]) up to a factor of  $\alpha_0$ ; therefore,

$$\beta_2 = -\frac{m_r^2}{2}, \quad (170)$$

as it should be for the quadratic part of the potential of the scalar field with mass  $m_r$ .

Unfortunately, the formulas for  $\alpha_1$ ,  $\alpha_2$ ,  $\beta_3$ , and  $\beta_4$  cannot be represented as known elementary or special functions of the parameters of the multidimensional theory. Therefore, we represent their approximate formulas as the first terms of expansions in series in the following small dimensionless combinations of the model parameters:

$$\xi = \frac{m_r}{k}, \quad \sigma = \frac{u}{k}, \quad \rho = \frac{\phi_0}{2M^3}. \quad (171)$$

Since the constants  $\alpha_j$  and  $\beta_j$  are dimensional, it is reasonable to switch to some dimensionless expressions obtained from the original ones using a suitable dimensional factor. These factors are the constant  $A^{-1}$  of the interaction of a radion with the SM fields and the mass  $m_r$  of the radion itself. The constants  $\alpha_1$  and  $\alpha_2$  are of the order of  $A^{-1}$  and  $A^{-2}$ , respectively, so the natural normalization parameter for them is  $A$ . The constant  $\beta_2$  is naturally normalized to  $m_r$  (see (170)). For the constant  $\beta_3$ , the natural normalization should be different, since it is of the order of  $m_r^2 A^{-1}$ , and the constant  $\beta_4$  is generally dimensionless. On the other hand, to compare the potential of radion self-interaction with the Higgs boson potential, it is convenient to factor out the factor  $m_r^2$  in it. As a result, taking into account Eqns (155) and (156), we arrive at the following form of the effective Lagrangian of the radion self-interaction with dimensionless constants  $\bar{\alpha}_1$ ,  $\bar{\alpha}_2$ ,  $\bar{\beta}_3$ , and  $\bar{\beta}_4$ :

$$\begin{aligned} L_r &= -\left( \frac{1}{2} + \frac{\bar{\alpha}_1}{A} r + \frac{\bar{\alpha}_2}{A^2} r^2 \right) \eta^{\mu\nu} r_{,\mu} r_{,\nu} \\ &- m_r^2 \left( \frac{1}{2} r^2 + \frac{\bar{\beta}_3}{A} r^3 + \frac{\bar{\beta}_4}{A^2} r^4 \right), \end{aligned} \quad (172)$$

where

$$\alpha_1 \equiv \frac{1}{A} \bar{\alpha}_1, \quad \alpha_2 \equiv \frac{1}{A^2} \bar{\alpha}_2, \quad \beta_3 \equiv \frac{m_r^2}{A} \bar{\beta}_3, \quad \beta_4 \equiv \frac{m_r^2}{A^2} \bar{\beta}_4.$$

The analytical formulas for the dimensionless constants  $\bar{\alpha}_1$ ,  $\bar{\alpha}_2$ ,  $\bar{\beta}_3$ , and  $\bar{\beta}_4$ , even in the lower orders of expansions in small

parameters (171), are rather cumbersome. Study [52] presents formulas for these coefficients and for the effective constant of interaction of a radion with the SM fields,  $\Lambda^{-1}$ , with an accuracy of  $O(\sigma^3)$  and  $O(\xi^3)$ . Here, we present a formula for the effective 4D Lagrangian of the radion with an accuracy of up to zeroth order for the introduced combinations of model parameters:

$$L_r = -\left(\frac{1}{2} - \frac{2}{\Lambda} r + \frac{1}{\Lambda^2} r^2\right) \eta^{\mu\nu} r_{,\mu} r_{,\nu} - \frac{m_r^2}{2} r^2 - \frac{5m_r^2}{2\Lambda} r^3 - \frac{1}{\Lambda^2} \left(18\tilde{k}^2 - \frac{5}{3} m_r^2\right) r^4. \quad (173)$$

This formula shows that, when taking into account the nonlinear interactions of the radion field, its kinetic term has a nonstandard form. There is a nonlinear transformation of the radion field  $r \rightarrow \tilde{r}$ , which transforms the kinetic term into a canonical form [52]. Unfortunately, it is not possible to express  $r$  through  $\tilde{r}$  using known elementary or special functions. Nevertheless, with an accuracy of  $\tilde{r}^3$ , it is easy to obtain the following expansion in a series in  $\tilde{r}$ :

$$r = \tilde{r} - \frac{\alpha_1}{2} \tilde{r}^2 + \frac{1}{3} (2\alpha_1^2 - \alpha_2) \tilde{r}^3 + \dots \quad (174)$$

The third order in expansion (174) is sufficient to derive a formula for the potential  $U$  with an accuracy of up to the fourth power in  $\tilde{r}$ ,

$$U(\tilde{r}) = \frac{m_r^2}{2} \tilde{r}^2 + \lambda_3 \tilde{r}^3 + \lambda_4 \tilde{r}^4 + O(\tilde{r}^5), \quad (175)$$

where

$$\lambda_3 \equiv \frac{m_r^2}{\Lambda} \left(\bar{\beta}_3 - \frac{\bar{\alpha}_1}{2}\right), \quad \lambda_4 \equiv \frac{m_r^2}{\Lambda^2} \left(\bar{\beta}_4 - \frac{3\bar{\alpha}_1\bar{\beta}_3}{2} + \frac{19\bar{\alpha}_1^2 - 8\bar{\alpha}_2}{24}\right).$$

According to [52], with an accuracy of zeroth order in small parameters of the model ( $\xi$  and  $\sigma$  (see (171))), for  $\lambda_3$  and  $\lambda_4$  we can obtain the following approximate expressions:

$$\lambda_3 \approx \frac{m_r^2}{\Lambda} \left(\frac{5}{2} + \exp(2Lu)\right) \approx \frac{7}{2} \frac{m_r^2}{\Lambda}, \quad (176)$$

$$\lambda_4 \approx \frac{m_r^2}{\Lambda^2} \left(\frac{47}{12} \exp(2Lu) + \frac{19}{4}\right) + \frac{18\tilde{k}^2}{\Lambda^2} \approx \frac{18\tilde{k}^2}{\Lambda^2}. \quad (177)$$

Note that the factor  $\tilde{k}^2/\Lambda^2$  in the second term on the right side of the formula for  $\lambda_4$  is greater than the factor  $m_r^2/\Lambda^2$  in the first term by 2 to 4 orders of magnitude ( $\xi^{-2}$  times). Then, taking into account relation (7) between the Planck mass and the fundamental energy scale, we obtain that  $\tilde{k} \sim \Lambda^{-1}$ :

$$\frac{18\tilde{k}^2}{\Lambda^2} \approx \frac{18}{\Lambda^2 L^2} \ln^2 \left( \sqrt{\frac{3}{8}} \frac{M_{\text{Pl}}}{\Lambda} \right). \quad (178)$$

Hence, for example, at  $\Lambda \sim 10$  TeV and  $L \sim 10$  TeV $^{-1}$ , we obtain the estimate  $\tilde{k} \sim 3.3$  TeV,  $18\tilde{k}^2/\Lambda^2 \sim 1.9$ , while at  $\Lambda \sim 20$  TeV and  $L \sim 20$  TeV $^{-1}$ , we have  $\tilde{k} \sim 1.6$  TeV and  $18\tilde{k}^2/\Lambda^2 \sim 0.11$ .

To date, it has been assumed that the values of the parameters  $\tilde{k}$  and  $\Lambda$  range from several units to several ten TeV. If we additionally assume that the resulting effective theory should be perturbative, the value of  $\beta_4$  should not exceed some maximum value of  $\beta_{4\text{max}}$ , which provides an

additional constraint on the ratio of the parameters  $\tilde{k}$  and  $\Lambda$ :

$$\tilde{k} < \Lambda \sqrt{\frac{\beta_{4\text{max}}}{18}}. \quad (179)$$

The self-interaction parameter

$$\lambda_3 \approx \frac{7}{2} \frac{m_r^2}{\Lambda}$$

with the cubic term  $\tilde{r}^3$  has the dimension of mass, while the parameter

$$\lambda_4 \approx \frac{18\tilde{k}^2}{\Lambda^2}$$

with the fourth-power term  $\tilde{r}^4$  is dimensionless, so a direct comparison of these quantities is incorrect. Nevertheless, in a certain sense, the value of the second parameter is much greater than that of the first. For example, in the amplitudes of processes described by diagrams with four external radion lines, in the low-energy limit, the contribution from a tree diagram with two three-prong vertices is proportional to  $\lambda_3^2/m_r^2$ , while the contribution from a diagram with one four-prong vertex is proportional to  $\lambda_4$ , i.e., it is  $72\tilde{k}^2/49m_r^2$  times greater. The large (compared to  $\lambda_3^2/m_r^2$ ) value of  $\lambda_4$  also guarantees that in the effective model obtained after the reduction, the radion is at a true minimum. Indeed, the derived quartic potential could have, in addition to the minimum located at zero, a couple more minima, should the equation

$$\frac{dU}{d\tilde{r}} = \{m_r^2 + 3\lambda_3\tilde{r} + 4\lambda_4\tilde{r}^2\}\tilde{r} = 0 \quad (180)$$

have more than one solution. For this, the discriminant of the corresponding quadratic equation must be positive. However, this is not the case:

$$D = 9\lambda_3^2 - 16\lambda_4m_r^2 = 16m_r^2\lambda_4 \left( \frac{49m_r^2}{128\tilde{k}^2} - 1 \right) < 0. \quad (181)$$

The nonlinear transformation  $r \rightarrow \tilde{r}$  makes it possible to formulate the entire model obtained after the reduction in terms of  $\tilde{r}$ —a scalar field with a standard kinetic term, a polynomial potential, and polynomial terms of interaction with the SM fields. However, this is not really necessary, since the analysis of interactions with the SM fields and the obtained results regarding the similarity of processes involving the radion and the Higgs boson are best seen using the standard definition of the radion field, which is used in all studies on this topic.

Thus, the complete theory of the scalar field (radion) arising in the stabilized RS model includes self-interaction terms in both the potential and kinetic terms. The interaction with the SM fields also contains additional terms, and only the interaction with vector fields is limited to a single linear (in radion) term, while the radion self-interaction and its interaction with spinor fields (but not with vector and scalar ones) are nonpolynomial.

It is also worth noting that the potential obtained in the approximation under consideration has a stable minimum at zero, i.e., no additional spontaneous shift of the radion field occurs. This attests to the correctness of the polynomial expansion near the zero value of the radion field.

## 7. Mixing of Higgs and radion fields

As we have already noted, the radion field and the fields of its KK tower have the same quantum numbers as the neutral Higgs field. Thus, the radion field and its excitations can mix with the Higgs field if there is an interaction between them. Initially, a bilinear interaction of the Higgs and radion fields in the unstabilized RS model, arising from the term of the Higgs field interaction with the brane curvature, was proposed in [72]. Later, such an interaction and the resulting mixing of the Higgs and radion in the case of the stabilized model were discussed in [73] without taking into account the KK tower of higher scalar excitations. The phenomenology of Higgs-radion mixing arising from the term of interaction between the Higgs field and curvature has also been discussed in connection with the unconfirmed observation of a Higgs-like scalar boson at the LHC [74, 75]; various proposals for masses and mixing of scalar states have been analyzed in [76–83]. In particular, it has been shown that a radion-dominated light state with a mass lower or higher than the observed 125 GeV Higgs boson is still not completely ruled out by all available stringent constraints on the electroweak parameters and the LHC data.

Although the term of interaction of the Higgs with curvature yields a bilinear interaction of the Higgs field with the radion field, after spontaneous symmetry breaking on the brane, it also gives rise to a brane-localized curvature term, which strongly affects the mass spectrum and the interaction of the graviton KK modes with matter [84]. Even for fairly large values of the model parameters in the range of several TeV, this can lead to quite small masses of the KK excitations of the graviton, which is in poor agreement or even in disagreement with current experimental constraints on such masses.

Below, following [85], we discuss a model in which the bilinear interaction of the Higgs and radion fields arises in a natural way due to a mechanism of spontaneous symmetry-breaking on the brane involving a stabilizing scalar field. This approach takes into account the effect of the KK tower of higher scalar excitations on the Higgs and radion mixing parameters, which turns out to be significant. It also has the advantage of altering only the scalar sector of the model and leaving the masses and coupling constants of the KK excitations of the graviton unchanged. Namely, we obtain the coupling of the Higgs and radion fields by combining the mechanisms of stabilizing the size of the extra dimension and spontaneous symmetry-breaking in the SM. In our analysis, we essentially use the results of [51] for fluctuations of the Goldberger–Wise scalar field in stabilized brane models. For the action (46) of the stabilized RS model, the vacuum solution for gravity and the stabilizing scalar field and the vacuum solution for the SM fields are independent. If we consider this brane world model as a unified theory, it is reasonable to assume that there should be a common interconnected vacuum solution for all of the fields. To do so, we change the action of the Goldberger–Wise field and the SM in (46) so that it contains an interaction of the stabilizing scalar field and the fourth-power Higgs field, which would simultaneously lead to stabilization of the size of the extra dimension and spontaneous symmetry-breaking in the SM:

$$S_{\phi+\text{SM}} = \int d^4x \int_{-L}^L dy \left( \frac{1}{2} g^{MN} \partial_M \phi \partial_N \phi - V(\phi) \right) \sqrt{g} - \int_{y=0} \sqrt{-\bar{g}} \lambda_1(\phi) d^4x + \int_{y=L} \sqrt{-\bar{g}} (-\lambda_2(\phi)) + L_{\text{SM-HP}} + L_{\text{int}}(\phi, H) d^4x, \quad (182)$$

where the Lagrangian  $L_{\text{SM-HP}}$  is the SM Lagrangian without the Higgs potential, which is replaced by the interaction Lagrangian

$$L_{\text{int}}(\phi, H) = -\lambda \left( |H|^2 - \frac{\xi}{M} \phi^2 \right)^2, \quad (183)$$

in which  $\xi$  is a positive dimensionless parameter. A similar interaction Lagrangian, quadratic in the stabilizing scalar field, was discussed in [86].

The background solutions for the metric and the scalar field that preserve Poincaré invariance in any four-dimensional subspace  $y = \text{const}$  have the same form as (55), (56); the background (vacuum) solution for the Higgs field is standard,

$$H_{\text{vac}} = \begin{pmatrix} 0 \\ \frac{v}{\sqrt{2}} \end{pmatrix}, \quad (184)$$

and all other SM fields are zero.

If we substitute this ansatz into the equations corresponding to action (182), we obtain a relation between the vacuum value of the Higgs field and the value of the field  $\phi$  on the brane at  $y = L$ :

$$\phi^2(L) = \frac{Mv^2}{2\xi}. \quad (185)$$

This relation implies that in such a scenario the vacuum value of the Higgs field, being proportional to the value of the stabilizing scalar field on the TeV brane, arises dynamically as a result of gravitational stabilization of the size of the extra dimension.

The gravitational background solution is obtained from the system of nonlinear differential equations (52)–(54) for the functions  $A(y), \bar{\phi}(y)$ . Suppose we have a solution  $A(y), \bar{\phi}(y)$  of this system for an appropriate choice of the parameters of the potentials such that the distance between the branes is stabilized and equal to  $L$ . Then, the vacuum energy of the scalar field has a minimum for this value of the distance.

Now, similarly to Eqns (60) and (61), the linearized theory is obtained by representing the metric, scalar, and Higgs field in the unitary gauge as

$$g_{MN}(x, y) = \bar{g}_{MN}(y) + \frac{1}{\sqrt{2M^3}} h_{MN}(x, y), \quad (186)$$

$$\phi(x, y) = \bar{\phi}(y) + \frac{1}{\sqrt{2M^3}} f(x, y), \quad (187)$$

$$H(x) = \begin{pmatrix} 0 \\ \frac{v + \sigma(x)}{\sqrt{2}} \end{pmatrix}, \quad (188)$$

substituting this representation into action (182), and retaining the second-order terms in  $h_{MN}, f$ , and  $\sigma$ . The Lagrangian of this action is the standard free SM Lagrangian (i.e., the masses of all SM fields except the Higgs field are expressed as usual in terms of the vacuum value of the Higgs field and the coupling constants) together with the standard Lagrangian of the second variation of the stabilized RS model [51], supplemented by the term of an interaction between the fields  $f$  and  $\sigma$ . The part of the Lagrangian related to the

mixing of the Higgs and radion fields is

$$\left[ -\frac{1}{2M^3} \left( \frac{1}{2} \frac{d^2 \lambda_2}{d\phi^2} + \frac{2\lambda v^2 \xi}{M} \right) f^2 + \frac{2\lambda v^2 \sqrt{\xi}}{M^2} f\sigma - \frac{1}{2} 2\lambda v^2 \sigma^2 \right] \delta(y-L). \quad (189)$$

The five-dimensional scalar field  $f$  can be expanded in Kaluza–Klein modes. In the case under consideration, we can derive equations for the mass spectrum and wave functions of KK excitations of scalar fields in a standard way, simply replacing

$$\frac{1}{2} \frac{d^2 \lambda_2}{d\phi^2} \rightarrow \frac{1}{2} \frac{d^2 \lambda_2}{d\phi^2} + \frac{2\lambda v^2 \xi}{M}$$

in the equations of [51] (note that the metric signature  $(-, +, +, +, +)$  was used in that publication, and therefore some formulas in [51] may differ in sign from the corresponding formulas in this review). Namely, that study showed that the scalar degrees of freedom of stabilized brane world models are most conveniently described by the field  $\varphi = \exp(-2A(y)) h_{44}(x, y)$ , associated with the field  $f$  by the gauge condition (62). The equations of motion and the boundary conditions on the branes for the field  $\varphi$  determine the wave functions  $\Psi_n(y)$  corresponding to the eigenvalues of the masses  $m_n^2$ . Expanding the field  $f$  in such modes, substituting the resulting expansion into the Lagrangian of the second variation, and integrating over the coordinate of the additional dimension  $y$ , we obtain a 4D Lagrangian which contains a bilinear interaction between the modes of the field  $f$  and the Higgs field, arising from the term

$$\frac{2\lambda v^2 \sqrt{\xi}}{M^2} f\sigma.$$

Using the gauge condition (62), the expansion in modes of the field  $\varphi(x, y)$ ,

$$\varphi(x, y) = \sum_{n=0}^{\infty} \varphi_n(x) \Psi_n(y),$$

and the boundary condition for the wave function of mode  $\Psi_n(y)$  at  $y = L$  [51] presented in terms of Eqn (189),

$$\left( \frac{1}{2} \frac{d^2 \lambda_2}{d\phi^2} + \frac{\bar{\phi}''}{\bar{\phi}'} + \frac{2\lambda v^2 \xi}{M} \right) \Psi_n' - m_n^2 \exp(2A) \Psi_n \Big|_{y=L} = 0,$$

we can express the field  $f$  in terms of  $\Psi_n(y)$  as follows:

$$\begin{aligned} \frac{f(x, L)}{3M^3} &= -\frac{\varphi' \exp(2A)}{\bar{\phi}'} \Big|_{y=L} = -\frac{\varphi'}{\bar{\phi}'} \Big|_{y=L} \\ &= -\sum_{n=1}^{\infty} \frac{m_n^2}{[(1/2)(d^2 \lambda_2/d\phi^2) + (\bar{\phi}''/\bar{\phi}') + (2\lambda v^2 \xi/M)] \bar{\phi}'} \\ &\quad \times \Psi_n(L) \varphi_n(x), \end{aligned}$$

where we have taken into account that  $A(L) = 0$ , so that the coordinates on the brane at  $y = L$  are Galilean [22].

Thus, the interaction of the modes with the Higgs field can be presented as

$$\sum_{n=1}^{\infty} m_n^2 a_n \varphi_n(x) \sigma(x),$$

where we introduced dimensionless quantities

$$-\frac{6\lambda M v^2 \sqrt{\xi}}{[(1/2)(d^2 \lambda_2/d\phi^2) + (\bar{\phi}''/\bar{\phi}') + (2\lambda v^2 \xi/M)] \bar{\phi}'} \Psi_n(L) = a_n, \quad (190)$$

which are assumed to be positive.

These interaction terms are proportional to the mode masses squared and can be fairly large at large  $n$ . We show below that it is the dimensionless quantities  $a_n$  that are of importance. They are proportional to the values of the wave functions of the modes on the brane and can be conveniently expressed in terms of the ratios of the latter and  $a_1$ :

$$a_n = a_1 \alpha_n, \quad \alpha_n = \frac{\Psi_n(L)}{\Psi_1(L)}. \quad (191)$$

These ratios must tend to zero at large  $n$ , so the overall effect of the KK tower of the radion is finite. In [51], the scalar wave functions  $\Psi_n(y)$  were found explicitly in a stabilized brane world model where the conformal factor is approximately equal to that in the unstabilized RS model. It can also be verified that the  $a_n$  values are indeed positive and the  $\alpha_n$  ratios in this case indeed fall off rather rapidly for large  $n$ . Finding them explicitly in stabilized brane world models where the conformal factor differs from the exponential of a linear function, as in the RS model, is fairly challenging. Such stabilized brane world models were studied in [22, 51] to conclude that they can also solve the hierarchy problem of gravitational interactions, providing masses of KK excitations in the TeV energy range. However, the corresponding equations cannot be solved exactly and must be explored numerically for each set of fundamental parameters of the model, which is a very challenging and time-consuming task.

Here, we do not make such calculations for a particular stabilized brane model, but rather give a qualitative description of the phenomena that are due to the interaction of the Higgs field with the radion and its KK tower, choosing the masses and coupling constants in a consistent way and taking into account modern theoretical and experimental constraints on their values.

**Effective Lagrangian of model with mixing.** The part of the extended SM Lagrangian containing the scalar fields in a linear or quadratic form is as follows:

$$\begin{aligned} L_{\text{part}} &= \frac{1}{2} \partial_\mu \sigma \partial^\mu \sigma - \frac{1}{2} 2\lambda v^2 \sigma^2 + \frac{1}{2} \sum_{n=1}^{\infty} \partial_\mu \phi_n \partial^\mu \phi_n \\ &\quad - \frac{1}{2} \sum_{n=1}^{\infty} m_n^2 \phi_n^2 + \sum_{n=1}^{\infty} m_n^2 a_n \phi_n \sigma - \sum_f \frac{m_f}{v} \bar{\psi}_f \psi_f \sigma \\ &\quad - \sum_{n=1}^{\infty} b_n \phi_n (T_\mu^\mu + \Delta T_\mu^\mu) + \frac{2M_W^2}{v} W_\mu^- W^{\mu+} \sigma \\ &\quad + \frac{M_Z^2}{v} Z_\mu Z^\mu \sigma + \frac{M_W^2}{v^2} W_\mu^- W^{\mu+} \sigma^2 + \frac{M_Z^2}{2v^2} Z_\mu Z^\mu \sigma^2, \end{aligned} \quad (192)$$

where  $T_\mu^\mu$  is the trace of the SM EMT, and  $\Delta T_\mu^\mu$  is the conformal anomaly of the massless vector fields, explicitly given by the equation

$$\Delta T_\mu^\mu = \frac{\beta(e)}{2e} F_{\rho\sigma} F^{\rho\sigma} + \frac{\beta(g_s)}{2g_s} G_{\rho\sigma}^{ab} G^{a\rho\sigma}_{ab}, \quad (193)$$

where  $\beta$  are the known QED and QCD  $\beta$ -functions.



The interaction of scalar modes with the EMT trace is described by the standard interaction Lagrangian for metric fluctuations [51], which leads to an expression for the parameters  $b_n$  in terms of the wave functions of the scalar modes:

$$b_n = \frac{1}{2\sqrt{8M^3}} \Psi_n(L). \quad (194)$$

In the case of the lowest scalar mode, the radion, this parameter is usually denoted as

$$b_1 = \frac{1}{\Lambda}, \quad (195)$$

where  $\Lambda$  is assumed to be of the order of the fundamental energy scale  $M$ . We use below  $\Lambda$  as a natural scale for the interactions of the radion and the interactions generated by its KK tower. For this reason, it is also convenient to express  $b_n$  in terms of  $\Lambda$  and  $\alpha_n$ , defined in Eqn (191) as

$$b_n = \frac{\alpha_n}{\Lambda}. \quad (196)$$

In what follows, we examine the phenomenology of the Higgs boson and radion in a range of energies much smaller than the masses of the radion excitations. In this case, we can move to the low-energy approximation for this Lagrangian by discarding the kinetic terms of the radion excitation fields and integrating them, which yields the following effective Lagrangian for the interactions of the Higgs and radion fields with the SM fields:

$$\begin{aligned} L_{\text{part-eff}} = & \frac{1}{2} \partial_\mu \sigma \partial^\mu \sigma - \frac{1}{2} (2\lambda v^2 - d^2) \sigma^2 + \frac{1}{2} \partial_\mu \varphi_1 \partial^\mu \varphi_1 \\ & - \frac{1}{2} m_1^2 \varphi_1^2 + m_1^2 a_1 \varphi_1 \sigma - \frac{1}{\Lambda} \varphi_1 (T_\mu^\mu + \Delta T_\mu^\mu) \\ & - \frac{c}{\Lambda} \sigma (T_\mu^\mu + \Delta T_\mu^\mu) - \sum_f \frac{m_f}{v} \bar{\psi}_f \psi_f \sigma \\ & + \frac{2M_W^2}{v} \mathbf{W}_\mu^- \mathbf{W}^{\mu+} \sigma + \frac{M_Z^2}{v} Z_\mu Z^\mu \sigma \\ & + \frac{M_W^2}{v^2} \mathbf{W}_\mu^- \mathbf{W}^{\mu+} \sigma^2 + \frac{M_Z^2}{2v^2} Z_\mu Z^\mu \sigma^2, \end{aligned} \quad (197)$$

where the new parameters are defined in terms of the old ones as follows:

$$c = a_1 \sum_{n=2}^{\infty} \alpha_n^2, \quad d^2 = a_1^2 \sum_{n=2}^{\infty} m_n^2 \alpha_n^2. \quad (198)$$

We have already mentioned that these series must converge. The positive parameter  $d^2$  can be of the order of  $v^2$ , because the mass term  $2\lambda v^2 - d^2$  must be positive, and, in the approach under consideration, the self-coupling constant of the Higgs boson  $\lambda$  can be larger than in the usual SM case. Possible restrictions on the parameter  $c$  are considered below.

Next, we consider the mass matrix of the fields  $\sigma$  and  $\varphi_1$ , which has the form

$$\mathcal{M} = \begin{pmatrix} 2\lambda v^2 - d^2 & -\frac{1}{2} m_1^2 a_1 \\ -\frac{1}{2} m_1^2 a_1 & m_1^2 \end{pmatrix}. \quad (199)$$

This matrix can be diagonalized using the rotation matrix

$$\mathcal{R} = \begin{pmatrix} \cos \theta & -\sin \theta \\ \sin \theta & \cos \theta \end{pmatrix}, \quad \mathcal{R}^T \mathcal{M} \mathcal{R} = \text{diag}(m_h^2, m_r^2),$$

where the rotation angle  $\theta$  is defined by the relation

$$\tan(2\theta) = \frac{m_1^2 a_1}{m_1^2 - 2\lambda v^2 + d^2}. \quad (200)$$

It is easy to see that it is sufficient to consider this angle in only the interval  $-\pi/4 < \theta < \pi/4$ , which is one full period of the function  $\tan(2\theta)$ .

The observed masses of the mass eigenstates are given by the formulas

$$\begin{aligned} m_h^2 = & 2\lambda v^2 - d^2 - \frac{m_1^2 - 2\lambda v^2 + d^2}{2} \\ & \times \left( \sqrt{1 + \frac{4a_1^2}{(m_1^2 - 2\lambda v^2 + d^2)^2}} - 1 \right), \\ m_r^2 = & m_1^2 + \frac{m_1^2 - 2\lambda v^2 + d^2}{2} \\ & \times \left( \sqrt{1 + \frac{4a_1^2}{(m_1^2 - 2\lambda v^2 + d^2)^2}} - 1 \right), \end{aligned}$$

which are presented in a form that explicitly shows that, due to mixing, the smaller mass becomes smaller and the larger mass becomes larger, which, notably, implies that the observed masses of  $m_r^2$  and  $m_h^2$  cannot be exactly equal in the presence of mixing, and the mixing angle  $\theta$  is negative for  $m_r^2 < m_h^2$  in accordance with the observation made in [73].

It is also worth noting that the mass matrix in Eqn (199) and the corresponding mixing with the rotation matrix  $\mathcal{R}$  are very similar to those appearing in the SM extended with an additional singlet scalar [87, 88].

The original unobservable parameters of the matrix  $\mathcal{M}$  can be expressed in terms of the observable parameters  $m_h^2$ ,  $m_r^2$ , and  $\theta$ , with a one-to-one correspondence, provided that for  $m_h^2 = m_r^2$  the mixing angle  $\theta = 0$ . The following formulas can then be easily obtained for the parameters  $a_1$  and  $c$  in terms of the physical masses and the mixing angle:

$$\begin{aligned} a_1 = & \frac{(m_r^2 - m_h^2) \sin(2\theta)}{m_r^2 \cos^2 \theta + m_h^2 \sin^2 \theta}, \\ c = & \frac{(m_r^2 - m_h^2) \sin(2\theta)}{m_r^2 \cos^2 \theta + m_h^2 \sin^2 \theta} \left( \sum_{n=2}^{\infty} \alpha_n^2 \right), \end{aligned}$$

with the latter parameter also depending on the sum of the ratios of the wave functions  $\alpha_n^2$ . Such ratios are certainly model dependent, and, although they must decrease with  $n$  for the sum to be convergent, it cannot be ruled out that in some models the first few ratios may be of the order of unity. Thus, this sum can also be estimated as having the order of unity, because, for example, in the stabilized model discussed in [51], the approximate wave functions of the scalar modes yield rather rough estimates for the value of this sum in the interval (0.02, 0.2) for the radion mass in the range  $100 < m_r < 500$  GeV and the mass of its first KK excitation of the order of 1–2 TeV. As a result, we obtain an estimate for

the parameter  $c$ ,

$$0 < c < \frac{(m_r^2 - m_h^2) \sin(2\theta)}{m_r^2 \cos^2 \theta + m_h^2 \sin^2 \theta}, \quad (201)$$

which is used in subsequent calculations.

The physical fields of mass eigenstates,  $h(x), r(x)$ , are easily expressed through the matrix  $\mathcal{R}$  and the original fields as

$$\begin{aligned} h(x) &= \cos \theta \sigma(x) + \sin \theta \varphi_1(x), \\ r(x) &= -\sin \theta \sigma(x) + \cos \theta \varphi_1(x). \end{aligned} \quad (202)$$

We call the  $h(x)$  field the Higgs-dominated field, and the  $r(x)$  field the radion-dominated field, because  $\cos \theta > |\sin \theta|$  in the interval  $-\pi/4 < \theta < \pi/4$  (recall that  $\theta < 0$  for  $m_r^2 < m_h^2$ ). The interaction of these fields with the SM fields is described by the following effective Lagrangian:

$$\begin{aligned} L_{h-r} &= \frac{1}{2} \partial_\mu h \partial^\mu h - \frac{1}{2} m_h^2 h^2 + \frac{1}{2} \partial_\mu r \partial^\mu r - \frac{1}{2} m_r^2 r^2 \\ &\quad - \frac{(c \cos \theta + \sin \theta)}{A} h(T_\mu^\mu + \Delta T_\mu^\mu) + \frac{(c \sin \theta - \cos \theta)}{A} \\ &\quad \times r(T_\mu^\mu + \Delta T_\mu^\mu) - \sum_f \frac{m_f}{v} \bar{\psi}_f \psi_f (h \cos \theta - r \sin \theta) \\ &\quad + \frac{2M_W^2}{v} W_\mu^- W^{\mu+} (h \cos \theta - r \sin \theta) + \frac{M_Z^2}{v} Z_\mu Z^\mu \\ &\quad \times (h \cos \theta - r \sin \theta) + \frac{M_W^2}{v^2} W_\mu^- W^{\mu+} (h \cos \theta - r \sin \theta)^2 \\ &\quad + \frac{M_Z^2}{2v^2} Z_\mu Z^\mu (h \cos \theta - r \sin \theta)^2. \end{aligned} \quad (203)$$

The effective 4D interaction Lagrangian (203), expressed in terms of the Higgs-dominated  $h(x)$  and radion-dominated  $r(x)$  physical fields, contains their interactions with the SM fields and includes only five parameters in addition to the SM parameters. They are the masses of the Higgs-dominated and radion-dominated  $m_h$  and  $m_r$  fields, the mixing angle  $\theta$ , the (inverse) constant of coupling of the radion to the trace of the EMT of the SM fields  $A$ , and the parameter  $c$ , which takes into account the contributions of the integrated heavy scalar modes. It should be noted that we do not assume a priori whether the 125 GeV boson observed at the LHC corresponds to a Higgs-dominated or radion-dominated state.

It is interesting to see what happens to Lagrangian (203) as the fundamental energy scale  $M$  tends to infinity. In the model under consideration, it is not possible to simply take the limit  $M \rightarrow \infty$  due to relation (185) for the model parameters, which includes the vacuum value of the Higgs field. In the stabilized brane world model discussed in [51], the mass of the radion turns out to be proportional to  $\phi^2(L)/M^3$ . Thus, to keep this mass fixed, we must take the limits  $M \rightarrow \infty$  and  $\xi \rightarrow 0$ , so that  $M^2 \xi = \text{const}$ . It is easy to see that in this case  $a_1$ , which is proportional to  $M\sqrt{\xi}$ , does not vanish, whereas the parameter  $A$  defined in Eqns (194) and (195) tends to infinity. As a result, in Lagrangian (203), the terms with the energy–momentum tensor proportional to  $1/A$  vanish, but all other terms remain unchanged, since the mixing angle must not be zero.

If we formally set the parameters  $a_1$ ,  $c$ , and  $\theta$  equal to zero, i.e., consider the case of zero mixing, Lagrangian (203) becomes simply the Higgs Lagrangian of the SM plus the

usual Lagrangian of the interaction of the radion with the SM fields via the SM EMT trace. In the case of nonzero mixing, additional terms appear in this Lagrangian, which can lead to certain changes in the collider phenomenology of the Higgs boson and radion.

**Some phenomenological implications of the model.** The effective Lagrangian (203) describes the interactions of the Higgs-dominated  $h(x)$  and radion-dominated  $r(x)$  fields with the SM fields and with each other. Several natural questions arise. What ranges of the model parameters are allowed by the available experimental data from the LEP and Tevatron, the discovery of the 125 GeV Higgs boson, the measurement of the Higgs signal strength for various signatures at the LHC, and the limits set by the search for the second Higgs boson at the LHC? Is it possible to interpret the observed boson as a radion-dominated state for some values of the model parameters?

We present below a phenomenological illustration involving only the two main channels in the LHC discovery, in which scalar particles are produced in gluon fusion and decay into two photons ( $\gamma\gamma$  mode) or into four leptons ( $ZZ^*$  mode).

The Feynman rules needed for our study, which can be easily derived from Lagrangian (203), are presented in [85]. They omit the terms coming from off-shell fermions, since the corresponding contributions to the physical processes are exactly compensated by additional diagrams with contact four-prong vertices coming from the next-order expansions of the trace of the SM energy–momentum tensor, as was proven in [68].

The Feynman rules were implemented as a ‘new model’ in a special version of the CompHEP package [89–91], also including a procedure for  $\chi^2$ -analysis of the strength of the Higgs boson signal in a manner similar to those used in [92, 93]. NLO corrections are taken into account in the CompHEP calculations by introducing appropriate form factors. NNLO corrections are taken into account in the corresponding analysis by multiplying the involved vertices by correction factors for each point in the model parameter space, such that the partial and total decay widths of the SM Higgs boson and the Higgs production cross sections in gluon fusion are exactly the same as those reported by the LHC Higgs Cross Section Working Group [94, 95]. Due to the similarity of Higgs and radion production and decay amplitudes, including the loop diagrams [68], the same correction factors were used for the Higgs-dominated and radion-dominated states.

We consider two possible scenarios where the observed 125 GeV boson is either a Higgs-dominated state or a radion-dominated one.

### 7.1 Higgs-dominated state with mass 125 GeV

To determine the mass range allowed for the radion-dominated state in this case, we first demonstrate the various production and decay properties of this state. Figure 11 shows the partial decay widths for the radion-dominated boson as a function of its mass.

Figure 11a shows the well-known behavior of the partial decay widths of the radion without Higgs mixing and with interaction with the SM fields only through the EMT trace. The main decay mode of the light radion is decay into two gluons, known to be due to anomaly enhancement. However, as soon as Higgs mixing is turned on, the picture changes

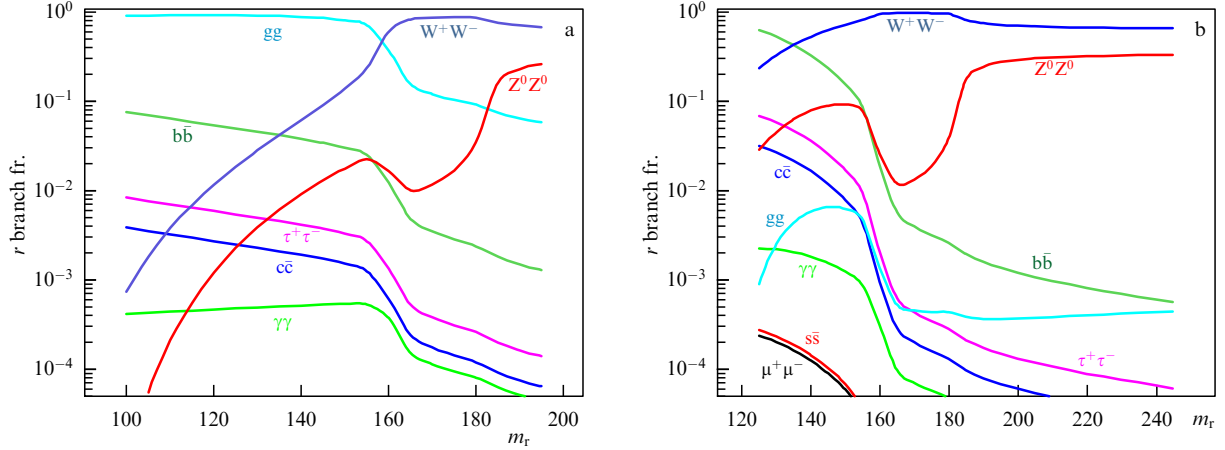


**Figure 11.** Partial decay widths for radion-dominated state as a function of  $m_r$  ( $m_h = 125$  GeV,  $\Lambda = 3$  TeV): (a)  $\sin \theta = 0$ ,  $c = 0$ , (b)  $\sin \theta = 0.7$ , parameter  $c$  is equal to its maximum value  $a_1$ .

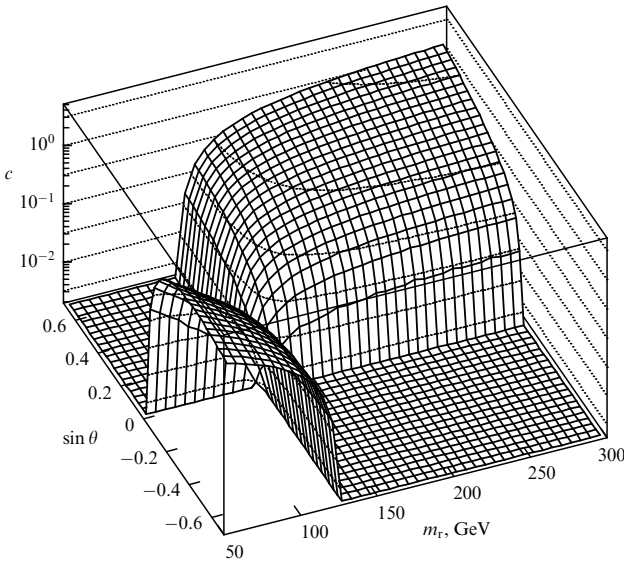


**Figure 12.** Two-dimensional plot of top-level  $c_{\max} = a_1$  of parameter  $c$  as a function of  $(m_r, \sin \theta)$ .

drastically due to the appearance of  $\sin \theta$ -like interactions in the radion-dominated state, similar to the Higgs boson, and also due to the influence of higher scalar modes encoded in the parameter  $c$ .

Figure 12 shows the behavior of the maximum possible value of this parameter as a function of the radion mass and the mixing angle. Recall that for  $\theta > 0$  the radion-dominated state is heavier than the Higgs-dominated state,  $m_r > m_h$ , and vice versa ( $\theta < 0$  for  $m_r < m_h$ ), and so for  $\theta < 0$ ,  $m_r > m_h$  and for  $\theta > 0$ ,  $m_r < m_h$ , the regions on the  $c = 0$  plane are not allowed.

If we take a fairly large mixing angle, for example,  $\sin \theta = 0.7$ , the mode of decay in  $b\bar{b}$  will dominate, as shown in Fig. 11b. Due to compensation at the gluon–gluon–radion vertex between the part of the anomalous term proportional to  $1/\Lambda$  and the part with the above-mentioned Higgs-type interaction proportional to  $\sin \theta/v$ , the vertex can be very small in some specific regions of the parameter space. This leads to the interesting feature shown in Fig. 11: the partial width of the decay of the radion-dominated state into two gluons can be smaller than the partial width of the decay into two photons.

Because of such compensations between different parts of the vertex of interaction between the radion-dominated state and gluons, the behavior of the total width and the production cross sections for the  $\gamma\gamma$  and  $ZZ^*$  modes in gluon-gluon fusion also has some minima, as can be seen in Figs 13 and 14. The cross sections can be used to obtain the corresponding signal strengths for the radion-dominated state, normalized to the SM Higgs boson cross sections.

In our analysis, for illustrative purposes, we use the Higgs boson signal levels for the  $\gamma\gamma$  and  $ZZ^*$  channels as reported by the CMS collaboration [96]:  $\mu_{\gamma\gamma} = 1.12 \pm 0.24$  and  $\mu_{ZZ^*} = 1.00 \pm 0.29$ . The standard  $\chi^2$  analysis yields regions in the parameter space (radion-dominated state mass and Higgs mixing angle) that are still allowed. The regions allowed if either the  $\gamma\gamma$  mode alone or the  $ZZ^*$  mode alone are considered are shown in Fig. 15a and b, respectively. The contours in all figures correspond to regions with confidence levels of 65%, 90%, and 99% with the best  $\Delta\chi^2$  fits of less than 2.10, 4.61, and 9.21, respectively, which is the standard representation of two-parameter fits that has been used in earlier studies (see, e.g., [92, 97]).

Thus, the blue region in Fig. 15 corresponds to the 65% confidence level of the fit; the green region, to the 90% confidence level; and the yellow region, to the 99% confidence level. It is easy to see that only the  $\gamma\gamma$  mode permits the presence of a radion-dominated state for masses both below and above 125 GeV.

The  $ZZ^*$  decay mode sets restrictions on the range of radion masses above the Z-boson pair threshold, where the cross section increases. The narrow allowed region in Fig. 15b is due to the above-mentioned compensation at the interaction vertices, leading to a smaller production cross section. The combined simultaneous  $\chi^2$  fit of the two modes further reduces the allowed region, as shown in Fig. 16. Here, there is an allowed region of heavier masses of the radion-dominated state, where its production probability decreases, so that the corresponding state can be allowed again. It is apparent that, if we consider large values of the parameter  $\Lambda$ , the cross section for the production of a radion-dominated state becomes smaller, while the allowed mass region for such a state increases. This is shown in Fig. 17, where the parameter  $\Lambda$  is chosen to be 5 TeV and all other parameters are the same as for the case  $\Lambda = 3$  TeV. The experimental lower bounds on the mass of such a heavy scalar state are currently about 3 TeV [98, 99].

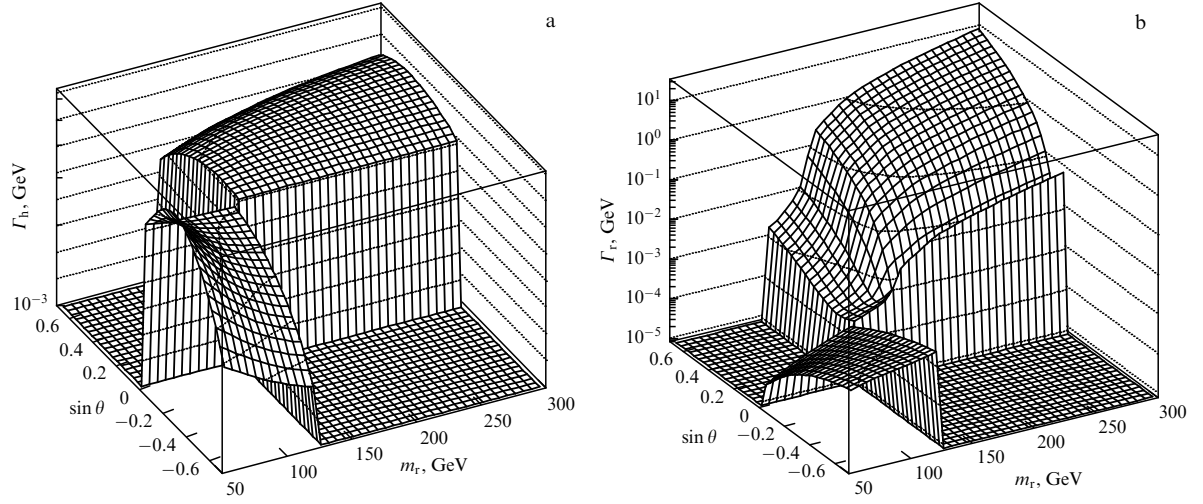


**Figure 13.** Three-dimensional plots of total width as a function of  $(m_r, \sin \theta)$  for LHC at  $\sqrt{s} = 8$  TeV and  $m_h = 125$  GeV,  $\Lambda = 3$  TeV,  $c = c_{\max}$ . (a) Higgs-dominated state,  $h(x)$ ; (b) radion-dominated state,  $r(x)$ .

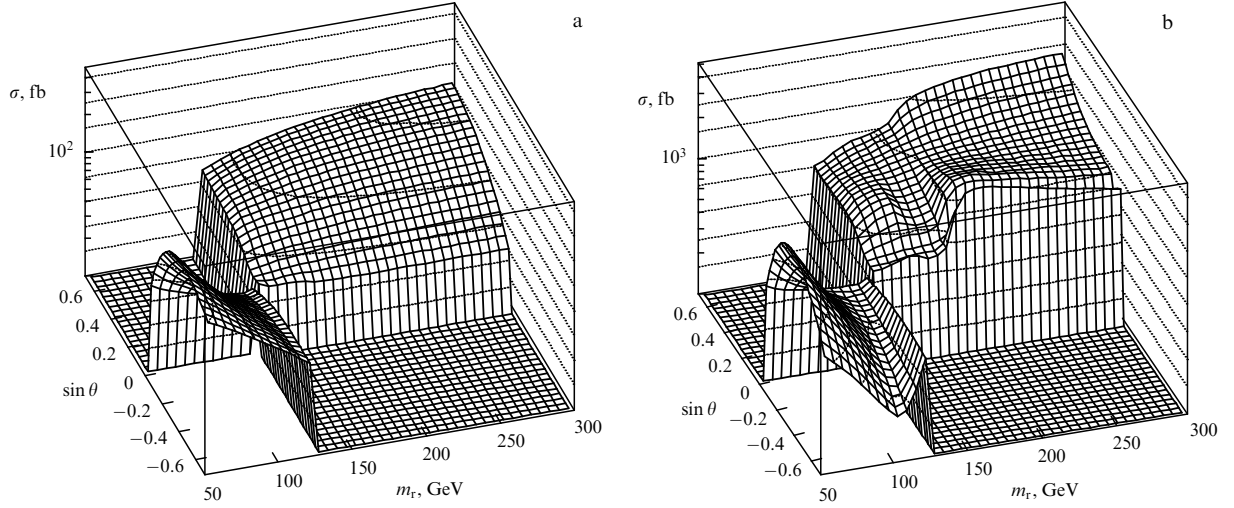


**Figure 14.** Three-dimensional plots of partial cross section as a function of  $(m_r, \sin \theta)$  for LHC at  $\sqrt{s} = 8$  TeV and  $m_h = 125$  GeV,  $\Lambda = 3$  TeV,  $c = c_{\max}$ . (a) Channel  $gg \rightarrow \gamma\gamma$ ; (b) channel  $gg \rightarrow ZZ^*$ .

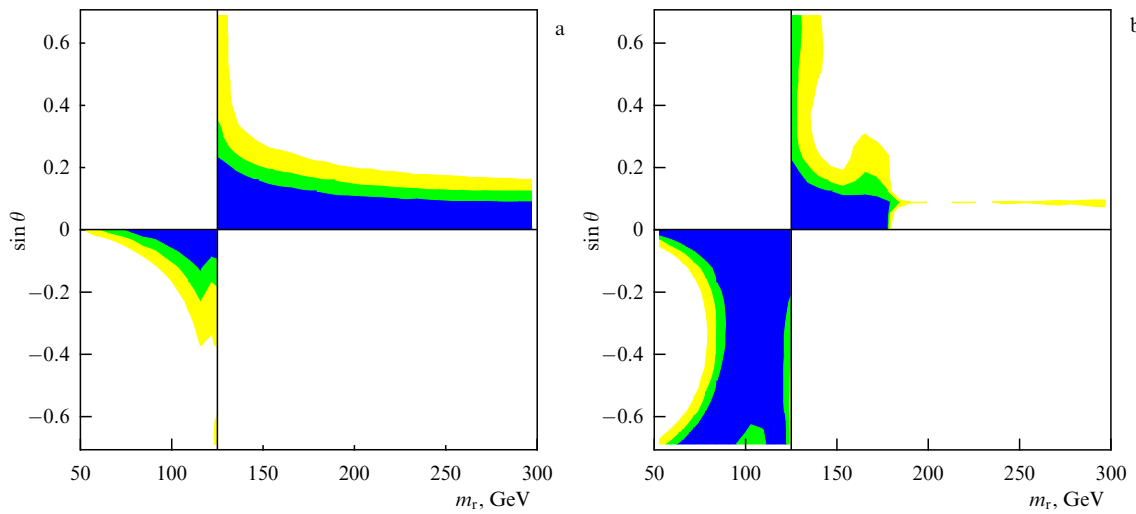


**Figure 15.** Exclusion contours for partial  $\chi^2$  fit in  $(m_r, \sin \theta)$  plane for LHC at  $\sqrt{s} = 7$  and 8 TeV,  $m_h = 125$  GeV,  $\Lambda = 3$  TeV,  $c = c_{\max}$ . Blue, green, and yellow areas correspond to 65%, 90%, and 99% confidence levels, respectively. (a) Channel  $gg \rightarrow \gamma\gamma$ ; (b) channel  $gg \rightarrow ZZ^*$ .

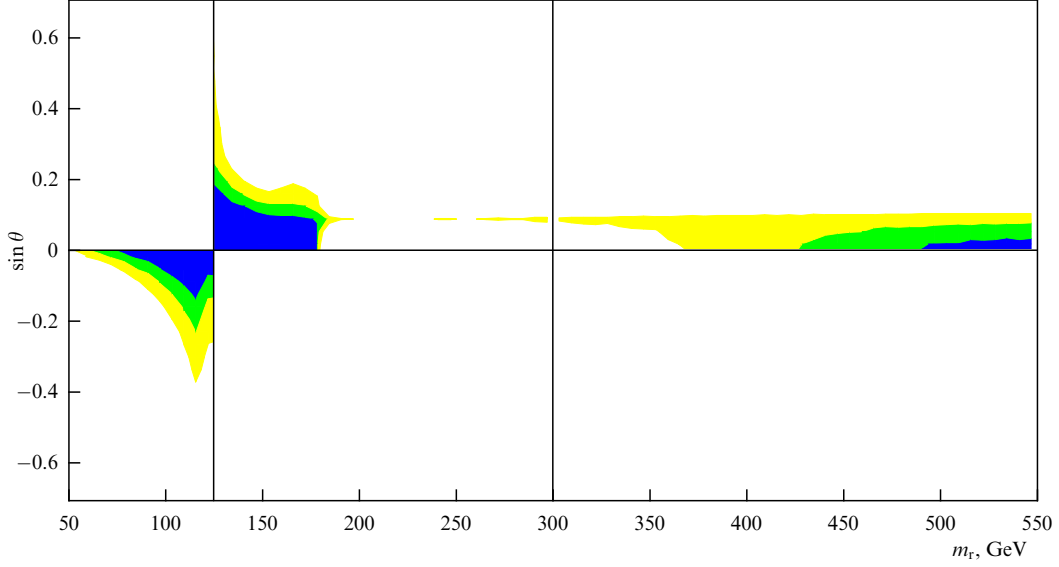


**Figure 16.** Exclusion contours for combined  $\chi^2$  fit in  $(m_r, \sin \theta)$  plane that includes both  $gg \rightarrow \gamma\gamma$  and  $gg \rightarrow ZZ^*$  channels for LHC at  $\sqrt{s} = 8$  TeV and  $m_h = 125$  GeV,  $\Lambda = 3$  TeV,  $c = c_{\max}$ . Blue, green, and yellow areas correspond to fit confidence level of 65%, 90%, and 99%, respectively.

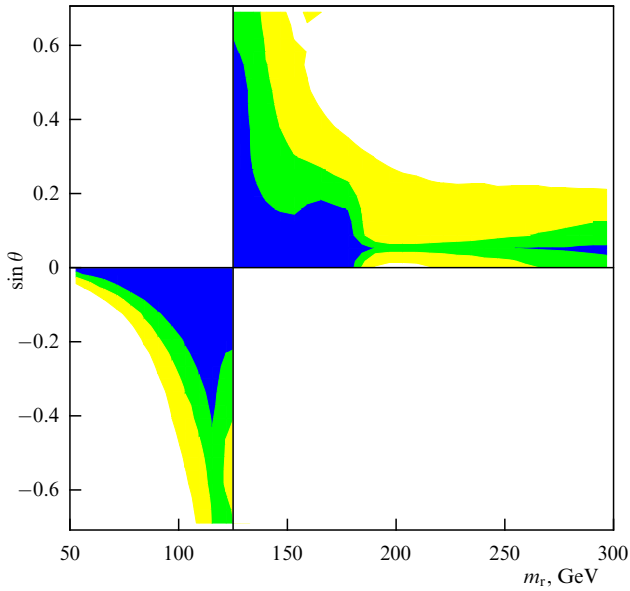


**Figure 17.** Exclusion contours for combined  $\chi^2$  fit in  $(m_r, \sin \theta)$  plane that includes both  $gg \rightarrow \gamma\gamma$  and  $gg \rightarrow ZZ^*$  channels for LHC at  $\sqrt{s} = 8$  TeV and  $m_h = 125$  GeV,  $\Lambda = 5$  TeV,  $c = c_{\max}$ . Blue, green, and yellow areas correspond to fit confidence level of 65%, 90%, and 99%, respectively.

## 7.2 Radion-dominated state with mass 125 GeV

We now briefly consider the case where the radion-dominated state has a mass of 125 GeV and, using the same analysis strategy, find the regions for the Higgs-dominated state mass and the mixing angle allowed by the two signal strengths. For this case, we made all the relevant calculations and plotted graphs similar to those displayed in Figs 12–17, which we are not presenting here for the sake of brevity. We only outline the result of the  $\chi^2$  analysis presented in Fig. 18.

As can be seen, this scenario is less favorable than the previous case. However, the mass of the Higgs-dominated state can still be very close to that of the radion-dominated one. This option exists in both scenarios. It can also be seen that, due to the specific cancellations between the anomaly and the SM-like parts in the interactions with gluons and

photons, a small allowed region appears for the sine of the mixing angle around  $\sin \theta \simeq -0.2$  and a mass immediately above the double W-boson mass.

The Higgs-radion mixing considered in this section is of course similar in many respects to that arising from the interaction of the Higgs field with the brane curvature. However, an important difference is the presence at low energies of an additional interaction of the Higgs-dominated field with the trace of the SM EMT, arising from the interaction of such a field with heavy scalar states of the radion KK tower. Although the interaction of a single higher excited scalar state with the Higgs field can be weak, it turns out that their cumulative effect on the mixing of the Higgs boson and radion can be observable. If they make significant contributions to the parameter  $c$ , this leads to certain changes in the collider phenomenology of the Higgs boson. A similar contribution of directly unobservable higher tensor KK modes to scattering processes was discussed in [100].

In this model, we studied two a priori possible scenarios according to which the scalar state detected at 125 GeV is either a Higgs-dominated state or a radion-dominated state. In our analysis, for simplicity and brevity, we used only two signal strengths, corresponding to the  $gg \rightarrow \gamma\gamma$  and  $gg \rightarrow ZZ^*$  channels. Our results show that the interpretation of the 125 GeV scalar state as a Higgs-dominated state is preferable, although the radion component in this state can be quite large. The regions allowed for the mass of the radion-dominated state were found as a function of the radion coupling constant  $\Lambda$ . It turned out that the radion-dominated state can either have a mass close to 125 GeV or a mass above 300 GeV, the allowed regions expanding with increasing radion coupling constant  $\Lambda$ .

We also showed that the interpretation of the 125 GeV scalar state as a radion-dominated state is not completely ruled out by the two leading measurements of signal strength, although in this case the constraints on the allowed masses of the Higgs-dominated state are very stringent. The mass of such a state can either be close to 125 GeV, which is consistent with our analysis of this 125 GeV state, or slightly exceed 160 GeV for a nonzero mixing angle.

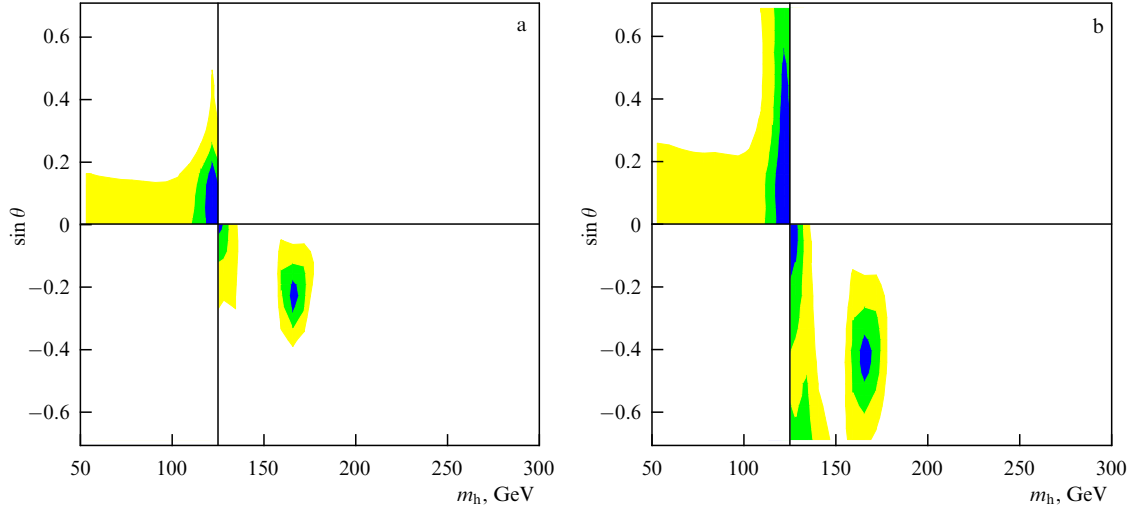


**Figure 18.** Exclusion contours for the combined  $\chi^2$  fit in  $(m_h, \sin \theta)$  plane, which includes both  $gg \rightarrow \gamma\gamma$  and  $gg \rightarrow ZZ^*$  channels for LHC at  $\sqrt{s} = 8$  TeV and  $m_t = 125$  GeV,  $c = c_{\max}$ . Blue, green, and yellow areas correspond to 65%, 90%, and 99% confidence levels of the fit, respectively, (a)  $A = 3$  TeV, (b)  $A = 5$  TeV.

## 8. Stability of Randall–Sundrum model with respect to quantum corrections

In the above-mentioned study by V. Rubakov [12], it was noted that, in the context of the braneworld, the problem of the cosmological constant should somehow be reduced to the question of why the vacuum energy density does not affect the curvature induced on the branes. In other words, it was assumed that, even if the vacuum energy density somehow affects the geometry of multidimensional spacetime as a whole, it only occurs in such a way that the 4D metric on our brane remains flat. As an explicit example of such an option, models with a single brane and a scalar field propagating throughout the entire multidimensional space, conformally coupled to the matter on the brane, were presented [12, 105, 106]. In such models, due to the symmetry of the problem, for some values of the conformal factor, only flat branes actually exist, featuring 4D Poincaré invariance [105]. However, the considered models with one brane and a conformal scalar field are plagued with a number of problems, one of which is the emergence of a ‘naked’ singularity in a multidimensional space at a finite distance  $r_{\text{sing}}$  from the brane [12].

Attempts to eliminate the naked singularity again lead to the problem of the cosmological constant in one form or another [107–110]. For example, if we place the second brane at a distance less than  $r_{\text{sing}}$  from the first brane, assuming that the model has an orbifold symmetry, it is apparent that no singularity arises within the orbifold itself. However, this approach requires fine-tuning the tension of the second brane, so that the metric of the model is a solution of the Einstein equations. Thus, we return to the problem of the cosmological constant, since such fine-tuning has no methodological advantages over adjusting the cosmological constant, which is usually carried out in 4D cosmological models [12]. Further analysis shows that, at least in some two-brane models, ‘flat’ branes or branes with a nonflat metric induced on them appear, depending on the fine-tuning of the parameters of the potentials on the branes themselves [111]. This raises the natural question as to what extent the ‘flat’ solutions obtained as a result of

fine-tuning are stable with respect to various corrections to the vacuum energy (for example, with respect to the Casimir effect).

It turns out that the stabilized RS model is stable with respect to the Casimir effect. In other words, the vacuum quantum corrections do not change the shape of the background solution, exerting only a negligible effect on the parameters of the model. We emphasize that, since such a small change in the parameters is a consequence of renormalization, it can hardly be obtained from other general considerations using any classical estimate. We consider this problem below in more detail.

### 8.1 Quantum corrections from scalar modes to energy–momentum tensor and to equations of motion of Randall–Sundrum model

According to Eqn (66), the five-dimensional scalar field  $\varphi(x, y)$  can be expanded in a basis of four-dimensional modes  $\varphi_n(x)$  satisfying the Klein–Gordon equation, and the wave functions  $\Psi_n(y)$  can be chosen in such a way that they are orthonormal with respect to the scalar product of the form (68). According to study [51], after substituting expansion (66) into the action of the stabilized RS model (46), we finally obtain for the part of the action quadratic in the scalar modes  $\varphi_n(x)$ , denoted as  $S^{(2)}$ ,

$$S^{(2)} = \frac{1}{2} \sum_{n,m=1}^{\infty} \int_{-L}^L \left\{ \frac{3}{4} \Psi_n \Psi_m - \frac{9M^3}{(\bar{\phi}')^2} \bar{g}^{44} (\partial_4 \Psi_n) (\partial_4 \Psi_m) \right\} \times \exp(2A) dy \int \left[ \eta^{\mu\nu} \partial_\mu \varphi_n \partial_\nu \varphi_m - \frac{1}{2} (m_n^2 + m_m^2) \varphi_n \varphi_m \right] d^4x. \quad (204)$$

For 4D scalar modes, the standard procedure of canonical quantization can be applied, expanding each mode in plane waves and declaring the corresponding coefficients of this expansion to be creation and annihilation operators, for which standard commutation relations are postulated.

Varying action (204) with respect to the background metric  $\bar{g}_{MN}$  and averaging the obtained expression over the vacuum, after expanding the modes in plane waves, we obtain



the lowest vacuum quantum correction from scalar modes in the EMT of the stabilized RS model:

$$\begin{aligned}\mathfrak{T}_{\mu\nu}(\varphi) &= \left\langle \frac{\delta S^{(2)}}{\delta \bar{g}^{\mu\nu}} \right\rangle = \exp(-2A) \left\langle \frac{\delta S^{(2)}}{\delta \eta^{\mu\nu}} \right\rangle \\ &= \frac{1}{2} \sum_{n=1}^{\infty} F_n^+(y) \int \frac{1}{2\omega_n} \left[ p_{n\mu} p_{n\nu} - \frac{1}{2} \eta_{\mu\nu} (p_n^2 - m_n^2) \right] d^3 p_n, \quad (205)\end{aligned}$$

$$\begin{aligned}\mathfrak{T}_{44}(\varphi) &= \left\langle \frac{\delta S^{(2)}}{\delta \bar{g}^{44}} \right\rangle = \frac{\exp(2A)}{2} \sum_{n=1}^{\infty} F_n^-(y) \\ &\times \int \frac{1}{2\omega_n} (p_n^2 - m_n^2) d^3 p_n \equiv 0, \quad (206)\end{aligned}$$

where

$$F_n^{\pm}(y) \equiv \frac{3\Psi_n^2}{4} \pm 9M^3 \frac{(\partial_4 \Psi_n)^2}{(\bar{\phi}')^2},$$

$$\omega_n = \sqrt{\mathbf{p}_n^2 + m_n^2}.$$

Due to the equality of the quantum correction  $\mathfrak{T}_{44}(\varphi)$  to zero, Eqn (53), which follows from Eqn (48) at  $M = N = 4$ , does not change when the quantum vacuum corrections are taken into account. Similarly, it can be shown that such corrections do not alter Eqn (52), except for the change in the potentials on the branes. Based on this observation, we can conclude that, in the case under consideration, when taking into account the vacuum quantum corrections, the form of the solutions  $A(y)$  and  $\phi(y)$  remains unaltered, and only the parameters of the model included in the solutions can change. These changes can be evaluated by calculating the contribution of the quantum corrections to such an integral characteristic of the model as, for example, the energy density. We calculate the Casimir energy density of scalar modes — the lowest vacuum quantum correction that scalar modes give to the energy density, defined as the zeroth component of a four-dimensional vector of the following form:

$$\begin{aligned}P^0 &\equiv 2 \int_0^L \mathfrak{T}^{\mu 0}(\varphi) \sqrt{\bar{g}} dy \\ &= \frac{1}{2} \sum_{n=1}^{\infty} \int \frac{1}{\omega_n} \left[ p_n^0 p_n^0 - \frac{1}{2} \eta^{\mu 0} (p_n^2 - m_n^2) \right] d^3 p_n. \quad (207)\end{aligned}$$

Its time component is apparently nothing more than the zero-point energy density of the scalar modes

$$P^0 = \frac{1}{2} \sum_{n=1}^{\infty} \int \omega_n d^3 p, \quad (208)$$

which is a standard result in the theory of the Casimir effect: the Casimir energy density is the sum of the zero-point energy densities [112].

## 8.2 Regularization and renormalization of Casimir energy density of scalar modes

The resulting expression for the Casimir energy density of scalar modes diverges if the spacetime dimension  $d$  is four. To regularize it and isolate the finite part depending on the distance between the branes, one can use the dimensional regularization method by calculating the corresponding

integrals in  $d$ -dimensional spacetime and summing the resulting divergent series using the Hurwitz zeta function. Up to zeroth order in parameter  $\varepsilon = 4 - d$ , the result obtained has the form

$$\begin{aligned}P^0 &= \mu^{4-d} I_d \sum_{n=1}^{\infty} m_n^d = \mu^{4-d} I_d m_r^d + \mu^{4-d} I_d v^d \sum_{n=2}^{\infty} (n + \theta)^d \\ &= \mu^{4-d} I_d m_r^d + \mu^{4-d} I_d v^d \zeta(-d, 2 + \theta) \\ &= -\frac{\pi}{2} X \varepsilon^{-1} + \frac{\pi}{8} (3 - 2\gamma - 2 \ln \pi) X - \frac{\pi}{2} Y + O(\varepsilon), \quad (209)\end{aligned}$$

where  $\zeta(-d, 2 + \theta)$  is the Hurwitz zeta function analytically continued to the region  $d > -1$ ,  $\zeta'$  is its derivative with respect to the first argument, and  $\mu$  is the scale factor of dimensional regularization. The mass of the lightest mode (radion)  $m_1 \equiv m_r$  is given by Eqn (77), and the masses of other modes, according to [113], are  $m_n \approx v(n + \theta)$ , where  $v = \pi \bar{k}$ , and the parameter  $\theta$  is close to  $1/4$ . The factor  $I_d$  in Eqn (209) is equal to

$$\begin{aligned}I_d &\equiv S_{d-2} \int_0^{\infty} \sqrt{q^2 + 1} q^{d-2} dq = \frac{\pi}{2\varepsilon} - \frac{\pi}{8} (3 - 2\gamma - 2 \ln \pi) \\ &+ \frac{\pi}{96} (21 - 18\gamma + 6\gamma^2 + \pi^2 + (-18 + 12\gamma + 6 \ln \pi) \ln \pi) \varepsilon + O(\varepsilon). \quad (210)\end{aligned}$$

The following expressions hold for the coefficients  $X$  and  $Y$  in expansion (209) in powers of  $\varepsilon$ :

$$\begin{aligned}X &\equiv m_r^4 + v^4 \zeta(-4, 2 + \theta), \quad (211) \\ Y &\equiv m_r^4 \ln \left( \frac{m_r}{\mu} \right) + v^4 \zeta(-4, 2 + \theta) \ln \left( \frac{v}{\mu} \right) - v^4 \zeta'(-4, 2 + \theta). \quad (212)\end{aligned}$$

In deriving Eqn (209), analytic continuation in the spacetime dimension was used to calculate the divergent integrals, which corresponds to discarding the contribution to the energy density from scalar modes in Minkowski space. This procedure, in turn, is equivalent to renormalizing the energy density by means of normal ordering of the field operators [114]. Nevertheless, the resulting expression is still divergent as the spacetime dimension  $d$  tends to four. A divergence of this type in the resulting expression for the Casimir energy density is due to the presence of boundaries (branes) in the spacetime of the RS model. Note that the occurrence of such ‘surface divergences’ in EMT models with boundaries is a typical phenomenon, and, to eliminate them, the renormalization procedure should be refined [112, 115].

Note that in Eqn (209) the contribution from the first mode (radion)

$$\mu^{4-d} I_d m_r^d = -\frac{\pi}{2} m_r^4 \varepsilon^{-1} + \frac{\pi}{8} \left( 3 - 2\gamma - 2 \ln \pi - \ln \left( \frac{m_r}{\mu} \right) \right) m_r^4$$

exactly coincides with the contribution that a scalar field with mass  $m_r$  would make to the Casimir energy density in  $d$ -dimensional Minkowski space. Therefore, the contribution of the radion to the Casimir energy density  $P^0$  can be renormalized by discarding this contribution. This is usually

done in the theory of the Casimir effect, when the contribution from this field in Minkowski space is subtracted from the expression for the Casimir energy density of some field in the spacetime under consideration.

The contribution of the KK tower to the Casimir energy density (209) can be formally represented, taking into account Eqns (210)–(212), as a contribution from some single mode with mass  $m_\Phi \equiv v \sqrt[4]{\zeta(-4, 2 + \theta)}$ :

$$\begin{aligned} & \mu^{4-d} I_d v^d \sum_{n=2}^{\infty} (n + \theta)^d \\ &= -\frac{\pi}{2} m_\Phi^4 \varepsilon^{-1} + \frac{\pi}{8} \left[ 3 - 2\gamma - 2 \ln \pi - \ln \left( \frac{m_\Phi}{\mu} \right) \right] m_\Phi^4 \\ & - v^4 \left[ \frac{1}{4} \zeta(-4, 2 + \theta) \ln \zeta(-4, 2 + \theta) + \zeta'(-4, 2 + \theta) \right]. \end{aligned} \quad (213)$$

Therefore, such a contribution can be renormalized similarly to that of radion by discarding the term

$$\mu^{4-d} I_d m_\Phi^d = -\frac{\pi}{2} m_\Phi^4 \varepsilon^{-1} + \frac{\pi}{8} \left[ 3 - 2\gamma - 2 \ln \pi - \ln \left( \frac{m_\Phi}{\mu} \right) \right] m_\Phi^4, \quad (214)$$

which would be provided to the Casimir energy density in the  $d$ -dimensional Minkowski space by a scalar mode with mass  $m_\Phi$ .

Thus, for the total contribution of all scalar modes to the Casimir energy, we obtain the finite renormalized formula:

$$P_{\text{ren}}^0 = -\frac{\pi}{2} v^4 \left[ \frac{1}{4} \zeta(-4, 2 + \theta) \ln \zeta(-4, 2 + \theta) + \zeta'(-4, 2 + \theta) \right], \quad (215)$$

which numerically agrees with high accuracy with the formula for the Casimir energy of scalar fields obtained for this model in a different way [113]. It should be noted that the considered scheme for renormalizing the Casimir energy density satisfies a set of conditions [112, 116] that ensure the uniqueness of the renormalization procedure.

For the model parameter values  $m = 5$  TeV,  $\tilde{k}L = 35$ ,  $\beta_2^2 = \tilde{k} = 53$  TeV,  $m_r = 1$  TeV, and  $\theta = 0.2518$ , chosen according to current experimental constraints on models with extra spacetime dimensions [117], numerical calculations yield the value for the Casimir energy density:

$$P_{\text{ren}}^0 \sim -1.98 \times 10^9 \text{ TeV}^4. \quad (216)$$

Calculations for other model parameter values confirm this estimate and show that the renormalized Casimir energy density  $P_{\text{ren}}^0$  is negative. Thus, in this case, the Casimir effect leads to an attraction between the branes, which, in the considered stabilized RS model, should lead to a decrease in the physical distance between them.

### 8.3 Change in model parameters due to Casimir effect

To estimate the decrease in the distance between the branes due to quantum effects, we should compare the Casimir energy density  $P_{\text{ren}}^0$  of scalar modes with the similar classical quantity obtained from the EMT of the classical background scalar field and defined by the following integral:

$$P_{\text{cl}}^0 \equiv \int_0^L T^{00} \sqrt{g} dy. \quad (217)$$

In accordance with current experimental constraints on models with extra spacetime dimensions [117], we choose the fundamental five-dimensional energy scale  $M$  equal to 5 TeV and assume that the mass of the radion is about 1 TeV. In this case, the conditions  $uL \sim 0.1$ ,  $k \approx \tilde{k}$  must be satisfied. These conditions are consistent if  $\tilde{k}L \sim 35$ ,  $k \sim 53$  TeV. Then, substituting Eqn (50) for the EMT of the Goldberger–Wise field into Eqn (217) and using Eqns (51)–(56) for the equations of motion and background solutions of the stabilized RS model, we can represent an approximate formula for  $P_{\text{cl}}^0$  in the following form:

$$P_{\text{cl}}^0 \approx \left( \frac{3\tilde{k}}{\kappa^2} - \frac{u}{2} \phi_0^2 + \frac{3\kappa^2 u^2}{16\tilde{k}} \phi_0^4 \right) \exp(2\tilde{k}L). \quad (218)$$

The numerical value of the classical energy density of scalar modes with this choice of parameters of the stabilized RS model is

$$P_{\text{cl}}^0 \sim 4.15 \times 10^{34} \text{ TeV}^4. \quad (219)$$

To compare the classical energy density  $P_{\text{cl}}^0$  with the quantum correction arising from the Casimir effect, the contribution of tensor modes should be taken into account for the latter. This contribution is calculated in a way completely similar to the calculation of the contribution to the Casimir energy density of scalar modes and leads to a result of the same order for each of the five polarizations of the tensor field [113]. Therefore, taking into account Eqn (216), the total contribution of tensor and scalar modes to the Casimir energy density can be estimated as

$$P_{\text{ren}}^0 \sim -1.2 \times 10^{10} \text{ TeV}^4. \quad (220)$$

Using Eqn (218) for  $P_{\text{cl}}^0$ , we can estimate  $\delta P_{\text{cl}}^0$ , taking into account the formula for the variation of  $\delta\phi_0 = u\phi_0\delta L$  and the smallness of the  $u/\tilde{k}$  ratio:

$$\delta P_{\text{cl}}^0 \approx 2\tilde{k}P_{\text{cl}}^0 \delta L. \quad (221)$$

Based on the fact that  $P_{\text{ren}}^0 \sim \delta P_{\text{cl}}^0$ , we obtain the following estimate for the relative change in the distance between branes  $\delta L/L$ :

$$\frac{P_{\text{ren}}^0}{P_{\text{cl}}^0} \approx 2\tilde{k}L \frac{\delta L}{L}. \quad (222)$$

Taking into account numerical estimates (219) and (220) and the fact that  $2\tilde{k}L \approx 70$ , we can use Eqn (221) to easily estimate the relative decrease in the distance between branes, which turns out to be of the order of  $\delta L/L \sim 10^{-26}$ , i.e., negligibly small.

In a completely similar way, we can estimate the change in the background field parameter  $\delta\phi_0$  due to the Casimir effect. Taking into account  $\delta\phi_0 = u\phi_0\delta L$  and Eqn (221), we obtain

$$\delta\phi_0 = u\phi_0\delta L \approx \frac{u\phi_0}{2\tilde{k}} \frac{\delta P_{\text{cl}}^0}{P_{\text{cl}}^0}.$$

The remaining parameters of the model either are not altered when the Casimir effect is taken into account, since they enter into Eqns (52) and (53) unchanged with respect to the lowest quantum corrections, or are not independent and are expressed through the parameters  $\phi_0$  and  $L$ . Indeed, the



parameters of the RS model potentials are chosen in such a way that the background solution determined by them corresponds to static flat branes located at a distance  $L$  from each other, i.e., certain constraints are set on the parameters of the model. With arbitrary values of the parameters, the background solution of the model would generally not be homogeneous and isotropic, and the branes would have a nonzero constant curvature.

Thus, the quantum corrections considered above do not alter the form of the background solution of the model, and a change in its parameters is actually reduced to a negligibly small variation of the physical distance between the branes and an equally insignificant change in the background field parameter. It is shown in this way that the stabilized RS model is stable with respect to quantum corrections leading to the Casimir effect. It should be noted that the obtained result agrees well with the conclusions of the classical work by Goldberger et al. [25, 118] on the impossibility of stabilizing the RS model by quantum corrections alone and, conversely, disagrees with the conclusions of studies [119–121], which allowed possible stabilization of the distance between branes due to the Casimir effect in the unstabilized RS model. Indeed, in the considered approximation for the conformal factor (56), the metric of the stabilized RS model has the same form as that of the usually discussed unstabilized model. Therefore, the Casimir energy of scalar and tensor fields for both models should have approximately the same order of magnitude and the same analytical form. The same conclusion can be made regarding the Casimir force leading to the attraction of branes. However, unlike the stabilized RS model, the unstabilized model contains no forces that could fix the branes at a certain distance from each other. Therefore, in such a model, to stabilize the distance between branes, it is necessary to additionally consider nonlinear interactions of scalar fields, as was done, for example, in [52], and quantum corrections to the potentials describing these interactions. It is possible that in this case the distance between branes in the unstabilized RS model could be stabilized due to quantum corrections.

## 9. Conclusions

We reviewed the history of the development of theories with extra spacetime dimensions and discussed various versions of theories with large extra dimensions focusing on V. Rubakov's contribution to the development of such theories. We also outlined the main aspects of the RS model: the identification of physical degrees of freedom of this model and the determination of its energy scales, the mechanisms for stabilizing the size of the extra dimension, and some phenomenological implications of the stabilized model. Our presentation of the RS model is based on the Lagrangian description of linearized gravity, which seems to be the most consistent approach. This description enables a fairly simple identification of the physical degrees of freedom in the model, turns out to be naturally related to the observer on the brane, and therefore makes it possible to easily find canonically normalized 4D fields on each of the branes and to determine the constants of their coupling to the SM fields.

A very important issue, which is ignored in the overwhelming majority of studies on the RS model, is that, for observers located on different branes, five-dimensional gravity looks differently. This, in particular, is reflected in Eqns (6) and (7) for the relation between the 4D gravitational

constant and the fundamental energy scales on different branes. It should be especially noted that, in almost all studies, Eqn (6), which is valid for a brane with positive tension, is used for a brane with negative tension, and this leads to an erroneous conclusion about the Planck energy scale on this brane.

We considered some phenomenological implications of the stabilized RS model, in which the five-dimensional energy scale is of the order of  $M \sim 5 - 10$  TeV, while their parameters are such that the metric of this stabilized model for a radion mass of the order of several TeV is close to that of the unstabilized model. Namely, we analyzed the problem of searching for KK excitations of the gravitational field and discussed the similarity of the Higgs boson and radion in their associated production. We showed that the analytical formulas for the total amplitudes of associated production of the Higgs boson and radion and pair production of the Higgs boson are the same up to replacing the masses and vacuum expectation value of the Higgs field with the coupling constant of radion and rescaling the constant of triple self-interaction of the Higgs field. As a result, the contribution of the radion can imitate the deviation in the Higgs triple self-interaction constant from the SM prediction when the masses of the radion and Higgs boson have close values, which should be taken into account in the experimental study of this constant.

The nonlinear self-interaction of the radion and its interactions with SM fields were also discussed. It was shown that the interaction of a radion with vector fields is always linear in the radion field. Another important issue is that the self-interaction potential of a radion up to the fourth power inclusively has a stable minimum at zero, which indicates the classical stability of the RS model vacuum.

In addition, we considered the mixing of Higgs and radion fields that arises in stabilized brane world models due to the unification of the mechanism of stabilization of the size of the extra dimension and the Higgs mechanism of spontaneous symmetry breaking on the TeV brane and discussed its phenomenological implications. This mixing is, of course, in many aspects similar to that arising in the standard approach from the term of interaction between brane curvature and the Higgs field. However, an important difference is the presence at low energies of an additional interaction of the Higgs boson-dominated state with the SM EMT trace. Arising from the interaction of this field with the heavy scalar modes of the radion KK tower, it can lead to a significant modification of the interactions of this state compared to the Higgs boson of the SM.

We also discussed the stability of the RS model with respect to the lowest quantum corrections leading to the Casimir effect in the 4D space between the branes and showed that the model is stable with respect to such corrections.

Finally, it should be noted that interest in theories with extra dimensions and in supersymmetric theories has a wave-like character with ebbs and tides. The latest surge of interest in such theories was associated with the idea of localization of fields on a domain wall, first suggested by V. Rubakov and M. Shaposhnikov, and braneworld models with large extra dimensions in the spirit of the Randall–Sundrum model. However, numerous experimental searches at the LHC for particles and effects predicted by these models have not yet yielded any positive results, pushing the scale of possible manifestations of extra dimensions to the energy range of the

order of 10 TeV or more. This circumstance has led to a noticeable decline in interest in such models. However, their development continues; new interesting areas of research are emerging, for example, the Kaluza–Klein portal to the world of dark matter [122] based on the property of universality of the interaction of tensor and scalar KK modes of the RS model with matter fields. The search for physical consequences of models with extra dimensions in accelerator and nonaccelerator experiments is also ongoing, and new search options are being discussed WRT future colliders with higher energies, in particular, in the FCC project.

**Acknowledgments.** The authors are grateful to Yu.V. Gratz for useful discussions of the issues presented in the review. This study was conducted within the scientific program of the National Center for Physics and Mathematics, Section 5 “Particle Physics and Cosmology”.

## References

- Nordström G *Phys. Z.* **15** 504 (1914); physics/0702221
- Kaluza Th *Sitzungsber. Preuss. Akad. Wiss. Berlin Math. Phys. Kl.* 966 (1921); Translated into English: *Int. J. Mod. Phys. D* **27** 1870001 (2018); arXiv:1803.08616; Translated into Russian: in *Albert Einstein i Teoriya Gravitatsii* (Albert Einstein and the Theory of Gravity) (Ed. E S Kuranskii) (Moscow: Mir, 1979) p. 529
- Klein O Z. *Phys.* **37** 895 (1926); *Surv. High Energy Phys.* **5** 241 (1986)
- Klein O *Nature* **118** 516 (1926)
- Einstein A, Bargmann V, Bergmann P G, in *Theodore von Kármán Anniversary Volume. Contributions to Applied Mechanics and Related Subjects* (Pasadena, CA: California Institute of Technology, 1941) p. 212; Translated into Russian: in *Albert Einstein. Sobranie Nauchnykh Trudov* (Albert Einstein. Collected Scientific Papers) Vol. 2 *Raboty po Teorii Otnositel'nosti 1921–1955* (Works on the Theory of Relativity 1921–1955) (Eds I E Tamm, Ya A Smorodinskii, B G Kuznetsov) (Moscow: Nauka, 1966) p. 543
- Wess J, Bagger J *Supersymmetry and Supergravity* (Princeton, NJ: Princeton Univ. Press, 1983); Translated into Russian: *Supersimmetriya i Supergravitatsiya* (Moscow: Mir, 1986)
- Schwarz J H *Phys. Rep.* **89** 223 (1982)
- Hořava P, Witten E *Nucl. Phys. B* **460** 506 (1996); hep-th/9510209
- Lukas A et al. *Phys. Rev. D* **59** 086001 (1999); hep-th/9803235
- Witten E *Nucl. Phys. B* **471** 135 (1996)
- Rubakov V A, Shaposhnikov M E *Phys. Lett. B* **125** 136 (1983)
- Rubakov V A *Phys. Usp.* **44** 871 (2001); *Usp. Fiz. Nauk* **171** 913 (2001)
- Barnaveli A T, Kancheli O V *Sov. J. Nucl. Phys.* **52** 576 (1990); *Yad. Fiz.* **52** 905 (1990)
- Kehagias A, Tamvakis K *Phys. Lett. B* **504** 38 (2001)
- Shaposhnikov M, Tinyakov P *Phys. Lett. B* **515** 442 (2001)
- Smolyakov M N *Phys. Rev. D* **85** 045036 (2012); *Phys. Rev. D* **87** 029901 (2013) erratum; arXiv:1111.1366
- Smolyakov M N *Phys. Rev. D* **87** 104035 (2013); arXiv:1210.7978
- Arkani-Hamed N, Dimopoulos S, Dvali G *Phys. Lett. B* **429** 263 (1998)
- Arkani-Hamed N, Dimopoulos S, Dvali G *Phys. Rev. D* **59** 086004 (1999)
- Randall L, Sundrum R *Phys. Rev. Lett.* **83** 3370 (1999)
- Landau L D, Lifshitz E M *The Classical Theory of Fields* (Oxford: Pergamon Press, 1975); Translated from Russian: *Teoriya Polya* (Moscow: Nauka, 1973)
- Boos E E et al. *Nucl. Phys. B* **717** 19 (2005); hep-th/0412204
- Boos E E et al. *Class. Quantum Grav.* **19** 4591 (2002)
- Charmousis C, Gregory R, Rubakov V A *Phys. Rev. D* **62** 067505 (2000); hep-th/9912160
- Goldberger W D, Wise M B *Phys. Rev. Lett.* **83** 4922 (1999)
- DeWolfe O et al. *Phys. Rev. D* **62** 046008 (2000)
- Vecchi L J *High Energy Phys.* **2011** (11) 102 (2011); arXiv:1012.3742
- Geller M, Bar-Shalom S, Soni A *Phys. Rev. D* **89** 095015 (2014); arXiv:1312.3331
- Pomarol A *Phys. Lett. B* **486** 153 (2000); hep-ph/9911294
- Davoudiasl H, Hewett J L, Rizzo T G *Phys. Lett. B* **473** 43 (2000); hep-ph/9911262
- Chang S et al. *Phys. Rev. D* **62** 084025 (2000); hep-ph/9912498
- Gherghetta T, Pomarol A *Nucl. Phys. B* **586** 141 (2000); hep-ph/0003129
- Djouadi A, Moreau G, Singh R K *Nucl. Phys. B* **797** 1 (2008); arXiv:0706.4191
- Allanach B C et al. *J. High Energy Phys.* **2010** (03) 014 (2010); arXiv:0910.1350
- Agashe K, Perez G, Soni A *Phys. Rev. D* **75** 015002 (2007); hep-ph/0606293
- Agashe K et al. *Phys. Rev. D* **76** 036006 (2007); hep-ph/0701186
- Fitzpatrick L et al. *J. High Energy Phys.* **2007** (09) 013 (2007); hep-ph/0701150
- Lillie B, Randall L, Wang L T *J. High Energy Phys.* **2007** (09) 074 (2007); hep-ph/0701166
- Agashe K et al. *Phys. Rev. D* **77** 015003 (2008); hep-ph/0612015
- Burdman G et al. *Phys. Rev. D* **79** 075026 (2009); arXiv:0812.0368
- Agashe K et al., arXiv:1309.7847
- Rizzo T G *J. High Energy Phys.* **2007** (05) 037 (2007)
- Accomando E et al. *Phys. Rev. D* **79** 055020 (2009); arXiv:0807.5051
- Accomando E et al. *Phys. Rev. D* **83** 015012 (2011); arXiv:1010.0171
- Accomando E et al. *Phys. Rev. D* **84** 115014 (2011); arXiv:1107.4087
- Accomando E et al. *Phys. Rev. D* **85** 115017 (2012); arXiv:1110.0713
- Boos E E et al. *Phys. Part. Nucl.* **43** 42 (2012); *Fiz. Elem. Chast. At. Yad.* **43** 82 (2012)
- Boos E E et al. *Theor. Math. Phys.* **131** 629 (2002); *Teor. Matem. Fiz.* **131** 216 (2002)
- Kisselev A V *Phys. Rev. D* **73** 024007 (2006)
- Kisselev A V *Phys. Rev. D* **88** 095012 (2013)
- Boos E E et al. *Mod. Phys. Lett. A* **21** 1431 (2006); hep-th/0511185
- Volobuev I P, Keizerov S I, Rakhmetov E R *Theor. Math. Phys.* **205** 1318 (2020); *Teor. Matem. Fiz.* **205** 84 (2020)
- Sirunyan A M et al. (CMS Collab.) *J. High Energy Phys.* **2021** 208 (2021); arXiv:2103.02708
- Aad G et al. (ATLAS Collab.) *Phys. Lett. B* **822** 136651 (2021); arXiv:2102.13405
- Aad G et al. (ATLAS Collab.) *Phys. Rev. D* **102** 112008 (2020); arXiv:2007.05293
- Sirunyan A M et al. (CMS Collab.) *Eur. Phys. J. C* **81** 688 (2021); arXiv:2102.08198
- Boos E E et al. *J. High Energy Phys.* **2014** (06) 160 (2014); arXiv:1311.5968
- Weinberg S *Physica A* **96** 327 (1979)
- Buchmüller W, Wyler D *Nucl. Phys. B* **268** 621 (1986)
- Burgess C P, London D *Phys. Rev. D* **48** 4337 (1993); hep-ph/9203216
- Burgess C P et al. *Phys. Rev. D* **49** 6115 (1994); hep-ph/9312291
- Whisnant K et al. *Phys. Rev. D* **56** 467 (1997); hep-ph/9702305
- Yang J M, Young B-L *Phys. Rev. D* **56** 5907 (1997); hep-ph/9703463
- Boos E, Dudko L, Ohl T *Eur. Phys. J. C* **11** 473 (1999); hep-ph/9903215
- Ferreira P M, Santos R *Phys. Rev. D* **74** 014006 (2006); hep-ph/0604144
- Boos E E et al. *Theor. Math. Phys.* **149** 1591 (2006); *Teor. Matem. Fiz.* **149** 339 (2006)
- Davoudiasl H, Hewett J L, Rizzo T G *Phys. Rev. Lett.* **84** 2080 (2000); hep-ph/9909255
- Boos E et al. *Phys. Rev. D* **90** 095026 (2014); arXiv:1409.2796
- Boos E E et al. *Phys. Atom. Nucl.* **78** 1484 (2015); Translated from Russian: *Yad. Fiz. Inzhiniring* **5** 741 (2014)
- Boos E et al. *Phys. Rev. D* **94** 024047 (2016)
- Boos E E et al. *Phys. Part. Nucl.* **48** 745 (2017); *Fiz. Elem. Chast. At. Yad.* **48** 627 (2017)
- Giudice G F, Rattazzi R, Wells J D *Nucl. Phys. B* **595** 250 (2001); hep-ph/0002178
- Csáki C, Graesser M L, Kribs G D *Phys. Rev. D* **63** 065002 (2001); hep-th/0008151
- Aad G et al. (ATLAS Collab.) *Phys. Lett. B* **716** 1 (2012); arXiv:1207.7214
- Chatrchyan S et al. (CMS Collab.) *Phys. Lett. B* **716** 30 (2012); arXiv:1207.7235

76. Chacko Z, Franceschini R, Mishra R K *J. High Energy Phys.* **2013** (04) 015 (2013); arXiv:1209.3259
77. Chacko Z, Mishra R K, Stolarski D J *J. High Energy Phys.* **2013** 121 (2013); arXiv:1304.1795
78. Kubota H, Nojiri M *Phys. Rev. D* **87** 076011 (2013); arXiv:1207.0621
79. Cho G-C, Nomura D, Ohno Y *Mod. Phys. Lett. A* **28** 1350148 (2013); arXiv:1305.4431
80. Desai N, Maitra U, Mukhopadhyaya B J *J. High Energy Phys.* **2013** (10) 093 (2013); arXiv:1307.3765
81. Cox P et al. *J. High Energy Phys.* **2014** (02) 032 (2014); arXiv:1311.3663
82. Jung D-W, Ko P *Phys. Lett. B* **732** 364 (2014); arXiv:1401.5586
83. Bhattacharya S et al. *Phys. Rev. D* **91** 016008 (2015); arXiv:1410.0396
84. Davoudiasl H, Hewett J L, Rizzo T G *J. High Energy Phys.* **2003** (08) 034 (2003); hep-ph/0305086
85. Boos E E et al. *Phys. Rev. D* **92** 095010 (2015); arXiv:1505.05892
86. Volobuev I *PoS QFTHEP2011* 054 (2012) <https://doi.org/10.22323/1.138.0054>
87. Godunov S I et al. *Eur. Phys. J. C* **76** 1 (2016); arXiv:1503.01618
88. Robens T, Stefaniak T *Eur. Phys. J. C* **75** 104 (2015); arXiv:1501.02234
89. Boos E et al. (CompHEP Collab.) *Nucl. Instrum. Meth. Phys. Res. A* **534** 250 (2004); hep-ph/0403113
90. Boos E E et al. *PoS ACAT2008* 008 (2008); arXiv:0901.4757
91. Boos E E, Bunichev V, Dubinin M *PoS QFTHEP2013* 015 (2013)
92. Boos E E et al. *Phys. Rev. D* **89** 035001 (2014); arXiv:1309.5410
93. Boos E et al. *Phys. Lett. B* **739** 410 (2014); arXiv:1402.4143
94. Dittmaier S et al. (LHC Higgs Cross Section Working Group), arXiv:1101.0593; CERN-2011-002, <http://dx.doi.org/10.5170/CERN-2011-002>
95. Heinemeyer S et al. (LHC Higgs Cross Section Working Group), arXiv:1307.1347; CERN-2013-004, <http://dx.doi.org/10.5170/CERN-2013-004>
96. Khachatryan V et al. (CMS Collab.) *Eur. Phys. J. C* **75** 212 (2015); arXiv:1412.8662
97. Espinosa J R et al. *J. High Energy Phys.* **2012** (05) 097 (2012); arXiv:1202.3697
98. Aad G et al. (ATLAS Collab.) *Eur. Phys. J. C* **80** 1165 (2020); arXiv:2004.14636
99. Tumasyan A et al. (CMS Collab.) *Phys. Rev. D* **105** 032008 (2022); arXiv:2109.06055
100. Boos E E et al. *Phys. Rev. D* **79** 104013 (2009); arXiv:0710.3100
101. Hewett J L *Phys. Rev. Lett.* **82** 4765 (1999)
102. Gupta A K, Mondal N K, Raychaudhuri S, hep-ph/9904234
103. Cheung K, Landsberg G *Phys. Rev. D* **62** 076003 (2000); hep-ph/9909218
104. Vermaseren J A M *Nucl. Instrum. Meth. Phys. Res. A* **559** 1 (2006); math-ph/0010025
105. Arkani-Hamed N et al. *Phys. Lett. B* **480** 193 (2000); hep-th/0001197
106. Kachru S, Schulz M, Silverstein E *Phys. Rev. D* **62** 085003 (2000); hep-th/0002121
107. de Alwis S P *Nucl. Phys. B* **597** 263 (2001); hep-th/0002174
108. de Alwis S P, Flournoy A T, Irges N *J. High Energy Phys.* **2001** (01) 027 (2001); hep-th/0004125
109. Förste S et al. *Phys. Lett. B* **481** 360 (2000); hep-th/0002164
110. Csáki C et al. *Nucl. Phys. B* **584** 359 (2000); hep-th/0004133
111. Smolyakov M N *J. High Energy Phys.* **2009** (11) 077 (2009)
112. Birrell N D, Davies P C W *Quantum Fields in Curved Space* (Cambridge: Cambridge Univ. Press, 1982); Translated into Russian: *Kvantovannye Polya v Iskrivlennom Prostranstve–Vremeni* (Moscow: Mir, 1984)
113. Volobuev I P, Keizerov S I, Rakhmetov E R *Moscow Univ. Phys. Bull.* **79** 156 (2024) <https://doi.org/10.3103/S0027134924700358>; *Vestn. Mosk. Univ. Ser. 3 Fiz. Astron.* **79** (2) 2420103 (2024) <https://doi.org/10.55959/MSU0579-9392.79.2420103>
114. Grib A A, Mamaev S G, Mostepanenko V M *Vakuumnye Kvantovye Effekty v Sil'nykh Polyalkh* (Vacuum Quantum Effects in Strong Fields) (Moscow: Energoatomizdat, 1988)
115. Bordag M et al. *Advances in the Casimir Effect* (International Ser. of Monographs on Physics, Vol. 145) (Oxford: Oxford Univ. Press, 2009)
116. Wald R M *Ann. Physics* **110** 472 (1978)
117. Sirunyan A M et al. (CMS Collab.) *J. High Energy Phys.* **2019** (04) 114 (2019)
118. Goldberger W D, Rothstein I Z *Phys. Lett. B* **491** 339 (2000)
119. Toms D J *Phys. Lett. B* **484** 149 (2000)
120. Garriga J, Pujolàs O, Tanaka T *Nucl. Phys. B* **605** 192 (2001)
121. Flachi A, Toms D J *Nucl. Phys. B* **610** 144 (2001)
122. Chivukula R S et al., arXiv:2411.02509